DEGRADATION AND CRYSTALLIZATION STUDIES OF BRANCHED PLA PREPARED BY REACTIVE EXTRUSION

by

Heather Leigh Simmons

A thesis submitted to the Department of Chemical Engineering

In conformity with the requirements for

the degree of Master of Applied Science

Queen's University

Kingston, Ontario, Canada

April, 2019

Abstract

This thesis proposes strategies to improve the crystallinity and mechanical properties of poly(lactic acid) (PLA) and investigates the effects of these modifications on hydrolytic degradation. The effect of long-chain branching (LCB) on the hydrolytic degradation at 60°C was monitored through the mass loss, molar mass distributions, and thermal properties of degraded specimens. A three-week induction period prior to the onset of mass loss coupled with an immediate loss in molar mass of over 80% in the same timeframe pointed to a bulk erosion mechanism. The highest loss in molar mass was observed in the z-average molar mass (M_z) of LCB PLA, exceeding 90% in the first three-weeks, and was attributed to the cleavage of the LCB segments from the polymer chain. Degradation-induced crystallinity resulted from the enhanced chain mobility at the experimental conditions, owing to the combined influence of annealing and the plasticizing effect of water. Although the hydrolysis profile differed between the linear and branched PLAs, branching did not affect negatively the extent of degradation over a 12-week period.

Increases in the crystallinity of PLA from 5% to 20% were achieved through reactive extrusion and the addition of biofiller (BF), a novel type of cross-linked PLA-based nucleating agent. The crystallinity of the nucleated formulations was further increased to over 50% by annealing at temperatures between 80 and 120°C. The BF additive was particularly effective in improving the crystallinity due to its PLA-based nature, which provided good compatibility with the matrix material. Owing to the improved crystallinities, the annealed materials demonstrated over 30% increases in flexural moduli compared to the neat material, while impact strength was maintained. Annealing of the modified PLA also resulted in 10°C increases in the glass transition temperatures followed by improvements in the heat deflection temperature (HDT) by as much as 7°C. An annealing temperature of 100°C was selected as optimum, due to evidence of thermal degradation taking place above this temperature. When subjected to hydrolysis over a 12-week period, the nucleated and annealed PLA degraded to the same extent as the untreated PLA, with over 30% loss in mass and 90% loss in molar mass.

Co-Authorship

Chapter 3 presents results which have been published in the form of an original journal article, and Chapter 4 presents material that has been submitted for publication. The complete citations are provided below:

Chapter 3: **Simmons, H.**; Kontopoulou, M. Hydrolytic degradation of branched PLA produced by reactive extrusion. *Polymer Degradation and Stability*. **2018,** *158,* 228-237.

Chapter 4: **Simmons, H.**; Tiwary, P.; Colwell, J.E.; Kontopoulou, M. Improvements in the crystallinity and mechanical properties of PLA by nucleation and annealing. *Under review with Polymer Degradation and Stability*. **2019.**

The large majority of the experimental work, analysis, and writing of the above chapters has been conducted by the author. All chapters and manuscripts were co-authored and reviewed by the thesis supervisor Dr. Marianna Kontopoulou. The fourth chapter was also co-authored by Dr. Praphulla Tiwary and Mr. James E. Colwell. In this chapter, the author was responsible for conducting the controlled crystallization experiments and degradation studies, in addition to performing differential scanning calorimetry (DSC) analysis and mechanical property testing. Dr. Praphulla Tiwary assisted with BF-formulation development and processing, and Mr. James E. Colwell assisted with compression molding, DSC, and performing extractions throughout the degradation study.

As a result of the work of this thesis, a patent was generated: Chaloupli, N. N.; Kontopoulou, M.; **Simmons, H**.; Tiwary, P.; Biobased Additive for Thermoplastic Polyesters. *Patent Publication Number WO/2019/010574*, **2019**. The author contributed to the patent by investigating the effects of isothermal conditioning on the BF-based material and proposing an optimal range of temperatures for conditioning.

Acknowledgements

I would first like to express my immense gratitude to Dr. Marianna Kontopoulou for her knowledge and mentorship in my journey as a Master's student. Without her assistance I would not have grown or learned as much in the past two years. I am also thankful for the guidance and friendship of Dr. Praphulla Tiwary. His knowledge and understanding of my work greatly supported project development and idea generation.

Thank you to all my peers and colleagues who have been instrumental in my development as a graduate student and have made my time in Dupuis Hall more enjoyable. I would also like to thank Kelly Sedore, Brooke Belfall, and Dr. Ying Zhang for their tireless support with the research equipment.

I am extremely grateful for Connor, Rebecca, Emily, Richard, Luca, and Syafiqah. Their friendship has been a constant source of laughter and solace, and has made my time at Queen's immeasurably better. A very special thanks to Nat for making me smile everyday, for listening to my often-long-winded rants, and most importantly for his endless encouragement and understanding throughout this journey. This experience would not have been the same without our adventures, both big and small. Finally, a huge thank you to Jenny, Jeffrey, and my parents. This would not have been possible without their unwavering love and support.

Table of Contents

List of Figures

List of Tables

List of Nomenclature and Abbreviations

Nomenclature

dn/dc	Differential refractive index
Đ	Dispersity
h	Hours
k	Hydrolytic degradation rate constant ($days^{-1}$)
M_n	Number average molar mass ($kg \cdot mol^{-1}$)
M_w	Weight average molar mass ($kg \cdot mol^{-1}$)
M_z	Z-average molar mass ($kg \cdot mol^{-1}$)
min	Minute
ml	Millilitre
s	Seconds
T	Temperature (°C)
T_c	Crystallization temperature (°C)
T_{cc}	Cold crystallization temperature (°C)
T_g	Glass transition temperature (°C)
T_m	Melting temperature (°C)
t	Time
μm	Micrometers
wt %	Weight percent (%)
χ_c	Percent crystallinity (%)

Abbreviations

ASTM	American Society for Testing Materials
BF	Biofiller
BN	Boron nitride
CM	Compression molded
DCP	Dicumyl peroxide

DRI	Differential refractive index
DSC	Differential scanning calorimetry
GHG	Greenhouse gas
GMA	Glycidyl methacrylate
GPC	Gel permeation chromatography
HDT	Heat deflection temperature
ISO	International Standards Organization
IV	Intrinsic viscosity
LALS	Low angle light scattering
LAK	Aromatic sulphonate derivative
LCB	Long-chain branching
LS	Light scattering
MFI	Melt flow index
MM	Molar mass
MMD	Molar mass distribution
PBP	Petroleum based plastic
PBS	Phosphate buffer solution
PLA	Poly(lactic acid)
RALS	Right angle light scattering
TAM	Triallyl trimesate
THF	Tetrahydrofuran
TSE	Twin-screw extruder
XRD	X-ray diffraction

Chapter 1

Introduction

The widespread use of plastics has resulted in rapid industry growth, with global production surging from 50 million metric tons in 1976 to 348 million metric tons in 2017[1]. Although plastics are a convenient and versatile material, their functional benefits come at a cost to the environment. Many of the most commonly used plastics including polyethylene (PE), polypropylene (PP), and polystyrene (PS) are derived from non-renewable fossil fuels and are termed petroleum-based plastics (PBPs). The manufacturing of PBPs is responsible for 70 million tonnes of CO_2 emission per year, contributing to climate change through approximately 1% of the annual U.S. greenhouse gas emissions (GHG)[2]. Traditional PBPs do not degrade and contribute heavily to landfill waste. Given these issues, recent research and development efforts have focused on the use of bioplastics, which may offer an effective way to maintain the advantages of conventional plastics, while reducing environmental impact[3].

1.1 Bioplastics

A thermoplastic material is defined as a bioplastic if it is either biobased, biodegradable, or features both properties[4]. A biobased plastic is one that is derived from biomass, such as polysaccharides, cellulose, or bacteria, or renewable natural resources, such as corn, sugarcane, or rice. Biodegradable plastics are those which can breakdown through microbial action into compounds which include water, carbon dioxide, biomass, and humus[3].

Many inherent limitations have restricted the growth and development of bioplastics. From an economic standpoint, the higher cost of bioplastics relative to PBPs hinders their widespread market acceptance[5,6]. Furthermore, the thermal and mechanical properties of bioplastics must match or improve upon those of PBPs in order to effectively to replace them. Other issues such as a lack of policy development surrounding bioplastics and limited end-of-life composting facilities have also hindered their acceptance and implementation[5–8].

Despite these limitations, factors such as the geopolitical challenges associated with petroleum availability and the growing environmental concerns surrounding PBP production and disposal have contributed to significant interest in PBP alternatives and continued research and development in bioplastics. Bioplastics offer advantages compared with PBPs in their energy consumption during production, waste management, and carbon footprint, in addition to contributing to a circular economy through their sustainable life cycle[5–7,9]. The most popular and sustainable type of bioplastics are those which are both biobased and biodegradable, such as poly(hydroxyalkanoate) (PHA), poly(3-hydroxybutyrate) (PHB), poly(butylene succinate) (PBS), and poly(lactic acid) (PLA)[10].

1.2 Poly(lactic acid) (PLA)

One of the most promising bioplastics is PLA, which attracts wide interest as a viable alternative to traditional PBPs[11]. PLA is a colourless, glossy, stiff, thermoplastic polyester with mechanical properties that resemble those of commodity plastics such as polyethylene (PE), polypropylene (PP), and polystyrene (PS)[12].

PLA is an inherently sustainable material: it is derived from renewable resources and is biodegradable, recyclable, and compostable at the end of its life[13,14]. The production of PLA utilizes 30-50% less fossil fuels, requires 25-55% less energy, and generates 50-70% less CO_2 emissions compared to PBPs[15,16]. The biocompatibility of PLA is advantageous when considering potential medical applications. In-vivo, PLA hydrolyzes to lactic acid which is incorporated into the tricarboxylic acid cycle and excreted from the body as carbon dioxide and water[17,18].

1.2.1 Processing, Properties, and Applications

Given that PLA is derived from a chiral compound, lactic acid, its stereochemistry can be modified by polymerizing a controlled mixture of L- or D-isomers[19]. PLA is naturally hydrophilic due to its polar oxygen linkages[20] (Figure 1.1) and this characteristic is responsible for its decomposition in response to surrounding moisture and temperature. PLA is degraded by simple hydrolysis of the ester bond and does not require the presence of enzymes to catalyze this hydrolysis[21].

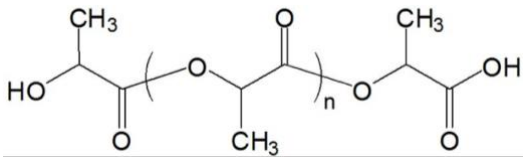

Figure 1.1: *Structure of PLA*

PLA can be processed using standard plastics equipment, such as injection molding, film casting, and extrusion, to yield molded parts, film, or fibers[12,22,23]. PLA has glass transition and melt temperatures of approximately 55°C and 175°C, respectively, and requires processing temperatures in excess of 185-190°C[12,24]. However, at temperatures above 200°C, PLA undergoes unzipping and chain scission reactions leading to loss of molar mass and thermal degradation[12]. Consequently, PLA has a very narrow processing window. PLA is also limited by its lack of melt strength, slow crystallization rates, and poor engineering properties such as impact strength and heat resistance[25]. These deficiencies mainly stem from the linear chain architecture of PLA, and limit its success in processing methods involving high stretch rates such as film blowing, thermoforming, and foaming[25].

Despite the processing difficulties, a number of consumer products currently use PLA[26]. Initially, most PLA applications were focused on high-value-added biomedical applications such as sutures, stents, and drug delivery systems due to the high initial cost of synthesizing PLA. More recently PLA has gained popularity in the packaging and textile industries[26,27], offering mechanical properties superior to polystyrene (PS) and comparable to polyethylene terephthalate (PET). According to the Food and Drug Administration (FDA), PLA is Generally Recognized As Safe (GRAS) when used in contact with food and therefore has become a sustainable material of choice in the food packaging industry[28]. PLA is also widely used as a material in the field of 3D printing[29].

1.2.2 Branching by Reactive Extrusion

To address the lack of melt strength and poor properties of PLA, several approaches have been proposed to achieve chain extension and/or branching in PLA. In contrast to adopting synthetic routes to develop branched PLA, methods which employ reactive modifications in the melt state are generally considered to be more convenient and industrially relevant[25]. Peroxide-initiated reactive extrusion in the melt state,

assisted by coagents, has frequently been used as a means to introduce long-chain branching in linear polymers, such as polypropylene[30,31]. More recently, branched or cross-linked PLA has been obtained through free-radical processing, initiated by organic peroxides[32,33], in the presence of multifunctional coagents, such as pentaerythritol triacrylate (PETA), trimethylolpropane triacrylate (TMPTA), and triallyl isocyanurate (TAIC)[34–39]. In comparison to commonly employed acrylate-based coagents, a trifunctional allylic coagent, triallyl trimesate (TAM), has been identified by our group as a particularly advantageous coagent at very low concentrations[25,40,41].

The solvent-free, peroxide-initiated grafting of TAM resulted in substantial improvements in the melt strength, strain-hardening, crystallinity, and crystallization kinetics of PLA[25,40]. Characterization of the chain architecture of TAM-modified PLA revealed that it is comprised of two types of chain populations: linear chains, which remain unreacted, and long-chain branched (LCB) structures generated through the combination of the trifunctional coagent with PLA macroradicals[34,38,42,43]. The formation of complex TAM structures interpenetrated within the PLA matrix was also proposed[42]. TAM is prone to oligomerization reactions and in the presence of peroxide, free radicals may react with the aliphatic unsaturated sites present in TAM, rather than abstracting hydrogen from the PLA chain[42,44,45]. The LCB structure was confirmed by the pronounced deviations of the intrinsic viscosity from the linear Mark-Houwink trends and its presence was associated with increases in molar mass, viscosity, elasticity, and strain hardening characteristics, along with pronounced shear thinning[42,46]. In addition, it was proposed that the branched chains act as nucleating sites, promoting crystallization under controlled cooling rates of $5°C \cdot min^{-1}$ provided by differential scanning calorimetry (DSC)[42].

Coagent modification using allylic coagents is very effective because of the better oligomer solubility in the ester-based matrix, compared to hydrocarbon systems[47]. Unlike TAM conversion in hydrocarbons, which leads to a precipitation polymerization reaction and thus loss of coagent[48], reactions with TAM conducted in polyesters do not incur loss of oligomeric intermediates. This phase stability advantage of

PLA allows all coagent charged to a formulation to be used for LCB production and is the cause of the remarkable LCB grafting yields of TAM-modified PLA[47].

The extensive studies on TAM-modified PLA have unambiguously confirmed improvements to the processing characteristics and properties of PLA, suggesting that peroxide-initiated reactive extrusion using TAM is an industrially relevant and promising approach for PLA modification. The improvements observed in TAM-modified PLA are expected to facilitate its use in operations such as foaming, injection molding, and film processing[25]. Despite such promise, there remain challenges which must be addressed, including the selection of processing conditions to optimize the crystallinity and mechanical properties, and the assessment of the effect of LCB on the degradability of PLA.

1.3 Thesis Objective

The peroxide-initiated reactive modification of PLA using multifunctional coagents has been well researched by our group[25,40,42,46,47]. However, despite the literature on the topic, the impact of such modifications on the degradation of PLA is largely unknown. The first objective of this thesis is to conduct an in-depth, long-term degradation study on reactively modified PLA, and to investigate the effect of LCB on the degradation characteristics of these materials. This knowledge will determine the relevance of this modification method, as degradability is a key contributor to the sustainability and market value of PLA.

Although TAM-modified PLA has accelerated crystallization kinetics compared to its parent material, such improvements were only demonstrated during controlled cooling conditions using DSC[25,42]. The second objective of this research is therefore to study the thermal and mechanical properties of PLA processed under well-controlled conditions. The detailed study of the structure-process-property relations of reactively modified PLA will enable the identification of processing conditions to achieve optimum thermal and mechanical properties.

1.4 Thesis Organization

This thesis is organized into five chapters. The present chapter, Chapter 1, has served as an introduction to bioplastics, and has demonstrated the motivation to use branched PLA. Chapter 2 is a comprehensive literature review focused on PLA lifecycle, degradation, and composting, as well as the structure-process-property relations of PLA and their relation to crystallinity development during processing. Chapter 3 focuses on the effects of branching on the hydrolytic degradation of LCB PLA. Chapter 4 examines the effects of annealing PLA at various temperatures on its thermal and mechanical properties. Finally, Chapter 5 summarizes the major conclusions of this work and recommends avenues of research to pursue in future work.

1.5 References

(1) Plastics Europe (PEMRG). Production of Plastics Worldwide from 1950 to 2017 https://www.statista.com/statistics/282732/global-production-of-plastics-since-1950/ (accessed Feb 14, 2019).

(2) United States Environmental Protection Agency. *Inventory of U.S. Greenhouse Gas Emissions and Sinks*; 2015.

(3) Jamshidian, M.; Tehrany, E. A.; Imran, M.; Jacquot, M.; Desobry, S. *Compr. Rev. Food Sci. Food Saf.* **2010**, *9* (5), 552.

(4) Chen, Y. J. *J. Chem. Pharm. Res.* **2014**, *6* (1), 226.

(5) Song, J. H.; Murphy, R. J.; Narayan, R.; Davies, G. B. H. *Philos. Trans. R. Soc. B Biol. Sci.* **2009**, *364* (1526), 2127.

(6) Lettner, M.; Schöggl, J.-P.; Stern, T. *J. Clean. Prod.* **2017**, *157*, 289.

(7) Lackner, M. In *Kirk-Othmer Encyclopedia of Chemical Technology*; John Wiley & Sons, Inc.: Hoboken, NJ, USA, 2015; pp 1–41.

(8) Brockhaus, S.; Petersen, M.; Kersten, W. *J. Clean. Prod.* **2016**, *127*, 84.

(9) Babu, R. P.; O'Connor, K.; Seeram, R. *Prog. Biomater.* **2013**, *2* (1), 8.

(10) Carrasco, F.; Pagès, P.; Gámez-Pérez, J.; Santana, O. O.; Maspoch, M. L. *Polym. Degrad. Stab.* **2010**, *95*, 116.

(11) Maharana, T.; Mohanty, B.; Negi, Y. S. *Prog. Polym. Sci.* **2009**, *34* (1), 99.

(12) Garlotta, D. *J. Polym. Environ.* **2001**, *9* (2), 63.

(13) Sawyer, D. J. *Macromol. Symp.* **2003**, *201* (1), 271.

(14) Drumright, R. E.; Gruber, P. R.; Henton, D. E. *Adv. Mater.* **2000**, *12* (23), 1841.

(15) Álvarez-Chávez, C. R.; Edwards, S.; Moure-Eraso, R.; Geiser, K. *J. Clean. Prod.* **2012**, *23* (1), 47.

(16) Vink, E. T. H.; Raago, K. R.; Glassner, D. A.; Gruber, P. R. *Polym. Degrad. Stab.* **2003**, *80* (3), 403.

(17) Athanasiou, K. *Biomaterials* **1996**, *17* (2), 93.

(18) Kimura, Y.; Shirotani, K.; Yamane, H.; Kitao, T. *Macromolecules* **1988**, *21* (11), 3338.

(19) Vink, E. T.; Rabago, K. R.; Glassner, D. A.; Springs, B.; O'Connor, R. P.; Kolstad, J.; Gruber, P. *Macromol Biosci* **2004**, *4* (6), 551.

(20) Ndazi, B. S.; Karlsson, S. *Express Polym. Lett.* **2011**, *5* (2), 119.

(21) Gopferich, A. *Biomoterials* **1996**, *17*, 103.

(22) Lim, L.-T.; Auras, R.; Rubino, M. *Prog. Polym. Sci.* **2008**, *33* (8), 820.

(23) Auras, R.; Harte, B.; Selke, S. *Macromol. Biosci.* **2004**, *4* (9), 835.

(24) Spinu, M.; Jackson, C.; Keating, M. Y.; Gardner, K. H. *J. Macromol. Sci. Part A Pure Appl. Chem.* **1996**, *33* (10), 1497.

(25) Nerkar, M.; Ramsay, J. A.; Ramsay, B. A.; Kontopoulou, M. *Macromol. Mater. Eng.* **2014**, *299* (12), 1419.

(26) Groot, W. J.; Borén, T. *Int J Life Cycle Assess* **2010**, *15*, 970.

(27) Mitchell, M. K.; Hirt, D. E. *Polym. Eng. Sci.* **2015**, *55* (7), 1652.

(28) Conn, R. E.; Kolstad, J. J.; Borzelleca, J. F.; Dixler, D. S.; Filer, L. J.; Ladu, B. N.; Pariza, M. W. *Food Chem. Toxicol.* **1995**, *33* (4), 273.

(29) Lasprilla, A. J. R. R.; Martinez, G. A. R. R.; Lunelli, B. H.; Jardini, A. L.; Filho, R. M. *Biotechnol. Adv.* **2012**, *30* (1), 321.

(30) Graebling, D. *Macromolecules* **2002**, *35* (12), 4602.

(31) Passaglia, E.; Coiai, S.; Augier, S. *Prog. Polym. Sci.* **2009**, *34* (9), 911.

(32) Takamura, M.; Nakamura, T.; Kawaguchi, S.; Takahashi, T.; Koyama, K. *Polym. J.* **2010**, *42* (7), 600.

(33) Takamura, M.; Nakamura, T.; Takahashi, T.; Koyama, K. *Polym. Degrad. Stab.* **2008**, *93* (10), 1909.

(34) Fang, H.; Zhang, Y.; Bai, J.; Wang, Z.; Wang, Z. *RSC Adv.* **2013**, *3* (23), 8783.

(35) Xu, H.; Fang, H.; Bai, J.; Zhang, Y.; Wang, Z. *Ind. Eng. Chem. Res.* **2014**, *53* (3), 1150.

(36) Quynh, T. M.; Mitomo, H.; Nagasawa, N.; Wada, Y.; Yoshii, F.; Tamada, M. *Eur. Polym. J.* **2007**, *43* (5), 1779.

(37) Yang, S.-L.; Wu, Z.-H.; Yang, W.; Yang, M.-B. *Polym. Test.* **2008**, *27* (8), 957.

(38) You, J.; Lou, L.; Yu, W.; Zhou, C. *J. Appl. Polym. Sci.* **2013**, *129* (4), 1959.

(39) Chen, C.-Q.; Ke, D.-M.; Zheng, T.-T.; He, G.-J.; Cao, X.-W.; Liao, X. *Ind. Eng. Chem. Res.* **2016**, *55* (3), 597.

(40) Nerkar, M.; Ramsay, J. A.; Ramsay, B. A.; Vasileiou, A. A.; Kontopoulou, M. *Polymer (Guildf).* **2015**, *64*, 51.

(41) Tiwary, P.; Park, C. B.; Kontopoulou, M. *Eur. Polym. J.* **2017**, *91*, 283.

(42) Tiwary, P.; Kontopoulou, M. *ACS Sustain. Chem. Eng.* **2018**, *6* (2), 2197.

(43) Wang, Y.; Yang, L.; Niu, Y.; Wang, Z.; Zhang, J.; Yu, F.; Zhang, H. *J. Appl. Polym. Sci.* **2011**, *122* (3), 1857.

(44) Wu, W.; Parent, J. S.; Sengupta, S. S.; Chaudhary, B. I. *J. Polym. Sci. Part A Polym. Chem.* **2009**, *47* (23), 6561.

(45) El Mabrouk, K.; Parent, J. S.; Chaudhary, B. I.; Cong, R. *Polymer (Guildf).* **2009**, *50* (23), 5390.

(46) Tiwary, P.; Kontopoulou, M. *J. Rheol. (N. Y. N. Y).* **2018**, *62* (5), 1071.

(47) Dawidziuk, K.; Simmons, H.; Kontopoulou, M.; Parent, J. S. S. *Polymer (Guildf).* **2018**, *158*, 254.

(48) Parent, J. S.; Bodsworth, A.; Sengupta, S. S.; Kontopoulou, M.; Chaudhary, B. I.; Poche, D.; Phane Cousteaux, S. *Polymer (Guildf).* **2008**, *50* (1), 85.

Chapter 2

Literature Review

2.1 Life Cycle Analysis

Life cycle assessment (LCA) is a commonly used methodology to assess the environmental performance and impact of products, considering all stages of life[1]. According to ISO standards, a LCA consists of four phases: i) goal and scope definition (establishing the extent of the analysis and system boundaries); ii) inventory analysis (input/output analysis of mass and energy flows from operations along the product's value chain); iii) impact assessment (evaluation of environmental effects and relevance); and iv) interpretation (e.g. optimization potential)[2,3]. LCA can be useful for product development and improvement, strategizing plans, making public policies, and developing new marketing norms[4].

LCA considers materials as product systems, accounting for various stages throughout their life. Optimally, LCA is performed by a cradle-to-grave analysis, including all inputs and outputs, extending from the production of raw materials (the "cradle") to the final disposal of all possible consumer products (the "grave")[5] (Figure 2.1). The scope of an LCA can be narrowed through a cradle-to-gate study, which starts with the extraction of raw material and ends when the finished product leaves the factory gate. Cradle-to-cradle analysis is sometimes used in place of cradle-to-grave and indicates that a product can be disposed of and returned back to the natural environment[2].

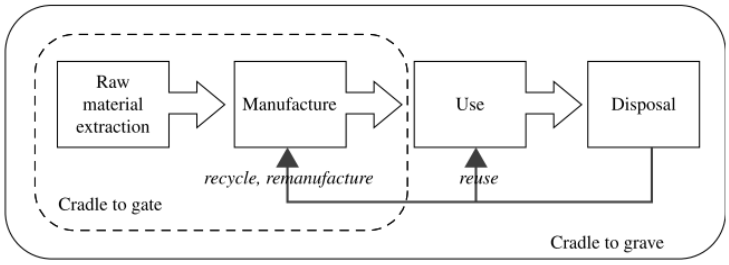

Figure 2.1: *Life cycle stages, from Landis 2010* [2]

PLA is generally regarded as a sustainable material, due to its inherent renewability and ability to be recycled and to degrade. The life cycle of PLA is based on a closed loop system which includes:

polymerization, processing and production, distribution, consumption or use, collection and sorting, recycling, and composting (Figure 2.2).

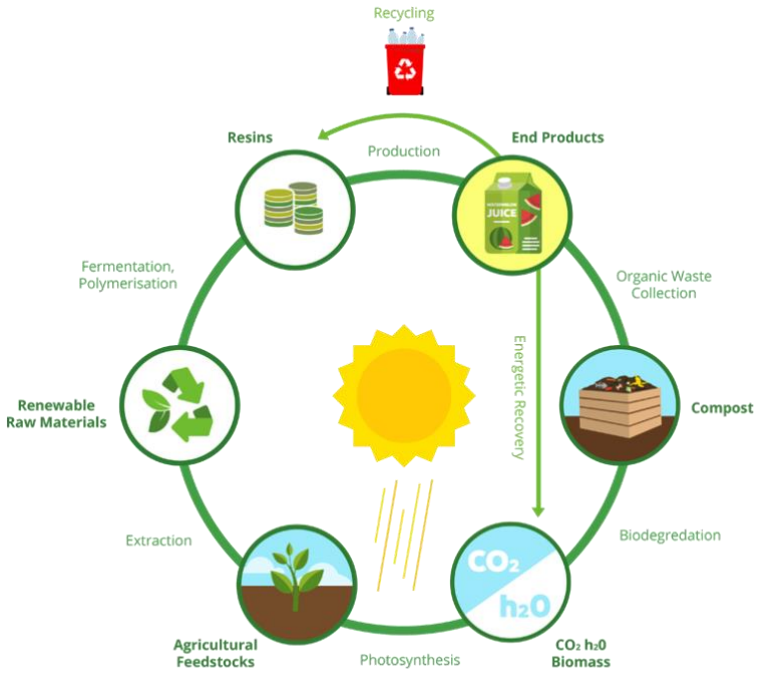

Figure 2.2: *Life cycle of PLA, from Environmental Resources Ltd* [6]

A significant amount of research has been conducted on the life cycle of PLA, with findings supporting its sustainability and potential to reduce the environmental impact of plastic products compared to PBPs[7]. A comparative LCA of cold drink cups composed of PLA, polyethylene terephthalate (PET), and polypropylene (PP) showed that the PET life cycle had the highest demand for non-renewable resources, followed by PP, and then PLA[7].

Vink et al. published a series of LCAs considering PLA production from cradle-to-gate[5,8,9]. The PLA production process presented less generation of greenhouse gases (GHGs), less use of material resources and non-renewable energy, and a lower global warming potential compared to the processing of PBPs[9]. A similar study on PLA blends made from cane sugar reached the same conclusions, but also highlighted the contributions of PLA production to acidification, eutrophication, and farm land use[1].

LCAs have also been conducted on PLA end-of-life scenarios. Studies on PLA disposal showed that composting, chemical recycling, and mechanical recycling present low environmental impact. The

recycling methods had the lowest environmental impact due to the potential re-use and re-polymerization of the output material of such processes, thus extending the life cycle[10,11]. Other studies have compared mechanical and chemical recycling of PLA, showing that chemical recycling has a larger environmental footprint, while the use of mechanical recycling yields lower quality PLA with loss of polymer properties[12–15].

To provide context to LCA, it is important to have a fundamental understanding of the key life cycle stages. This literature review will highlight two aspects of the PLA life cycle, namely, the production and processing of PLA, along with the disposal of PLA through degradation and composting mechanisms.

2.2 Structure-Process-Property Relations of PLA

2.2.1 Effects of Chemical Structure on Crystallinity

It is well known that the crystallinity, crystalline morphology, and spherulite size of PLA affect its processability, mechanical strength, biodegradability, and service temperature[16–20]. Crystallization of a thermoplastic polymer is limited by the mobility of chain segments, which depends on the polymer microstructure, molecular weight, and temperature[21,22].

The chiral nature of lactic acid results in distinct forms of PLA, namely, poly(L-lactide) (PLLA), poly(D-lactide) (PDLA), and poly(D,L-lactide) (PDLLA), synthesized from the L-, D-, and meso (D,L-) lactide monomers, respectively[23,24] (Figure 2.3). The ratio of the lactides influences polymer chain stereochemistry, mechanical properties, crystallinity, and degradation characteristics[25,26]. PLLA and PDLA are crystalline polymers due to the enantiomeric purity of the monomers and the stereoregularity of the polymer chain. Conversely, PDLLA, which is an equimolar relatively random copolymer of L- and D-lactic acid, is fully amorphous because of its irregular structure. For a commercial PLA, a blend of a higher amount of L-lactide and a lower amount of D-lactide is used to tune the crystallization properties as needed[27].

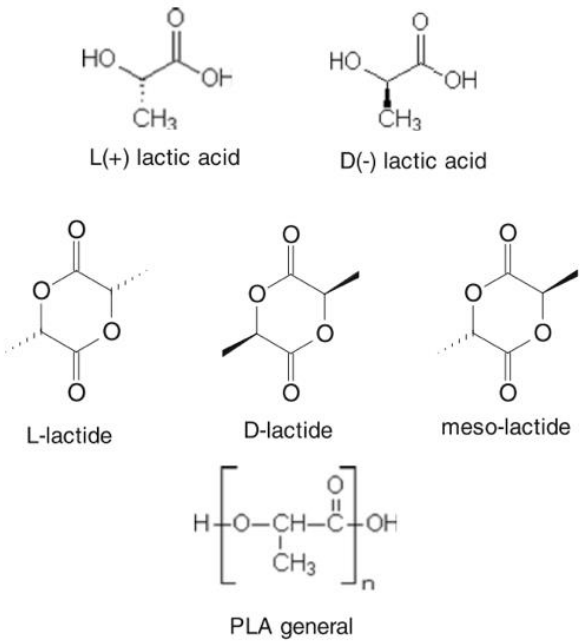

Figure 2.3: *Structures of lactic acid, lactide, and PLA, from Groot and Boren 2010* [1]

Many authors have studied the crystalline structure of PLA[17,28,37–39,29–36]. PLA crystals present three structural conformations which develop under various processing conditions[40]. Melt or cold crystallization and solution spinning processes at low drawing temperatures and/or ratios induce the formation of α-structures, characterized by a left-handed 10_3 helix that packs in an orthorhombic unit cell[41]. Stretching, solution spinning, or high hot draw ratios induce the formation of β-crystal structures with a chain conformation of left-handed 3_1 helices[42]. More recently, an additional crystalline form, γ, has been reported, which develops under epitaxial crystallization[43].

2.2.2 Effect of Crystalline Structure on Solid-State Properties

The crystalline phase of PLA tends to increase stiffness and tensile strength, while the amorphous phase is more effective in absorbing impact energy[44,45]. Therefore an increase in the total percentage crystallinity of PLA can effectively improve its HDT, stiffness, and chemical resistance, while the impact strength of PLA usually varies inversely with the percent crystallinity[46]. The tensile properties of PLA depend on the degree of crystallinity, in addition to the molecular weight and molecular orientation[47,48]. A lower extrusion temperature[49], collection speed increase[50–52], draw ratio increase, and hot drawing[50] have

strong effects on the tensile strength of PLA fibers due to higher molecular orientation and crystallinity development under these conditions. In addition, increasing the crystallization rate of PLA is of great importance, as higher amounts of the crystalline form contribute to HDT[53].

Given the strong correlation between crystallinity and material properties, many methods and processing techniques have been implemented to improve the level of crystallinity in PLA products[54]. PLA with high crystallinity has been obtained through methods such as block copolymerization, chemical modification, nucleation, plasticization[18,55–60], polymer blending[61–64], compounding with inorganic particles[63,65,66], strain-induced crystallization[67–69], and isothermal annealing[70–72].

2.2.3 Processing

Melt processing is by far the most widely adopted method for converting PLA resins into various end products[73]. It involves heating the polymer above its melting point, shaping the molten polymer, and cooling to stabilize its dimensions. Examples of melt processed PLA include injection molded disposable cutlery, thermoformed containers and cups, injection stretch blown bottles, extruded cast and oriented films, and melt-spun fibers for textiles[27,74]. Melt processing is affected by the stereochemical makeup and the structural and rheological properties of the PLA resins, while also having a significant influence on the final properties of the end products.

The processing of PLA is intimately related to its thermal properties. The glass transition temperature (T_g) of PLA can range from 35 to 60°C depending on the molecular weight, presence of plasticizers, physical aging, polymer architecture, degree of crystallinity, and thermal history of the polymer[75]. In extrusion, the process temperature must be greater than T_m to form a homogeneous melt, but low enough to minimize thermal degradation. During the cooling phase, sufficient in-mold cooling time must be given such that the part is cooled below the T_g to stabilize its dimensions. The degree of crystallinity of a polymeric part is dictated by the processing conditions. Quenching the polymer from the melt at a high cooling rate results in a highly amorphous polymer, while a slow rate of cooling allows for crystallinity development.

2.2.4 Nucleation and Thermal Treatment (Annealing)

The addition of nucleating agents during the processing of a thermoplastic can have a positive effect on the crystallization kinetics and morphology, by offering nucleating sites for initializing the crystallization process. A variety of nucleating agents for PLA have been reported, including talc[76], calcium carbonate[77], cellulose[78,79], and nanoclays[65,66,80–87]. Nucleating agents lower the surface free energy barrier for nucleation and enable crystallization at higher temperatures[27]. Lowering of the crystallization half time achieved with the presence of a nucleating agent can also help in shortening the molding cycle times[88].

In addition to various additives and chemical modification techniques, changes to PLA processing conditions have also been proposed to enhance its crystallization. Typically, in conventional processing techniques, obtaining a highly crystalline part remains difficult, due to the high cooling rates coupled with the slow crystallization rate of PLA[18,25]. To maximize the degree of crystallinity, the cooling rate must be slow, which leads to a long cycle time, or alternatively, annealing of the post-processed part is required[18,89–91]. Annealing can be done offline and in batches, offering a cost-effective way to improve the performance of PLA parts without impacting cycle time.

Originally used in metallurgy to increase the strength of metal objects, annealing is a heat treatment method which can change the physical properties of a material without changing its existing shape. In the plastics industry, annealing is the process of heating a plastic to a controlled temperature, often approximately half the polymer melting temperature, for a duration of time before cooling it down to room temperature[92]. This treatment increases the sample crystallinity since at a temperature above T_g, polymer chains gain mobility, which allows for the rearrangement of segments and the formation of an ordered phase[89,90]. Increasing the crystallinity through annealing also enhances the mechanical properties of the material[93]. The improvements offered by annealing treatment to the thermal and mechanical properties of PLA have been the focus of recent literature[18,25,94–97].

The effect of annealing on the fracture toughness of PLLA has been investigated in the work of Park et al.[98]. PLLA samples prepared by annealing showed slight increases in T_g and T_m, and drastic increases in

crystallinity compared to quenched samples[98]. The density and size of spherulites also increased with annealing time and temperature[99]. Reported increases in mechanical properties for annealed PLA reach a maximum at a crystallinity of 65%[73], since above this value, material embrittlement becomes predominant[100]. Carrasco et al. extensively studied the chemical structure, crystallinity, thermal stability, and mechanical properties of PLA after processing with or without annealing treatment[15]. Upon evaluation of the degree of crystallinity, it was found that mechanical processing led to the quasi disappearance of crystal structure, whereas it was recovered after annealing. In addition, annealed samples showed an increase in Young's modulus and in yield strength, attributed to the higher degree of crystallinity of these materials[15].

2.3 Composting and Biodegradation

A degradable plastic is one which undergoes a significant change in its chemical structure under specified environmental conditions, while a biodegradable plastic is one in which the degradation results from the action of naturally occurring microorganisms such as bacteria, fungi, and algae[101]. Standards related to the composting of plastics include ASTM D6400, ISO 17088, EN 13432, and DIN 14995[101–104], which define a compostable plastic as one that undergoes degradation by biological processes to yield carbon dioxide, water, inorganic compounds, and biomass at a rate consistent with other known compostable materials, leaving no visually distinguishable or toxic residues[101].

Composting requires specific conditions, including temperature, moisture, aeration, pH, and carbon to nitrogen (C/N) ratio, and consists of three phases: i) the mesophilic phase, ii) the thermophilic phase, and iii) the cooling and maturation phase[105]. In the first phase, mesophilic bacteria and fungi degrade organic matter over the duration of a few hours to several days. This phase results in the production of organic acids and a decrease in pH[106]. Temperature starts to rise spontaneously as heat is released from exothermic degradation reactions and the compost enters the thermophilic phase when the temperature reaches 40°C[106]. In this stage, thermophilic bacteria and fungi take over, and the degradation rate increases. After peak heating, the pH stabilizes to a neutral level. The thermophilic phase can last from a

few days to several months. In the maturation phase, the compost starts to cool and become stable as mesophilic bacteria and fungi reappear. The biological processes are slow in this phase, but the compost continues to be further humified, becoming mature.

Composting of polymers occurs mainly through mechanical, thermal, and chemical degradation. Photodegradation is only present on the surface of a compost pile where the material is exposed to ultraviolet (UV) and gamma radiation[107]. Of all the degradation mechanisms, chemical degradation is the most important for biodegradable polymers. Chemical degradation initiates the process of polymer erosion since biodegradable polymers have hydrolysable functional groups in the polymer backbone, which are susceptible to attack by water[107].

2.3.1 PLA as a Biodegradable and Compostable Polymer

PLA is a fully compostable polymer when composted in a large-scale operation with temperatures of 60°C and above[108]. The high moisture content and temperature in compost promote PLA hydrolysis and assimilation by thermophilic microorganisms[109–111]. On the contrary, PLA degradation in soil is much slower.

Biodegradation of PLA proceeds via a two-step mechanism[112]. Chemical degradation occurs in the first step, where the ester bond of the PLA backbone is cleaved through hydrolysis. This step can be accelerated by acid or bases and is affected by both temperature and moisture levels[113]. In this primary degradation phase, no microorganisms are involved. As the molar mass of the material decreases, microorganisms begin to digest the lower molecular weight lactic acid oligomers, producing carbon dioxide and water. According to the most commonly suggested mechanism, microorganisms can degrade PLA only after the molecular weight of PLA falls to 10,000 Da or less[109,112,121,122,113–120]. This is a distinct feature of PLA, since typically biodegradable polymers are degraded by microbial attack in a single step[112].

2.4 Hydrolysis

The first stage of PLA degradation is hydrolysis, which yields water soluble compounds and lactic acid, then followed by metabolization by microorganisms into carbon dioxide, water, and biomass[123]. Many researchers exclusively study hydrolysis as this provides an initial understanding of the propensity of a PLA-based material towards degradation, without requiring the complexity of a composting set-up.

2.4.1 Mechanism

PLA is susceptible to hydrolysis due to the hydrolysable functional groups in its backbone[113,124,125]. The hydrolytic degradation of PLA occurs via chain end scission and random cleavage of the ester bond, which are controlled by four basic parameters: the rate constant, the amount of absorbed water, the diffusion coefficient of chain fragments within the polymer, and the solubility of degradation products[126,127]. Random hydrolytic cleavage of ester bonds proceeds upon the diffusion of water into the amorphous regions (Figure 2.4). Chain end scission occurs through the action of carboxylic end groups accelerating the hydrolytic degradation of PLA in a self-catalyzed and self-maintaining process[128–131]. It has been reported in previous work that the scission kinetic constant of the terminal groups is much larger than that of the internal esters[132–134]. Following scission and cleavage of the polymer bonds, oligomers which are soluble in the surrounding aqueous medium can diffuse from the matrix. Soluble oligomers close to the surface can diffuse out easily, while those in the core of the matrix remain entrapped. As the latter fraction starts to degrade into lactic acid, it will lead to the reduction of pH in the core, further accelerating hydrolysis[135].

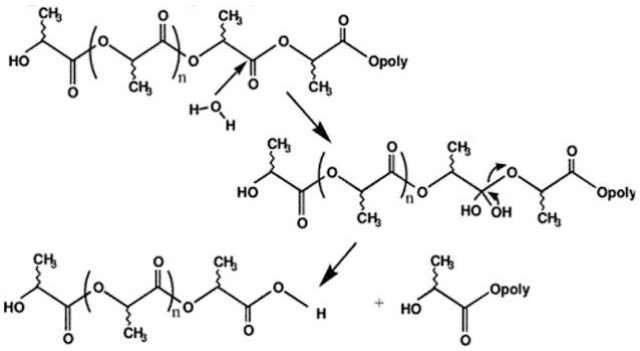

Figure 2.4: *Scheme of PLA hydrolysis mechanism, from Hartmann et al. 2000* [136]

The hydrolytic degradation of PLA-based solid polymer matrices can proceed through two different mechanisms: i) surface (heterogeneous) erosion or ii) bulk (homogeneous) erosion (Figure 2.5)[137]. The hydrolysis mechanism of PLA depends on the competition between the rate of diffusion of water molecules and the rate of hydrolysis reactions[138]. Surface erosion takes place when the hydrolytic degradation rate of the material surface is much higher than the diffusion of water molecules, causing hydrolysis to mainly occur in the near-surface regions[139]. On the contrary, bulk erosion occurs when the diffusion rate of water molecules is higher than the hydrolysis rate, causing hydrolysis to occur throughout the polymer matrix irrespective of the thickness of the material[73]. Degradation has been found to become a bulk process above the glass transition temperature (T_g), and is restricted to the surface below such temperature[140]. Material thickness is another important factor in determining the hydrolytic degradation mechanism. As expected, the hydrolytic degradation mechanism changes from bulk erosion to surface erosion when the material thickness exceeds a threshold device dimension, termed the critical thickness, $L_{critical}$, which is 7.4 cm for PLA[73,141].

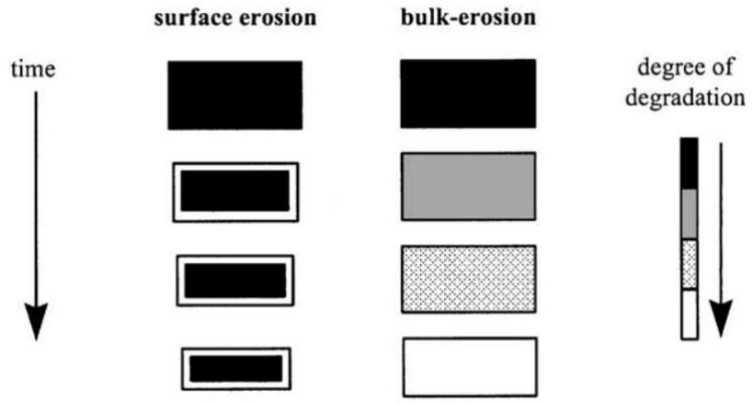

Figure 2.5: *Schematic illustration of changes to a polymer matrix during surface and bulk erosion, from Burkersroda et al. 2002*[141]

When PLA-based materials are hydrolytically degraded via the bulk erosion mechanism, the degradation occurs in three distinct stages: i) initial hydration and water absorption, ii) gradual decrease in molecular weight without weight loss, and iii) weight loss through the formation and dissolution of water-soluble

oligomers and monomers[142]. In a surface erosion mechanism, weight loss is observed nearly instantaneously, while molecular weight does not change for a period of time[143].

2.4.2 Parameters Influencing Degradation

Polymer degradation is the result of the interplay between chemical hydrolysis and the diffusion of water and oligomers[141,144] and largely depends on the molecular weight, crystallinity, geometry, and surrounding environment (temperature, moisture, pH, presence of micro-organisms, etc)[145].

The hydrolytic degradation rate of PLA is a strong function of pH, which can affect both the degradation mechanism and kinetics. Both alkaline and acidic media have been found to accelerate the hydrolytic degradation of PLA materials[134,139,146–151]. Schliecker et al. investigated the degradation of D,L-lactic acid oligomers at varying pH conditions, finding that the degradation rate was higher at two extreme pH conditions than at 4.5[126]. The mode of the reaction was chain-end cleavage under acidic conditions, while degradation proceeded via random ester cleavage under basic conditions. Shih also reports that acid-catalyzed hydrolysis proceeds predominantly through a chain-end scission mechanism, with the scission kinetic constant of the terminal groups exceeding that of the internal esters 10-fold[152]. Similar results were obtained by Batycky et al. who found that the difference in reaction rate between terminal and backbone esters under acidic conditions is 4-fold[153].

Crystallinity can largely impact the rate of hydrolysis, since the chains in crystalline regions of PLA are more resistant to hydrolysis, compared to those in amorphous regions. Therefore, diffusion and chain cleavage proceed preferentially in the amorphous regions, resulting in an increase in the crystallinity of samples as degradation proceeds[154–156]. Due to the preferential degradation of amorphous regions, hydrolytic degradation rates tend to decrease with increasing sample crystallinity[148,149,156,157]. In the early stages of hydrolytic degradation, the crystalline thickness of a sample only has an indirect effect on degradation. However, in the late stages of hydrolytic degradation wherein the crystalline residues are degraded, the effect of crystalline thickness has direct and crucial influence on the rate of degradation[149,158–160].

The temperature of hydrolytic degradation (T_h) has a strong effect on the rate of degradation and can occur within three ranges, depending upon its relation to the glass transition temperature, T_g and melting temperature, T_m, of the polymer: $T_h < T_g$, $T_g < T_h < T_m$, and $T_m < T_h$[161]. Reed and Gilding revealed that the rate of hydrolytic degradation dramatically increased when the degradation temperature was elevated over T_g[162]. This is attributed to enhanced chain mobility above T_g, which can enhance the diffusion of water[161]. At T_h exceeding T_m, crystalline regions melt and disappear, and hydrolytic degradation in the melt takes place homogeneously.

The molecular weight can have a strong influence on degradation behaviour and rates[161]. The effect of the initial molecular weight on degradation has been found to be minimal; however, as degradation proceeds, the effect of the degraded low molecular weight material becomes significant[158,163–165]. Decreases in molecular weight result in elevated molecular mobility, increased density of hydrophilic and catalytic terminal carboxyl groups, and higher probability of the formation of water-soluble oligomers and monomers, all of which contribute to the overall degradation process.

The rate of PLA degradation also depends on sample thickness[166,167]. Grizzi et al. demonstrated that materials with a greater thickness degrade faster than those that are thinner[166]. This is attributed to the autocatalytic effect of PLA terminal groups[161]. Decreased thickness results in quick removal of formed oligomers and monomers, resulting in a reduced autocatalytic effect, and therefore a lower degradation rate[161]. Conversely, core-accelerated erosion takes place in the case of PLA materials with a thickness of over 2 mm[100,168–172].

Various modification approaches to PLA such as copolymerization, terminal group modification, blending, and branching can impact the hydrolysis rate by affecting the crystallinity and diffusivity of water. Branching in PLA was found to increase the rate of hydrolytic degradation during later stages compared to linear PLA, due to the increased density of hydrophilic and catalytic carboxyl end groups[173]. While branches are thought to increase the rate of degradation, cross-linking reduces hydrolyzability due to the reduced diffusion of water and a reduction in the number of catalytic terminal groups[161].

2.4.3 Structural and Property Changes

PLA degradation leads to changes in mechanical and thermal properties, molecular weight, and morphology[132,145,166,168–170,174–177]. As PLA degrades and chain cleavage occurs, there is a decrease in molecular weight and the release of low molecular weight soluble oligomers and monomers[73,113]. The loss of molecular weight can be evaluated by means of gel permeation chromatography (GPC) or by conducting intrinsic viscosity measurements[178]. Since only monomeric and oligomeric degradation products are soluble, very large reductions in both the molecular weight and mechanical strength typically occur before a decrease in the weight of the sample is observed[179].

At a late stage in the hydrolytic degradation of PLA, a decrease in the mechanical properties occurs, resulting from the loss in molecular weight[161]. However, during the early stages of degradation, mechanical properties may increase due to the stabilized chain packing in amorphous regions, resulting from low-temperature annealing in the presence of water molecules as a plasticizer[130,155].

Crystallization of PLA is known to occur during hydrolytic degradation[130,148,155,163,168–170,180]. Crystalline regions are hydrolysis resistant, and experience slower rates of hydrolysis compared to amorphous regions. This is attributed to the preferential diffusion of water and hydrolysis in amorphous regions, which results in an increase in crystallinity over degradation time[114,130,149,160,161,181,182].

The thermal properties of PLA also change as a result of degradation. At a late stage in the hydrolytic degradation of high molecular weight PLA, T_g decreases due to enhanced molecular mobility resulting from reduced molecular weight, and T_m decreases due to the decreased crystalline thickness and surface structural changes of crystalline regions[130,155,183]. However, at an early stage of hydrolytic degradation, the effect of stabilized chain packing in the presence of water is higher than the reduced molecular weight effect, causing an increase in T_g[130,155,183]. An increase in T_m can also take place at early stages of degradation due to the thickening of crystallites and reduced disorder in the crystalline lattice[130,155,183]. As degradation proceeds, the selective degradation and removal of amorphous chains occurs, causing the peak area of melting to increase while that of cold crystallization decreases[130,139,148,149,155,170,180].

2.5 References

(1) Groot, W. J.; Borén, T. *Int J Life Cycle Assess* **2010**, *15*, 970.

(2) Landis, A. E. In *Poly(Lactic Acid): Synthesis, Structures, Properties, Processing, and Application*; Auras, R., Lim, L.-T., Selke, S. E. M., Tsuji, H., Eds.; John Wiley & Sons, Inc, 2010; pp 431–441.

(3) ISO 14044. *Environmental management - Life cycle assessment - Requirements and guidelines*; 2006.

(4) Madival, S.; Auras, R.; Singh, S. P.; Narayan, R. *J. Clean. Prod.* **2009**, *17* (13), 1183.

(5) Vink, E. T. H.; Raago, K. R.; Glassner, D. A.; Gruber, P. R. *Polym. Degrad. Stab.* **2003**, *80* (3), 403.

(6) Environmental Resources LTD. Bioplastics Life Cycle Assessment https://biotuff.com.au/why-biotuff/bioplastics (accessed Apr 19, 2018).

(7) PE Americas. *Comparative Life Cycle Assessment Ingeo biopolymer, PET, and PP Drinking Cups*; 2009.

(8) Vink, E. T.; Rabago, K. R.; Glassner, D. A.; Springs, B.; O'Connor, R. P.; Kolstad, J.; Gruber, P. *Macromol Biosci* **2004**, *4* (6), 551.

(9) Vink, E. T. H.; Davies, S. *Ind. Biotechnol.* **2015**, *11* (3), 167.

(10) Detzel, A.; Kruger, M. *Life Cycle Assessment of Polylactide (PLA)*; 2006.

(11) Papong, S.; Malakul, P.; Trungkavashirakun, R.; Wenunun, P.; Chom-In, T.; Nithitanakul, M.; Sarobol, E. *J. Clean. Prod.* **2014**, *65*, 539.

(12) Piemonte, V.; Sabatini, S.; Gironi, F. *J. Polym. Environ.* **2013**, *21* (3), 640.

(13) Zenkiewicz, M.; Richert, J.; Rytlewski, P.; Moraczewski, K.; Stepczynska, M.; Karasiewicz, T. *Polym. Test.* **2009**, *28*, 412.

(14) Pillin, I.; Montrelay, N.; Bourmaud, A.; Grohens, Y. *Polym. Degrad. Stab.* **2008**, *93*, 321.

(15) Carrasco, F.; Pagès, P.; Gámez-Pérez, J.; Santana, O. O.; Maspoch, M. L. *Polym. Degrad. Stab.* **2010**, *95*, 116.

(16) Wang, X.; Kumar, V.; Li, W. *Cell. Polym.* **2012**, *31* (1), 1.

(17) Tsuji, H.; Ikada, Y. *Polymer (Guildf).* **1995**, *36* (14), 2709.

(18) Harris, A. M.; Lee, E. C. *J. Appl. Polym. Sci.* **2008**, *107* (4), 2246.

(19) Park, S.-D.; Todo, M.; Arakawa, K. *J. Mater. Sci.* **2005**, *40* (4), 1055.

(20) Batista, N. L.; Olivier, P.; Bernhart, G.; Rezende, M. C.; Botelho, E. C. *Mater. Res.* **2016**, *19* (1), 195.

(21) Vincent, J. F. V. *Structural biomaterials*; Princeton University Press, 2012.

(22) Saeidlou, S.; Huneault, M. A.; Li, H.; Park, C. B. *Prog. Polym. Sci.* **2012**, *37* (12), 1657.

(23) Gupta, A. P.; Kumar, V. *Eur. Polym. J.* **2007**, *43* (10), 4053.

(24) Garlotta, D. *J. Polym. Environ.* **2001**, *9* (2), 63.

(25) Tabi, T.; Sajo, I. E.; Szabo, F.; Luyt, A. S.; Kovacs, J. G. *Express Polym. Lett.* **2010**, *4* (10), 659.

(26) Di Maio, L.; Scarfato, P.; Garofalo, E.; Galdi, M. R.; D'Arienzo, L.; Incarnato, L. In *AIP Conference Proceedings*; 2014; Vol. 1593, pp 308–311.

(27) Lim, L.-T.; Cink, K.; Vanyo, T. In *Poly(Lactic Acid): Synthesis, Structures, Properties, Processing, and Application*; Auras, R., Tak, L. T., Selke, S. E. M., Tsuji, H., Eds.; John Wiley & Sons, Ltd, 2010; pp 189–213.

(28) Jamshidi, K.; Hyon, S.-H.; Ikada, Y. *Polymer (Guildf).* **1988**, *29* (12), 2229.

(29) Migliaresi, C.; Cohn, D.; De Lollis, A.; Fambri, L. *J. Appl. Polym. Sci.* **1991**, *43* (1), 83.

(30) Marega, C.; Marigo, A.; Di Noto, V.; Zannetti, R.; Martorana, A.; Paganetto, G. *Die Makromol. Chemie* **1992**, *193* (7), 1599.

(31) Iannace, S.; Nicolais, L. *J. Appl. Polym. Sci.* **1997**, *64* (5), 911.

(32) Miyata, T.; Masuko, T. *Polymer (Guildf).* **1997**, *38* (16), 4003.

(33) Kolstad, J. J. *J. Appl. Polym. Sci.* **1996**, *62* (7), 1079.

(34) Perego, G.; Cella, G. D.; Bastioli, C. *J. Appl. Polym. Sci.* **1996**, *59* (1), 37.

(35) Sarasua, J.-R.; Prud'homme, R. E.; Wisniewski, M.; Le Borgne, A.; Spassky, N. *Macromolecules* **1998**, *31* (12), 3895.

(36) Di Lorenzo, M. L. *Polymer (Guildf).* **2001**, *42* (23), 9441.

(37) Di Lorenzo, M. L. *J. Appl. Polym. Sci.* **2006**, *100* (4), 3145.

(38) Di Lorenzo, M. L. *Macromol. Symp.* **2006**, *234* (1), 176.

(39) Yuryev, Y.; Wood-Adams, P.; Heuzey, M.-C.; Dubois, C.; Brisson, J. *Polymer (Guildf).* **2008**, *49* (9), 2306.

(40) Di Lorenzo, M. L. *Eur. Polym. J.* **2005**, *41* (3), 569.

(41) De Santis, P.; Kovacs, A. J. *Biopolymers* **1968**, *6* (3), 299.

(42) Hoogsteen, W.; Postema, A. R.; Pennings, A. J.; ten Brinke, G.; Zugenmaier, P. *Macromolecules* **1990**, *23* (2), 634.

(43) Cartier, L.; Okihara, T.; Ikada, Y.; Tsuji, H.; Puiggali, J.; Lotz, B. *Polymer (Guildf).* **2000**, *41* (25), 8909.

(44) Osswald, T. A.; Baur, E.; Brinkmann, S.; Oberbach, K.; Schmachtenberg, E. *International Plastics Handbook*; Carl Hanser Verlag GmbH & Co. KG: München, 2006.

(45) Srithep, Y.; Javadi, A.; Pilla, S.; Turng, L.-S.; Gong, S.; Clemons, C.; Peng, J. *Polym. Eng. Sci.* **2011**, *51* (6), 1023.

(46) Kfoury, G.; Raquez, J.-M.; Hassouna, F.; Leclère, P.; Toniazzo, V.; Ruch, D.; Dubois, P. *Polym. Eng. Sci.* **2015**, *55* (6), 1408.

(47) Blackburn, R. S. *Biodegradable and sustainable fibres*; Woodhead Publishing, 2005.

(48) Eling, B.; Gogolewski, S.; Pennings, A. J. *Polymer (Guildf).* **1982**, *23* (11), 1587.

(49) Yuan, X.; Mak, A. F. T.; Kwok, K. W.; Yung, B. K. O.; Yao, K. *J. Appl. Polym. Sci.* **2001**, *81* (1), 251.

(50) Fambri, L.; Pegoretti, A.; Fenner, R.; Incardona, S. D. D.; Migliaresi, C. *Polymer (Guildf).* **1997**, *38* (1), 79.

(51) Schmack, G.; Tandler, B.; Vogel, R.; Beyreuther, R.; Jacobsen, S.; Fritz, H.-G. *J. Appl. Polym. Sci.* **1999**, *73* (14), 2785.

(52) Kim, M. S.; Kim, J. C.; Kim, Y. H. *Polym. Adv. Technol.* **2008**, *19* (7), 748.

(53) Li, M.; Hu, D.; Wang, Y.; Shen, C. *Polym. Eng. Sci.* **2010**, *50* (12), 2298.

(54) Drieskens, M.; Peeters, R.; Mullens, J.; Franco, D.; Lemstra, P. J.; Hristova-Bogaerds, D. G. *J. Polym. Sci. Part B Polym. Phys.* **2009**, *47* (22), 2247.

(55) Kfoury, G.; Raquez, J.-M.; Hassouna, F.; Odent, J.; Toniazzo, V.; Ruch, D.; Dubois, P. *Front. Chem.* **2013**, *1* (32), 1.

(56) Liu, H.; Zhang, J. *J. Polym. Sci. Part B Polym. Phys.* **2011**, *49* (15), 1051.

(57) Liu, J.; Lou, L.; Yu, W.; Liao, R.; Li, R.; Zhou, C. *Polymer (Guildf).* **2010**, *51* (22), 5186.

(58) Liu, H.; Song, W.; Chen, F.; Guo, L.; Zhang, J. *Macromolecules* **2011**, *44* (6), 1513.

(59) Zhang, K.; Mohanty, A. K.; Misra, M. *ACS Appl. Mater. Interfaces* **2012**, *4* (6), 3091.

(60) Zhang, K.; Nagarajan, V.; Misra, M.; Mohanty, A. K. *ACS Appl. Mater. Interfaces* **2014**, *6* (15), 12436.

(61) Yu, L.; Dean, K.; Li, L. *Prog. Polym. Sci.* **2006**, *31* (6), 576.

(62) Pillin, I.; Montrelay, N.; Grohens, Y. *Polymer (Guildf).* **2006**, *47* (13), 4676.

(63) Li, H.; Huneault, M. A. *Int. Polym. Process.* **2008**, *23* (5), 412.

(64) Yeh, J.-T.; Wu, C.-J.; Tsou, C.-H.; Chai, W.-L.; Chow, J.-D.; Huang, C.-Y.; Chen, K.-N.; Wu, C.-S. *Polym. Plast. Technol. Eng.* **2009**, *48* (6), 571.

(65) Day, M.; Nawaby, A. V.; Liao, X. *J. Therm. Anal. Calorim.* **2006**, *86* (3), 623.

(66) Li, H.; Huneault, M. A. *Polymer (Guildf).* **2007**, *48* (23), 6855.

(67) Chapleau, N.; Huneault, M. A.; Li, H. *Int. Polym. Process.* **2007**, *22* (5), 402.

(68) Mihai, M.; Huneault, M. A.; Favis, B. D. *J. Appl. Polym. Sci.* **2009**, *113* (5), 2920.

(69) Kokturk, G.; Piskin, E.; Serhatkulu, T. F.; Cakmak, M. *Polym. Eng. Sci.* **2002**, *42* (8), 1619.

(70) Yasuniwa, M.; Tsubakihara, S.; Iura, K.; Ono, Y.; Dan, Y.; Takahashi, K. *Polymer (Guildf).* **2006**, *47* (21), 7554.

(71) Yasuniwa, M.; Iura, K.; Dan, Y. *Polymer (Guildf).* **2007**, *48* (18), 5398.

(72) Tsuji, H.; Takai, H.; Saha, S. K. *Polymer (Guildf).* **2006**, *47* (11), 3826.

(73) Auras, R.; Tak, L. T.; Selke, S. E. M.; Tsuji, H. *Poly(Lactic Acid): Synthesis, Structures, Properties, Processing, and Application.*; John Wiley & Sons, Inc.: Hoboken, NJ, USA, 2010.

(74) Weber, C. J.; Haugaard, V.; Festersen, R.; Bertelsen, G. *Food Addit. Contam.* **2002**, *19* (sup1), 172.

(75) Baker, G.; Vogel, E.; Smith, M. *Polym. Rev.* **2008**, *48* (1), 64.

(76) Battegazzore, D.; Bocchini, S.; Frache, A. *Express Polym. Lett.* **2011**, *5* (10), 849.

(77) Liang, J.-Z.; Zhou, L.; Tang, C.-Y.; Tsui, C.-P. *Compos. Part B Eng.* **2013**, *45* (1), 1646.

(78) Frone, A. N.; Berlioz, S.; Chailan, J.-F.; Panaitescu, D. M. *Carbohydr. Polym.* **2013**, *91* (1), 377.

(79) Kowalczyk, M.; Piorkowska, E.; Kulpinski, P.; Pracella, M. *Compos. Part A Appl. Sci. Manuf.* **2011**, *42* (10), 1509.

(80) Sinha Ray, S.; Yamada, K.; Okamoto, M.; Ogami, A.; Ueda, K. *Chem. Mater.* **2003**, *15* (7), 1456.

(81) Sinha Ray, S.; Yamada, K.; Okamoto, M.; Fujimoto, Y.; Ogami, A.; Ueda, K. *Polymer (Guildf).*

2003, *44* (21), 6633.

(82) Zhang, J.; Jiang, L.; Zhu, L.; Jane, J.-L.; Mungara, P. *Biomacromolecules* **2006**, *7* (5), 1551.

(83) Pluta, M. *Polymer (Guildf)*. **2004**, *45* (24), 8239.

(84) Lewitus, D.; McCarthy, S.; Ophir, A.; Kenig, S. *J. Polym. Environ.* **2006**, *14* (2), 171.

(85) Nam, J. Y.; Sinha Ray, S.; Okamoto, M. *Macromolecules* **2003**, *36* (19), 7126.

(86) Krikorian, V.; Pochan, D. J. *Macromolecules* **2004**, *37* (17), 6480.

(87) Liao, R.; Yang, B.; Yu, W.; Zhou, C. *J. Appl. Polym. Sci.* **2007**, *104* (1), 310.

(88) Suryanegara, L.; Okumura, H.; Nakagaito, A. N.; Yano, H. *Cellulose* **2011**, *18* (3), 689.

(89) Andjelić, S.; Scogna, R. C. *J. Appl. Polym. Sci.* **2015**, *132* (38), 42066.

(90) Ivey, M.; Melenka, G. W.; Carey, J. P.; Ayranci, C. *Adv. Manuf. Polym. Compos. Sci.* **2017**, *3* (3), 81.

(91) Zhou, H.; Green, T. B.; Joo, Y. L. *Polymer (Guildf)*. **2006**, *47* (21), 7497.

(92) Pérez-Fonseca, A. A.; Robledo-Ortíz, J. R.; González-Núñez, R.; Rodrigue, D. *J. Appl. Polym. Sci.* **2016**, *133* (31), 43750.

(93) Huang, T.; Yamaguchi, M. *J. Appl. Polym. Sci.* **2017**, *134* (24), 44960.

(94) Dong, T.; Yu, Z.; Wu, J.; Zhao, Z.; Yun, X.; Wang, Y.; Jin, Y.; Yang, J. *Polym. Sci. Ser. A* **2015**, *57* (6), 738.

(95) Srithep, Y.; Nealey, P.; Turng, L.-S. *Polym. Eng. Sci.* **2013**, *53* (3), 580.

(96) Wach, R. A.; Wolszczak, P.; Adamus-Wlodarczyk, A. *Macromol. Mater. Eng.* **2018**, *303* (9), 1800169.

(97) Takayama, T.; Todo, M.; Tsuji, H. *J. Mech. Behav. Biomed. Mater.* **2011**, *4* (3), 255.

(98) Park, S.-D.; Todo, M.; Arakawa, K. *J. Mater. Sci.* **2004**, *39* (3), 1113.

(99) Park, S. D.; Todo, M.; Arakawa, K.; Koganemaru, M. *Polymer (Guildf)*. **2006**, *47* (4), 1357.

(100) Södergård, A.; Stolt, M. *Prog. Polym. Sci.* **2002**, *27* (6), 1123.

(101) ASTM Standard D6400. *Labeling of Plastics Designed to be Aerobically Composted in Municipal or Industrial Facilities*; 2012.

(102) ISO 17088. *Specifications for compostable plastics*; 2012.

(103) BS EN 13432. *Requirements for packaging recoverable through composting and biodegradation*; 2000.

(104) DIN EN 14995. *Plastics - Evaluation of compostability - Test scheme and specifications*; 2007.

(105) Rudnik, E. *Compostable Polymer Materials*; Elsevier Ltd, 2008.

(106) Tuomela, M. Degradation of lignin and other 14 C-labelled compounds in compost and soil with an emphasis on white-rot fungi, University of Helsinki, 2002.

(107) Kale, G.; Auras, R.; Singh, S. P. *J. Polym. Environ.* **2006**, *14* (3), 317.

(108) Tokiwa, Y.; Calabia, B. P. *Appl. Microbiol. Biotechnol.* **2006**, *72* (2), 244.

(109) Itävaara, M.; Karjomaa, S.; Selin, J.-F. *Chemosphere* **2002**, *46* (6), 879.

(110) Ohkita, T.; Lee, S.-H. *J. Appl. Polym. Sci.* **2006**, *100* (4), 3009.

(111) Kamiya, M.; Asakawa, S.; Kimura, M. *Soil Sci. Plant Nutr.* **2007**, *53* (5), 568.

(112) Lunt, J. *Polym. Degrad. Stab.* **1998**, *59* (1–3), 145.

(113) Auras, R.; Harte, B.; Selke, S. *Macromol. Biosci.* **2004**, *4* (9), 835.

(114) Kale, G.; Auras, R.; Singh, S. P. *Packag. Technol. Sci.* **2007**, *20* (1), 49.

(115) Mohanty, A. K.; Misra, M.; Drzal, L. T. (Lawrence T. *Natural fibers, biopolymers, and biocomposites*; Taylor & Francis, 2005.

(116) Agarwal, M.; Koelling, K. W.; Chalmers, J. J. *Biotechnol. Prog.* **1998**, *14* (3), 517.

(117) Torres, A.; Li, S. M.; Roussos, S.; Vert, M. *J. Appl. Polym. Sci.* **1996**, *62* (13), 2295.

(118) Ghorpade, V.; Gennadios, A.; Hanna, M. A. *Bioresour. Technol.* **2001**, *76* (1), 57.

(119) Sangwan, P.; Wu, D. Y. *Macromol. Biosci.* **2008**, *8* (4), 304.

(120) Copinet, A.; Legin-Copinet, E.; Erre, D. *Materials (Basel)*. **2009**, *2* (3), 749.

(121) Longieras, A.; Tanchette, J.-B.; Erre, D.; Braud, C.; Copinet, A. *J. Polym. Environ.* **2007**, *15* (3), 200.

(122) Saadi, Z.; Rasmont, A.; Cesar, G.; Bewa, H.; Benguigui, L. *J. Polym. Environ.* **2012**, *20* (2), 273.

(123) Nolan-ITU; ExcelPlas Australia; Environment Australia. *Biodegradable Plastics - Developments and Environmental Impacts*; 2002.

(124) Tsuji, H.; Saeki, T.; Tsukegi, T.; Daimon, H.; Fujie, K. *Polym. Degrad. Stab.* **2008**, *93* (10), 1956.

(125) Lim, L.-T.; Auras, R.; Rubino, M. *Prog. Polym. Sci.* **2008**, *33* (8), 820.

(126) Schliecker, G.; Schmidt, C.; Fuchs, S.; Kissel, T. *Biomaterials* **2003**, *24* (21), 3835.

(127) Fischer, E. W.; Sterzel, H. J.; Wegner, G. *Kolloid-Zeitschrift und Zeitschrift für Polym.* **1973**, *251* (11), 980.

(128) Paul, M.-A.; Delcourt, C.; Alexandre, M.; Degée, P.; Monteverde, F.; Dubois, P. *Polym. Degrad. Stab.* **2005**, *87* (3), 535.

(129) Zhou, Q.; Xanthos, M. *Polym. Degrad. Stab.* **2008**, *93* (8), 1450.

(130) Tsuji, H.; Ikada, Y. *Polym. Degrad. Stab.* **2000**, *67* (1), 179.

(131) Tsuji, H. *Polymer (Guildf).* **2002**, *43* (6), 1789.

(132) de Jong, S. J.; Arias, E. R.; Rijkers, D. T. S.; van Nostrum, C. F.; Kettenes-van den Bosch, J. J.; Hennink, W. E. *Polymer (Guildf).* **2001**, *42* (7), 2795.

(133) van Nostrum, C. F.; Veldhuis, T. F. J.; Bos, G. W.; Hennink, W. E. *Polymer (Guildf).* **2004**, *45* (20), 6779.

(134) Belbella, A.; Vauthier, C.; Fessi, H.; Devissaguet, J.-P.; Puisieux, F. *Int. J. Pharm.* **1996**, *129* (1–2), 95.

(135) Vert, M.; Mauduit, J.; Li, S. *Biomaterials* **1994**, *15* (15), 1209.

(136) Hartmann, M.; Whiteman, N. In *TAPPI Polymers, Laminations & Coatings Conference*; Chicago, IL, United States, 2000; pp 467–474.

(137) Siepmann, J.; Gopferich, A. *Adv. Drug Deliv. Rev.* **2001**, *48* (2–3), 229.

(138) Lyu, S.; Schley, J.; Loy, B.; Lind, D.; Hobot, C.; Sparer, R.; Untereker, D. *Biomacromolecules* **2007**, *8* (7), 2301.

(139) Yuan, X.; Mak, A. F. T.; Yao, K. *Polym. Degrad. Stab.* **2003**, *79* (1), 45.

(140) Canevarolo, S. V. *Polym. Degrad. Stab.* **2000**, *70* (1), 71.

(141) Burkersroda, F. von; Schedl, L.; Göpferich, A. *Biomaterials* **2002**, *23* (21), 4221.

(142) Gopferich, A. *Macromolecules* **1997**, *30*, 2598.

(143) Tsuji, H.; Hayashi, T. *Polym. Degrad. Stab.* **2014**, *102*, 59.

(144) Grayson, A. C. R.; Cima, M. J.; Langer, R. *Biomaterials* **2005**, *26* (14), 2137.

(145) Mitchell, M. K.; Hirt, D. E. *Polym. Eng. Sci.* **2015**, *55* (7), 1652.

(146) Makino, K.; Arakawa, M.; Kondo, T. *Chem. Pharm. Bull. (Tokyo).* **1985**, *33* (3), 1195.

(147) Makino, K.; Ohshima, H.; Kondo, T. *J. Microencapsul.* **1986**, *3* (3), 203.

(148) Cam, D.; Hyon, S.; Ikada, Y. *Biomaterials* **1995**, *16* (11), 833.

(149) Tsuji, H.; Ikada, Y. *J. Polym. Sci. Part A Polym. Chem.* **1998**, *36* (1), 59.

(150) Taddei, P.; Monti, P.; Simoni, R. *J. Mater. Sci.* **2002**, *13* (1), 469.

(151) Chu, C. C. *Ann. Surg.* **1982**, *195* (1), 55.

(152) Shih, C. *J. Control. Release* **1995**, *34* (1), 9.

(153) Batycky, R. P.; Hanes, J.; Langer, R.; Edwards, D. A. *J. Pharm. Sci.* **1997**, *86* (12), 1464.

(154) Hakkarainen, M. In *Degradable Aliphatic Polyesters*; Springer Berlin Heidelberg: Berlin, Heidelberg, 2002; Vol. 157, pp 113–138.

(155) Tsuji, H.; Mizuno, A.; Ikada, Y. *J. Appl. Polym. Sci.* **2000**, *77* (7), 1452.

(156) Tsuji, H.; Miyauchi, S. *Polym. Degrad. Stab.* **2001**, *71* (3), 415.

(157) Tsuji, H.; Miyauchi, S. *Polymer (Guildf).* **2001**, *42* (9), 4463.

(158) Saha, S. K.; Tsuji, H. *Polym. Degrad. Stab.* **2006**, *91* (8), 1665.

(159) Tsuji, H.; Nakahara, K.; Ikarashi, K. *Macromol. Mater. Eng.* **2001**, *286* (7), 398.

(160) Tsuji, H.; Ikarashi, K.; Fukuda, N. *Polym. Degrad. Stab.* **2004**, *84* (3), 515.

(161) Tsuji, H. In *Poly(Lactic Acid): Synthesis, Structures, Properties, Processing, and Application*; Auras, R., Tak, L. T., Selke, S. E. M., Tsuji, H., Eds.; John Wiley & Sons, Inc., 2010; pp 345–376.

(162) Reed, A. M.; Gilding, D. K. *Polymer (Guildf).* **1981**, *22* (4), 494.

(163) Migliaresi, C.; Fambri, L.; Cohn, D. *J. Biomater. Sci. Polym. Ed.* **1994**, *5* (6), 591.

(164) Celikkaya, E.; Denkbas, E. B.; Piskin, E. *J. Appl. Polym. Sci.* **1996**, *61* (9), 1439.

(165) Hyon, S.-H.; Jamshidi, K.; Ikada, Y. *Polym. Int.* **1998**, *46* (3), 196.

(166) Grizzi, I.; Garreau, H.; Li, S.; Vert, M. *Biomaterials* **1995**, *16* (4), 305.

(167) Dunne, M.; Corrigan, O. I.; Ramtoola, Z. *Biomaterials* **2000**, *21* (16), 1659.

(168) Li, S. M.; Garreau, H.; Vert, M. *J. Mater. Sci. Mater. Med.* **1990**, *1* (3), 123.

(169) Li, S. M.; Garreau, H.; Vert, M. *J. Mater. Sci. Mater. Med.* **1990**, *1* (3), 131.

(170) Li, S. M.; Garreau, H.; Vert, M. *J. Mater. Sci. Mater. Med.* **1990**, *1* (4), 198.

(171) Stefani, M.; Coudane, J.; Vert, M. *Polym. Degrad. Stab.* **2006**, *91* (11), 2554.

(172) Li, S.; Anjard, S.; Rashkov, I.; Vert, M. *Polymer (Guildf)*. **1998**, *39* (22), 5421.

(173) Kim, S. H.; Kim, Y. H. In *Studies in Polymer Science*; Elsevier, 1994; Vol. 12, pp 464–469.

(174) Tsuji, H.; Sumida, K. *J. Appl. Polym. Sci.* **2001**, *79* (9), 1582.

(175) Auras, R. A.; Singh, S. P.; Singh, J. J. *Packag. Technol. Sci.* **2005**, *18* (4), 207.

(176) Gupta, B.; Revagade, N.; Anjum, N.; Atthoff, B.; Hilborn, J. *J. Appl. Polym. Sci.* **2006**, *100* (2), 1239.

(177) Copinet, A.; Bertrand, C.; Govindin, S.; Coma, V.; Couturier, Y. *Chemosphere* **2004**, *55* (5), 763.

(178) Griffith, L. G. *Acta Mater.* **2000**, *48* (1), 263.

(179) Elsawy, M. A.; Kim, K.-H.; Park, J.-W.; Deep, A. *Renew. Sustain. Energy Rev.* **2017**, *79*, 1346.

(180) Duek, E. A. .; Zavaglia, C. A. .; Belangero, W. . *Polymer (Guildf)*. **1999**, *40* (23), 6465.

(181) Reeve, M. S.; McCarthy, S. P.; Downey, M. J.; Gross, R. A. *Macromolecules* **1994**, *27* (3), 825.

(182) Höglund, A.; Odelius, K.; Albertsson, A.-C. *ACS Appl. Mater. Interfaces* **2012**, *4* (5), 2788.

(183) Gonzalez, M. F.; Ruseckaite, R. A.; Cuadrado, T. R. *J. Appl. Polym. Sci.* **1999**, *71* (8), 1223.

Chapter 3

Hydrolytic degradation of branched PLA produced by reactive extrusion*

3.1 Introduction

The ability to manufacture thermoplastic-based products from renewable resources is becoming increasingly important as both consumers and industry seek alternatives to the use of fossil fuels for commodity applications. Poly(lactic acid) or poly(lactide) (PLA) is a bioderived and biodegradable thermoplastic polyester, which attracts wide interest as a viable replacement for commercial petroleum-based polymers such as polyethylene, polypropylene, and polystyrene[1].

Even though PLA is used commercially in a variety of polymer processes, it suffers from slow crystallization kinetics[2,3] and poor melt strength[2,4–6]. These shortcomings pose limitations in the processing of PLA using conventional thermoplastics processing equipment, such as injection molding, blow molding, and film processing[7]. Reactive modification approaches have been implemented to produce PLA containing long-chain branching (LCB), thus extending the applicability and improving the processability of PLA[8–12]. The effects of various modification approaches, such as the addition of chain extenders[13,14] and other additives[15–17] on the degradation of PLA have also been investigated.

The hydrolysis of polyesters, including PLA, occurs via an auto-catalytic random chain scission reaction[18–23]. During hydrolysis, the ester bonds of PLA are broken down, forming carboxyl end groups which have been demonstrated to self-catalyze the hydrolysis reaction[24].

The physical structure of PLA impacts its degradation, as diffusion and chain cleavage of the ester bond proceeds preferentially in the amorphous regions, resulting in an increase in the crystallinity of degraded samples[25–27]. The rate of polymer degradation is controlled by kinetics and transport phenomena which can be affected by factors such as the shape of the specimens and the hydrolysis conditions including pH

* A version of this chapter has been published: **Simmons, H.**; Kontopoulou, M. Hydrolytic Degradation of Branched PLA Produced by Reactive Extrusion. *Polymer Degradation and Stability.* **2018,** *158,* 228-237.

and temperature[28–30]. It was demonstrated that degradation becomes a bulk process above the glass transition temperature, T_g, while at temperatures below T_g, degradation of the polymer matrix is restricted to its surface[31,32].

Recent work in our group showed that substantial improvements in the melt strength, crystallization properties, foaming, and strain hardening characteristics of PLA can be achieved by introducing branching through solvent-free, peroxide-initiated grafting of the multi-functional co-agent triallyl trimesate (TAM)[33–35]. However, the effects of this promising and industrially relevant modification on the degradability of PLA have not been studied. In this work, this is achieved by examining the evolution of molar mass distributions, mass, and thermal properties as a function of the degradation time. To further facilitate interpretation, the degradation profiles for branched and nucleated PLAs obtained by conventional means are compared to those obtained for TAM-modified formulations.

3.2 Materials and Methods

3.2.1 Materials

PLA 3251D, designated as PLA1 (MFI 35g·10 min^{-1} at 190°C / 2.16 kg, injection molding grade) was obtained from Natureworks®. PLA 2500HP, also obtained from Natureworks®, and designated as PLA2 (MFI 8 g·10 min^{-1} at 210°C / 2.16 kg, extrusion grade), is a high molar mass linear material, used for comparison with the reactively modified PLA1 formulations. Joncryl® ADR 4368, a multifunctional epoxide styrene-acrylic oligomeric chain extender with glycidyl methacrylate (GMA) functionality of 9, epoxy equivalent weight of 285 g·mol^{-1}, and molar mass of 6800 g·mol^{-1}, was supplied by BASF®. Boron Nitride (BN) powder (CarboTherm®, Grade CTP 05) was obtained from Saint-Gobain Ceramics and used as a nucleating agent. DCP (98% purity, Sigma-Aldrich), TAM (98% purity, Monomer-Polymer and Dajac Labs), and tetrahydrofuran (THF, HPLC grade, Sigma-Aldrich) were used as received.

3.2.2 Reactive Extrusion

Reactive extrusion of TAM-modified PLA1 formulations was conducted using a twin screw co-rotating extruder (TSE, Coperion ZSK 18 ML) equipped with a strand die, water cooling bath, and pelletizer, as

described in previous work[35]. A masterbatch was prepared by coating ground PLA powder with an acetone solution containing DCP and TAM and allowing the solvent to evaporate. The masterbatch was mixed with dried PLA1 in appropriate ratios to yield the desired concentrations of DCP and TAM (0.1 wt% - 0.3 wt %). The formulations of the coagent-modified PLA are designated as PLA1/a/b where 'a' and 'b' denote the concentrations of DCP and TAM respectively, in weight percentage. The extruder operated with a temperature of 190°C throughout (170°C in the feed zone), a hopper speed of 30 min^{-1}, screw speed of 120 min^{-1}, and an average residence time of 2.5 min to allow for a complete reaction. The neat PLA samples were processed in the twin screw extruder in a similar fashion.

We have previously demonstrated that PLA-TAM contains branching, and exhibits enhanced crystallization kinetics[35]. Therefore, standards for comparison were selected by preparing samples that contain LCB only, by reacting PLA with Joncryl (GMA), a multifunctional epoxide styrene-acrylic oligomeric chain extender, and a nucleated formulation containing Boron Nitride (BN), which is a well-known nucleating agent[34]. For the preparation of PLA1/GMA, PLA1 powder was coated with an acetone solution containing 1.2 wt% GMA and the solvent was allowed to evaporate. PLA1/BN was prepared by adding 0.5 wt% BN to PLA1. Both compounds were prepared using a co-rotating DSM micro-compounder operating at 100 rpm and a temperature of 180°C with a residence time of 6 minutes.

3.2.3 Specimen Preparation

Thin films with a thickness of 200 μm were prepared for the hydrolytic degradation tests by compression molding for 5 minutes using a Carver hydraulic press at 180°C and cooling rapidly in a room temperature press below the T_g. Prior to molding, pellets of each formulation were dried for 24 h under vacuum at a temperature of 60°C. The compression molding procedures were designed to minimize the impact of thermal degradation and remained consistent between each formulation.

3.2.4 Hydrolytic Degradation Tests

Long-term hydrolytic degradation tests were conducted at 60°C in a Thermo Scientific Forma 3911 environmental chamber. Individual films with dimensions of 1x3 cm^2 and a thickness of 200 μm were

placed in labelled and tared scintillation vials containing 20 ml of phosphate buffer solution (PBS) with a pH of 7.3. PBS was used to minimize the changes in pH throughout the study. Every week, two samples per formulation were extracted and the PBS was replaced for all remaining vials. The total duration of the study was 12 weeks (84 days). Photographs of the degraded films were taken after drying for 24 h under vacuum at 60°C.

3.2.5 Mass Loss

Mass loss measurements were carried out by weighing the samples after extraction. Each extracted vial was dried for 24 h under vacuum at 60°C. The mass of the sample was determined by subtracting the original tare of each vial and mass loss was calculated using Equation 3.1:

$$Mass\ Loss = \frac{M_i - M_f}{M_i} \times 100\% \tag{3.1}$$

where M_i is the initial mass of the sample and M_f is the final mass of the degraded sample extracted at each time period.

3.2.6 Gel Permeation Chromatography (GPC)

GPC characterization of the starting samples, and samples obtained after one week of hydrolytic exposure was performed using a Viscotek 270 max separation module equipped with triple detectors: differential refractive index (DRI), viscosity (IV), and light scattering (low angle, LALS and right angle, RALS). The separation module was maintained at 40°C and contained two porous PolyAnalytik columns in series with an exclusion molar mass limit of $20x10^6$ g·mol^{-1}. HPLC grade THF was used as the eluent at a flow rate of 1 ml·min^{-1}. Due to the drastic drop in molar mass, characterization of Week 2-Week 12 samples was performed using a Waters 2960 separation module connected to a Waters 410 differential refractometer (DRI) which allowed for better detection of low molar masses. Four Styragel columns were maintained at 35°C with HPLC grade THF as the eluent at a flow rate of 0.3 ml·min^{-1}. The DRI detector was calibrated by polystyrene standards with narrow dispersities over the range of 300-850,000 g·mol^{-1}. Samples were prepared for GPC analysis by dissolving a PLA film cross-section in THF to achieve solutions with

concentrations of 5 mg·ml^{-1} and 2 mg·ml^{-1} for the Viscotek and Waters machines respectively. Dissolved samples were filtered using Chromspec 13 mm UV syringe filters with a 0.22 µm pore size.

3.2.7 Differential Scanning Calorimetry (DSC)

DSC measurements were obtained using a DSC Q1000 by TA Instruments. Samples weighing 5-10 mg were sealed in aluminum hermetic pans and heated to 210°C at a rate of 5°C·min^{-1}. After the first heating, each sample was held isothermally at 210°C for 3 minutes before cooling at a rate of 5°C·min^{-1} to -30°C, to accurately determine the crystallization onset and peak. The second heating scanned from -30°C to 210°C at a rate of 5°C·min^{-1}. The percent crystallinity of each polymer formulation, χ_c, was calculated using Equation 3.2:

$$\chi_c = \frac{\Delta H_m - \Delta H_{cc}}{\Delta H_{100}} \times 100 \tag{3.2}$$

where ΔH_m is the enthalpy of melting, ΔH_{cc} is the enthalpy of cold crystallization, and ΔH_{100} is the theoretical enthalpy of melting for a 100% crystalline polymer, which is 93 J·g^{-1} for PLA[36].

3.3 Results

The formulations investigated in this work present a range of properties and structures. PLA1 and PLA2 are unmodified, linear grades, having low and high molar mass respectively. TAM-modified PLA formulations are nucleated and have long-chain branching, with a range of molar masses depending on the concentration of coagent used[34,35]. BN-modified PLA is nucleated, while GMA-modified PLA is branched. The range of PLA formulations used in this work allows the effects of branching and nucleation on the hydrolysis profile of PLA to be assessed.

3.3.1 Mass Loss

Figure 3.1 shows the mass loss of the PLA samples as a function of the degradation time. All formulations experienced substantial loss in mass, up to 40% over the 12 week study; however, there are notable differences in the trends between modified and unmodified samples.

Irrespective of their molar mass, both the linear unmodified samples, PLA1 and PLA2 showed negligible rates of mass loss in the first 70 days of the study, followed by a high rate of loss in the last 14 days. The modified samples demonstrated a more complex profile with an induction period for the first 20 days, followed by a high rate of loss between days 20 and 30, a plateau with minimal mass loss between days 30 and 56, and a period with a high rate of loss during the final 28 days.

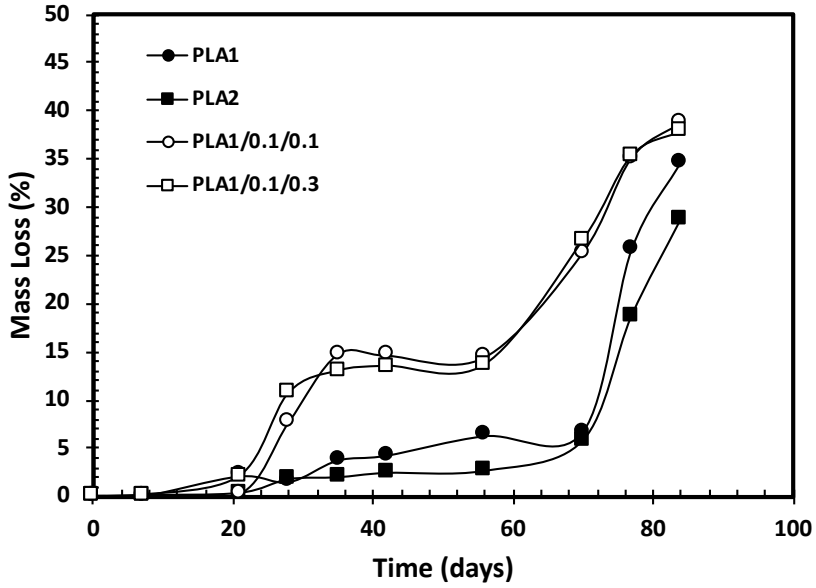

Figure 3.1: *Mass loss as a function of hydrolysis time. Lines are drawn to guide the eye.*

Although not illustrated in Figure 3.1, the branched PLA1/GMA followed similar trends to the TAM-modified PLA, whereas the nucleated PLA1/BN behaved similarly to the unmodified samples.

As degradation proceeded, the samples became progressively more brittle, with the original films being reduced to small powdered fragments over the course of the study. Figure 3.2 presents visual changes in extracted linear and branched specimens, depicting an increase in opacity as hydrolysis proceeds. Increased opacity is a known consequence of degradation and has been attributed to the increase in crystallinity of the polymer matrix[37,38]. This is further discussed in Section 3.4.3.

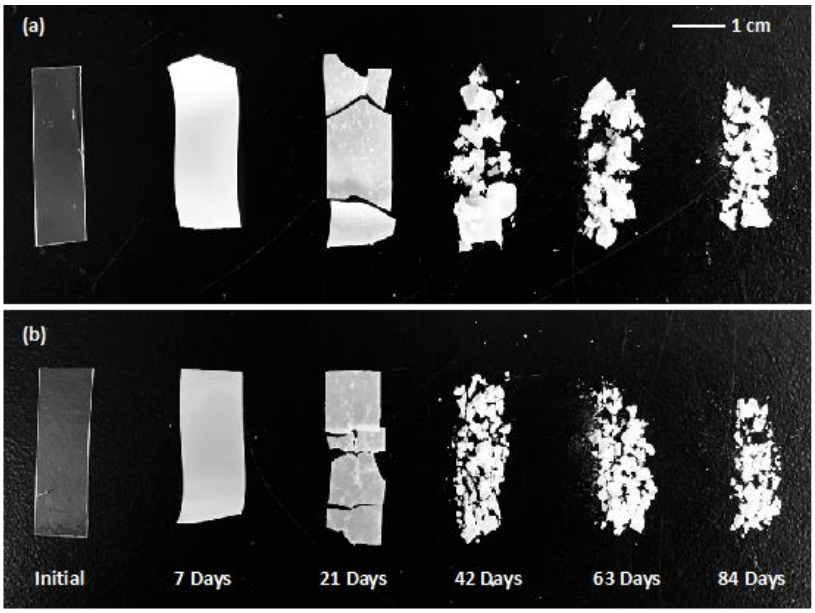

Figure 3.2: *Physical changes in PLA1 (a) and PLA1/0.1/0.3 (b) resulting from hydrolytic exposure*

3.3.2 Molar Mass Loss

The molar mass data of the starting materials, as compounded, is summarized in Table 3.1. The reaction of PLA with peroxide and coagent altered the molar mass and molar mass distributions compared with unmodified linear PLA. The formation of high molar mass fractions is evident by the significant increase in M_z from 129 kg·mol^{-1} for the neat PLA to over 600 kg·mol^{-1} in the modified formulations. Previous research has shown that TAM-modified PLA consists of two types of chain populations: linear chains which remain unreacted, and LCB structures which are generated through combination of the tri-functional coagent with the PLA macroradicals[35,39–41]. It must also be noted that TAM is prone to oligomerization reactions in the presence of free radicals, and may form highly crosslinked structures[42,43]. In the presence of peroxide and TAM, free radicals may react directly with the aliphatic unsaturated sites present in TAM rather than abstracting hydrogen from the PLA chain, favouring these side-reactions[42,43]. These free-radical pathways would contribute to the formation of complex short and long-chain TAM structures, interpenetrated with the PLA matrix[35], and thus result in a broad molar mass distribution (MMD), with distinct tails attributed to low and high molar mass fractions. This is illustrated in Figure

3.3 which presents representative MMD curves for PLA1 and PLA1/0.1/0.3, and is evident in Table 3.1, which shows that the modified samples had higher dispersity compared to the linear PLA.

Table 3.1: *Initial properties of various PLA formulations*

Sample	M_w (kg·mol^{-1})	Đ	M_z (kg·mol^{-1})	χ_C (%)
PLA1	84	1.5	129	8
PLA2	126	1.6	189	17
PLA1/0.1/0.1	156	3.0	640	52
PLA1/0.1/0.3	175	4.2	976	47
PLA1/0.3/0.1	187	4.2	1293	55
PLA1/BN	73	1.8	114	52
PLA1/GMA	159	3.1	438	2

M_w – Weight average molar mass

M_z – Z-average molar mass

Đ – Dispersity (M_w/M_n)

χ_c – Percent crystallinity determined from the second heating

Upon degradation, all the formulations experienced a shift in the MMD curve towards lower molar mass (Figure 3.3). In the modified formulations the high molar mass tail disappeared over time, indicating loss of the highly branched regions of the polymer, which are known to reside in the higher molar mass fractions[35]. The MMD curves became narrower as a result of degradation, and the dispersity was reduced, as shown in Figure 3.4. Owing to their broader initial dispersity, the branched formulations experienced a greater decrease in dispersity, from 3.0 to 1.2, compared with the linear PLA which only saw a marginal decrease in dispersity from 1.5 to 1.2.

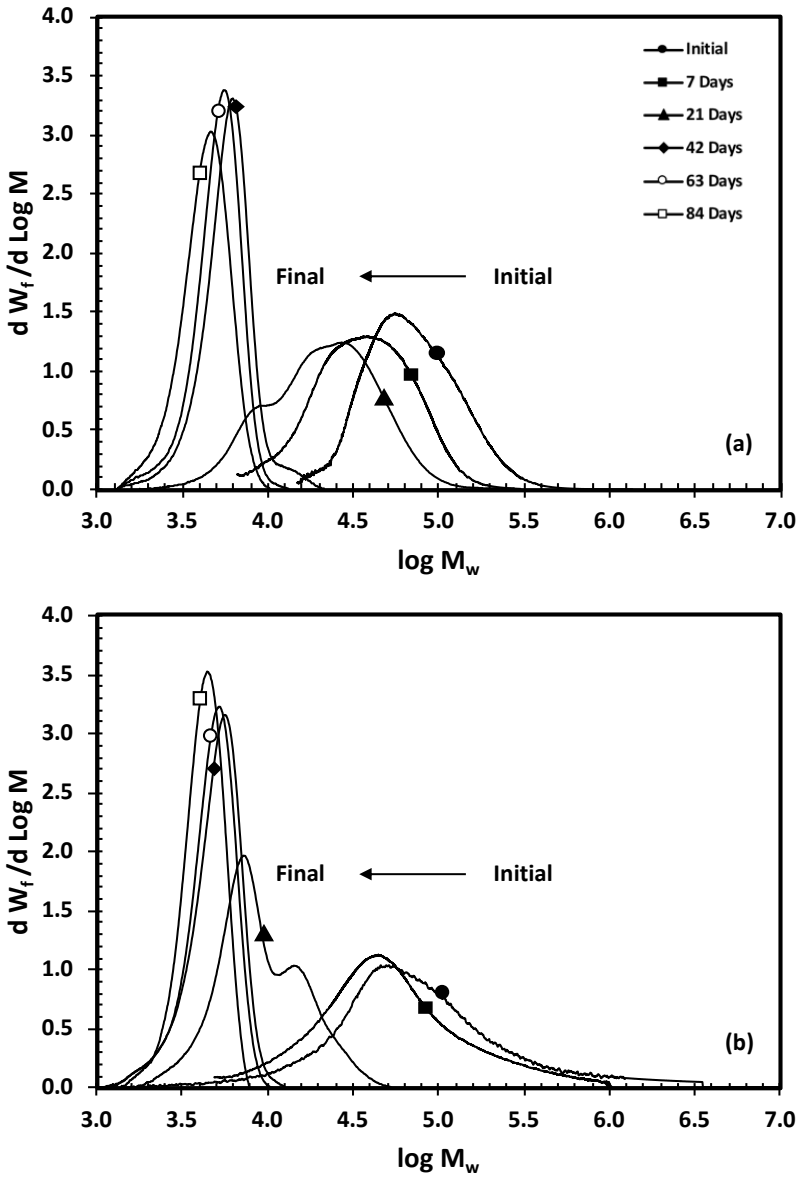

Figure 3.3: *Initial and final MMD curves for (a) PLA1 and (b) PLA1/0.1/0.3*

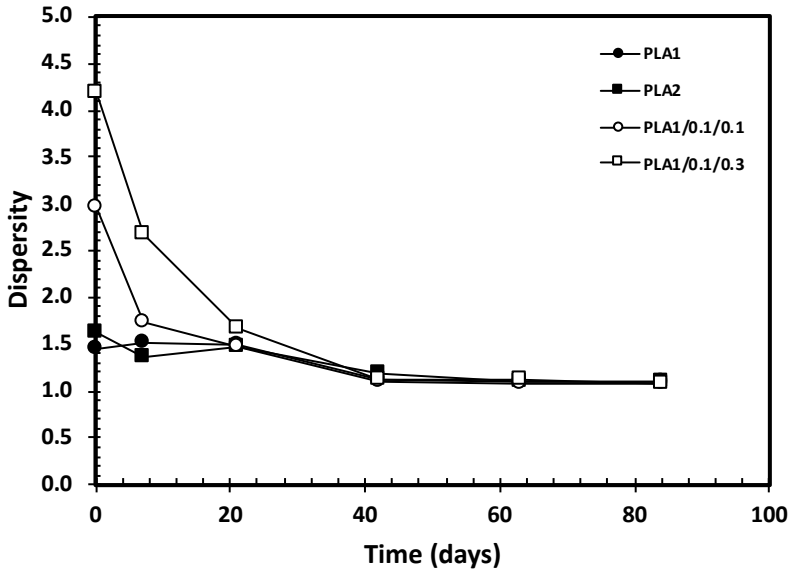

Figure 3.4: *Changes in dispersity as a function of degradation time*

Upon hydrolysis, significant decreases in molar mass averages were observed in all formulations, attributed to polymer degradation (Figure 3.5). Across all molar mass averages, the rate of loss was highest in the first three weeks, with all formulations exhibiting over 70% loss. Similar rates of loss are reported in the literature under comparable experimental conditions[14,44,45]. The final nine weeks of the study were characterized by minimal rate of change in molar mass.

Comparison of the Mz averages shown in Figure 3.5(c), reveals that the TAM-modified PLA exhibited the highest rates of loss in M_z, followed by the unmodified PLA, and lastly by the BN and GMA formulations.

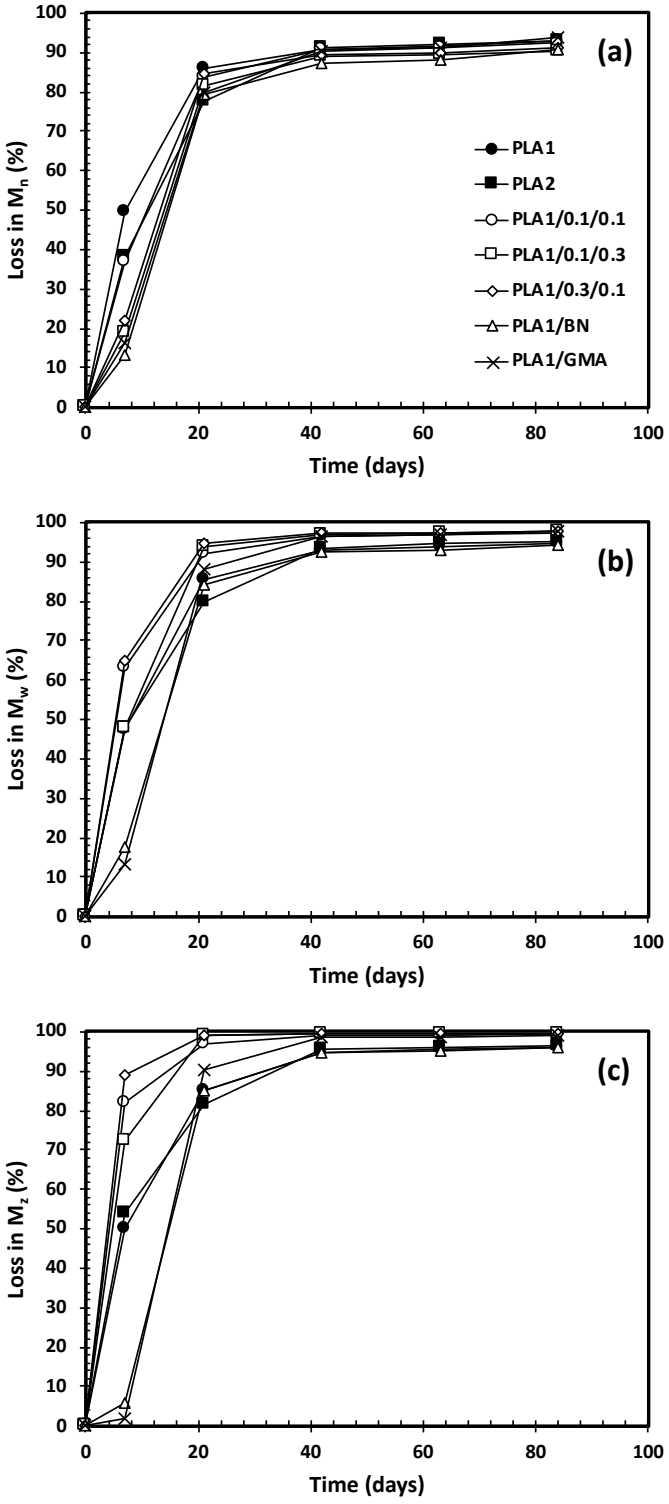

Figure 3.5: *Molar mass averages as a function of time (a) M_n; (b) M_w; and (c) M_z*

3.3.3 Thermal Properties

Figure 3.6 shows representative thermograms for PLA1 and PLA1/0.1/0.3. The rest of the modified compositions showed similar trends as the latter. The initial and final thermal properties are compared in Table 3.2.

As expected, the unmodified PLAs exhibited cold crystallization during both the first and second heating sequences (Figure 3.6). Unlike the starting materials, the degraded samples did not exhibit cold crystallization peaks in their first heating scans; however, in the second heating scan, cold crystallization peaks were observed for all unmodified and modified degraded samples (Figure 3.6). Both the cold crystallization and melting peaks shifted toward lower temperatures as hydrolysis proceeded. Additionally, broad and double melting peaks are observed which could be attributed to melting-recrystallization-remelting mechanisms or the occurrence of at least two distinct crystal populations[46].

While neat PLA did not exhibit crystallization upon cooling, sharp crystallization peaks were present in the modified PLA, along with the absence of the cold crystallization peak from the second heating scan. This is consistent with the previously reported presence of sharp crystallization peaks, and higher crystallinity of these modified materials[35]. However, the crystallization peak decreased in intensity upon degradation, and disappeared from 42 days onwards for the modified formulations, resulting in a reduction in the crystallinity of the samples upon second heating.

Degradation affects crystallinity substantially, as shown by Figure 3.7, which summarizes the crystallinity as a function of degradation time. During the first heating, an overall increase in crystallinity was observed with time (Figure 3.7(a)), while the data obtained during the second heating showed an overall decrease (Figure 3.7(b)).

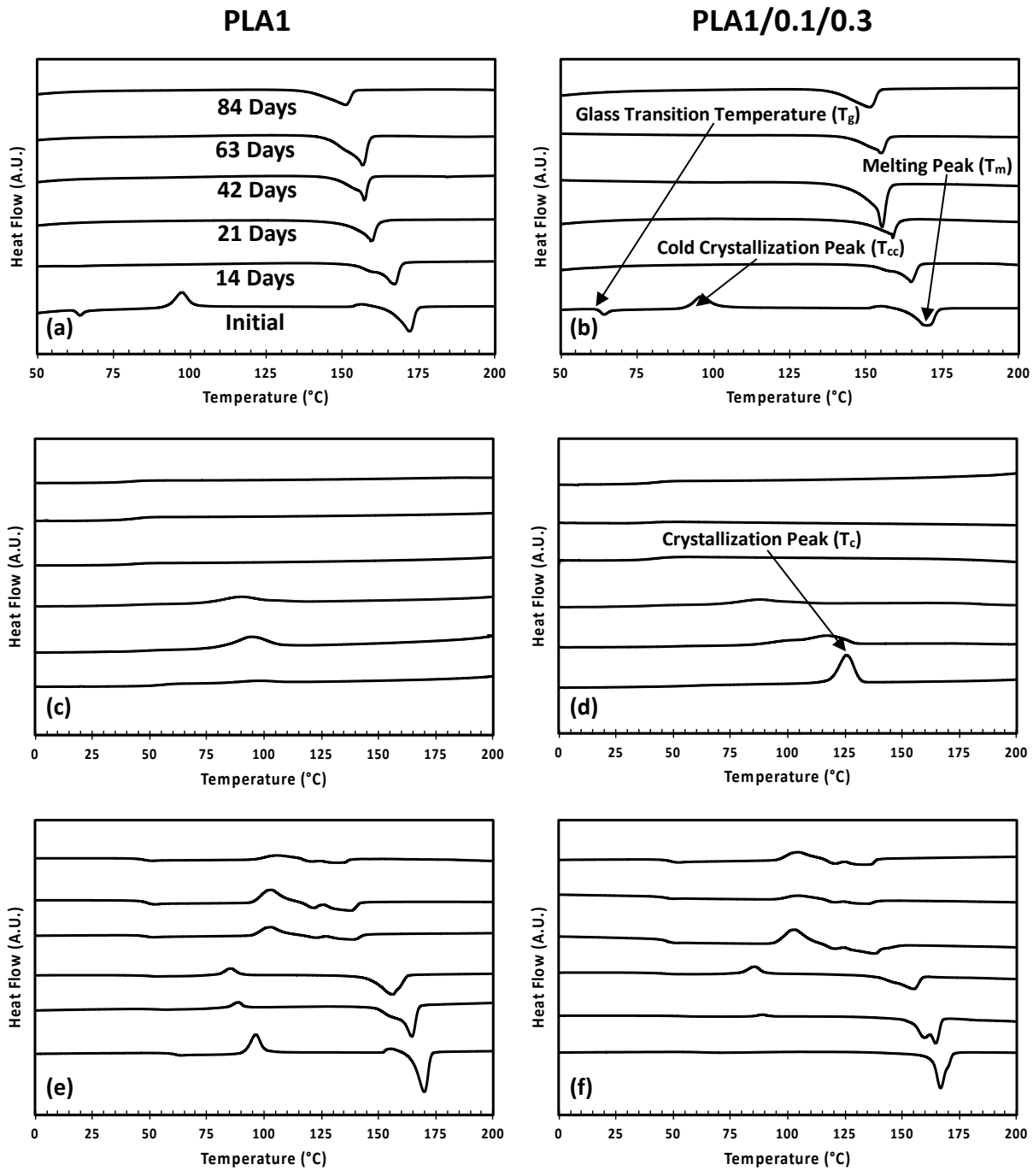

Figure 3.6: *DSC curves for PLA1 (a, c, e) and PLA1/0.1/0.3 (b, d, f). First heating (a-b), cooling (c-d), and second heating (e-f) curves are shown. Curves are shifted vertically by an arbitrary factor and exothermic peaks are up.*

Table 3.2: *Thermal properties of initial samples and final samples obtained after 84 days of degradation*

Sample	First Heating					Cooling		Second Heating			
	T_{cc1} [a]	T_{cc2} [b]	T_m [c]	T_g [d]	χ_c [e]	T_c [f]	T_{cc1}	T_{cc2}	T_m	T_g	χ_c
PLA1 (Initial)	98	157	172	62	5	-	97	155	170	59	8
PLA1 (Final)	-	-	151	-*	44	-	106	-	131	46	1
PLA2 (Initial)	94	162	180	60	8	-	96	162	178	60	17
PLA2 (Final)	-	-	160	-*	56	-	99	-	148	49	4
PLA1/0.1/0.1 (Initial)	99	157	171	62	5	123	-	-	166	59	52
PLA1/0.1/0.1 (Final)	-	-	151	-*	45	-	106	-	136	50	7
PLA1/0.1/0.3 (Initial)	98	155	170	62	14	126	-	-	167	59	47
PLA1/0.1/0.3 (Final)	-	-	151	-*	50	-	105	-	135	47	1
PLA1/BN (Initial)	96	156	171	58	2	119	-	-	167, 171	59	52
PLA1/BN (Final)	-	-	150	-*	36	-	-	-	131	45	7
PLA1/GMA (Initial)	93	154	169	59	2	94	95	154	168	59	5
PLA1/GMA (Final)	-	-	150	-*	43	-	-	-	140	42	1

[a] T_{cc1} – cold crystallization peak temperature measured in heating

[b] T_{cc2} – cold crystallization peak temperature measured in heating just before melting

[c] T_m – melting peak temperature measured in heating

[d] T_g – glass transition temperature measured in heating

[e] χ_c – percentage crystallinity

[f] T_c – crystallization peak temperature measured in cooling

* – T_g could not be detected

All temperatures are reported in °C.

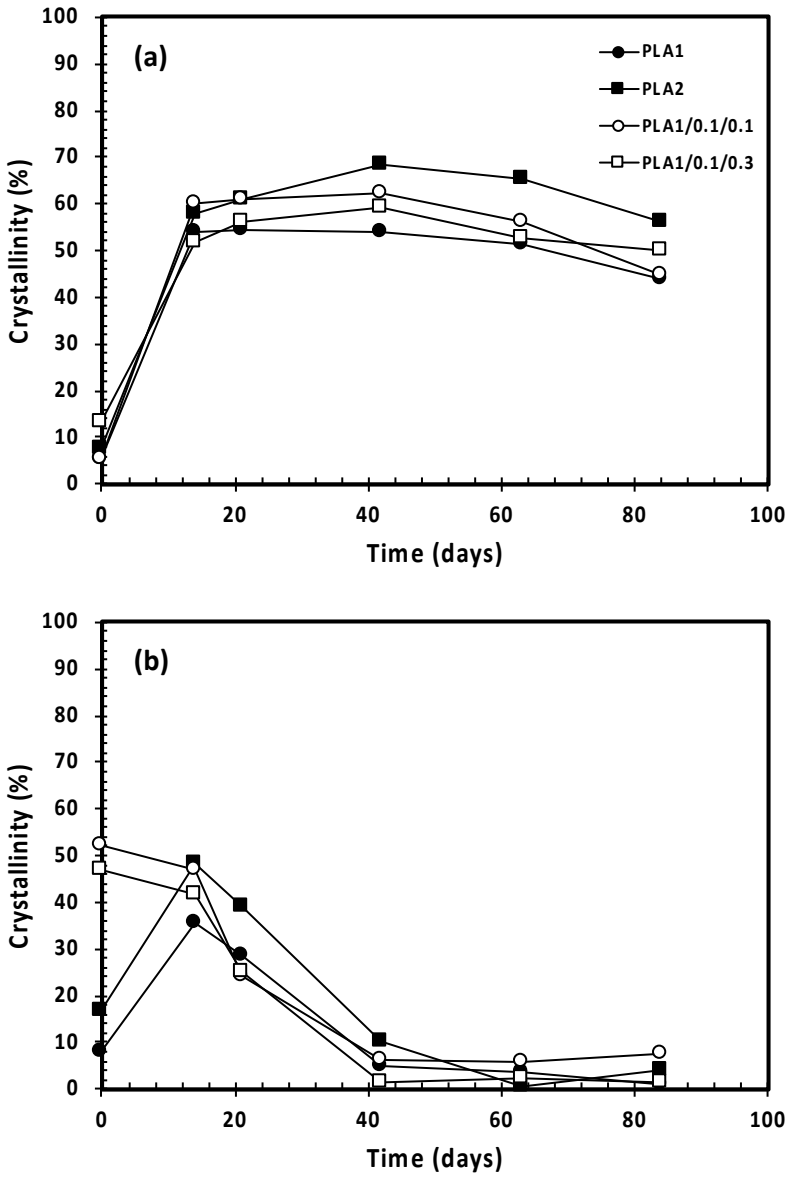

Figure 3.7: *PLA crystallinity calculated from the first heating (a) and second heating (b) scans. Lines are drawn to guide the eye*

3.4 Discussion

3.4.1 Mechanism and Kinetics of Degradation

The hydrolytic degradation of a solid polymer matrix may proceed through two alternative mechanisms: bulk (homogeneous) erosion, or surface (heterogeneous) erosion[47]. In surface eroding matrices, the rate of hydrolysis is higher than the rate of water diffusion. Degradation occurs mainly in the outermost polymer

layers before reaching the inner parts of a matrix. In contrast, bulk eroding polymers degrade slowly, with the rate of water diffusion into the system being higher than the rate of hydrolysis. This results in hydration and cleavage of polymer chains throughout the entire matrix.

Comparing molar mass loss and specimen mass loss provides insight into the predominant type of erosion mechanism. During bulk erosion, the process can be divided into two stages: in the first stage, significant molar mass decrease with minimal mass loss occurs, while in the second stage, significant mass loss takes place. In contrast, during surface erosion, significant mass loss occurs with no significant molar mass changes in the bulk. In all the PLA samples investigated in this work, comparison of Figure 3.1 and Figure 3.5 reveals that mass loss lagged behind molar mass loss, which implies that hydrolysis proceeded throughout the polymer bulk[44]. Materials which degrade through a bulk mechanism typically must reach a critical molar mass below which they are water soluble and mass loss can be observed[44]. This is substantiated by the observation that considerable mass loss only begins following the initial three weeks of rapid loss in molar mass.

The degradation of the samples through a bulk erosion mechanism is also supported by the critical device dimension ($L_{critical}$) for poly(α-hydroxy esters) such as PLA. This parameter was defined in work by von Burkersroda et al. and represents the device thickness at which the erosion mechanism of a polymer changes[48]. If the thickness of a matrix is larger than $L_{critical}$, then it will undergo surface erosion, whereas if it is smaller, bulk erosion is said to occur. The $L_{critical}$ for poly(α-hydroxy esters) is 7.4 cm[48], which is substantially larger than the sample thickness of 200 μm, pointing to a bulk mechanism. A bulk mechanism is also inferred by the MMD of the samples (Figure 3.5). With this type of erosion it is expected that changes in the shape of the curves are observed, along with an overall shift[13,49]. In all formulations, a shift in the MMD curve towards low molar mass was observed, along with a narrowing of the MMD towards the end of the study.

The scission of polymer chains during degradation is reflected by changes in the number-average molar mass, M_n. A number of relationships have been derived relating the changes in M_n to the hydrolysis rate

of the ester linkages[50]. A model accounting for the possibility of autocatalysis by the generated carboxylic acid end groups is described by Equation 3.3:

$$M_n(t) = M_n\,(t_0)e^{-kt} \tag{3.3}$$

where $M_n\,(t)$ is the number average molar mass at any time, $M_n\,(t_0)$ is the initial number average molar mass before hydrolytic degradation, k is the hydrolytic degradation rate constant, and t is time.

The values for the hydrolytic degradation rate constant (k) can be calculated from the evolution of logarithmic M_n values as a function of degradation time (Figure 3.8). Table 3.3 presents the hydrolytic degradation rate constants for all formulations used in this study.

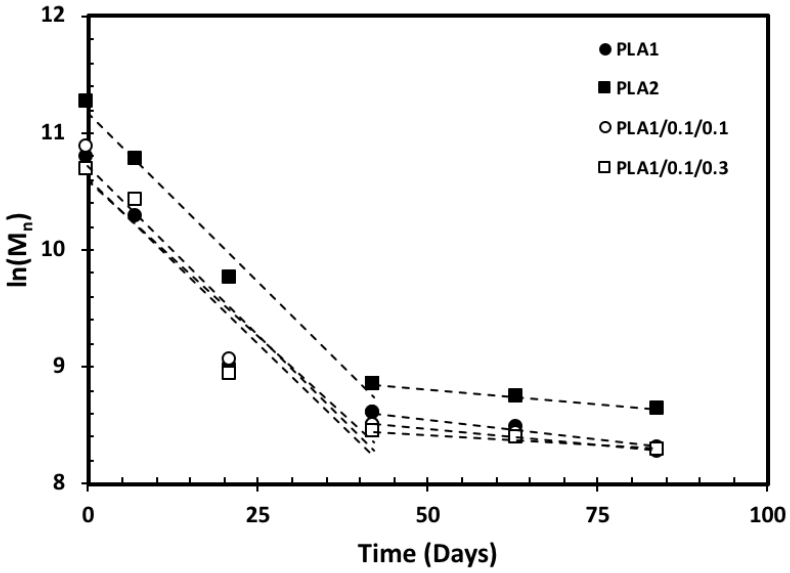

Figure 3.8: *Logarithmic number average molar mass during degradation*

Since the rate of loss in M_n differs between the periods of 0-42 days and 42-84 days, the k values were evaluated separately for these two periods (Table 3.3) and are comparable in magnitude to the rate constant values found in literature[24,51–54]. The k values for all formulations were higher during early degradation and correlate with the significant loss in M_n from 0-42 days (Figure 3.5(a)). The lower k values found for 42-84 days coincide with the minimal molar mass loss observed during the second half of the study. The rate constants among all formulations are comparable and decrease with degradation time. This suggests that the linear chains, which are present in both starting and modified PLA and are

represented by M_n, exhibit similar degradation kinetics. Hence the overall differences in the degradation profiles seen in Figure 3.1 stem from the presence of LCB in the modified formulations. This is further analyzed below.

Table 3.3: *Hydrolytic degradation rate constants for various timeframes during the study*

Sample	$k \cdot 10^{-3}$ (Days^{-1})	
	0-42 Days	**42-84 Days**
PLA1	53	7
PLA2	58	5
PLA1/0.1/0.1	58	5
PLA1/0.1/0.3	57	4
PLA1/0.3/0.1	58	4
PLA1/BN	53	8
PLA1/GMA	59	10

3.4.2 Mass Loss of Linear and LCB PLA

As PLA undergoes hydrolysis, changes in the mechanical properties, thermal properties, molar mass, and specimen mass take place[13,14,16,52,55,56]. These changes are strongly affected by the temperature of the degradation environment, which influences the chain mobility, especially close to the glass transition temperature, T_g. The temperature of 60°C used in this study is slightly above the T_g of PLA which allows measurable data to be obtained and is comparable to temperatures used in relevant standards[57,58] and literature[16,17,45,51,52].

PLA hydrolysis is a three-phase process comprised of: i) diffusion of water into the polymeric bulk, ii) hydrolysis reaction, iii) counter-diffusion of reaction products (ie. carboxylic acids, alcohols, oligomers, etc)[52]. These phases resulted in distinct degradation stages, which were unique to linear and branched PLA, as shown in Figure 3.9.

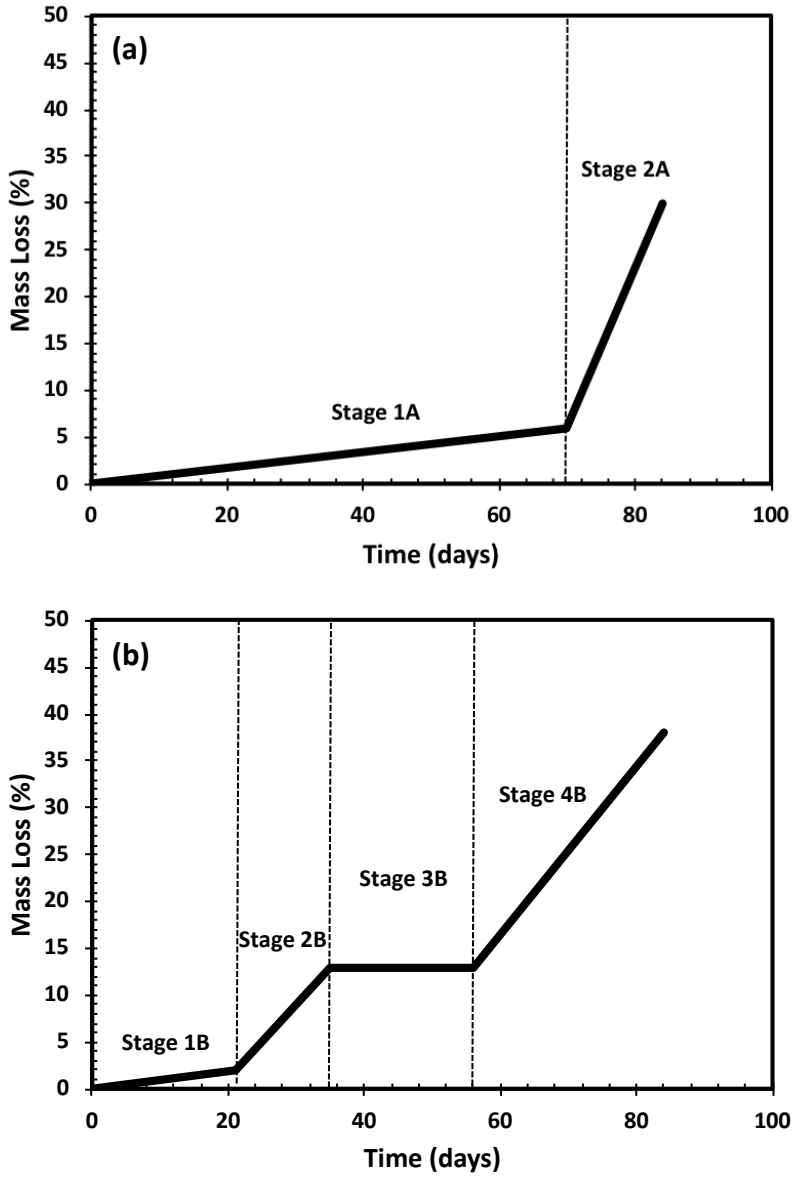

Figure 3.9: *Schematic depicting the phases of mass loss in linear PLA (a) and LCB PLA (b)*

Mass loss during hydrolytic degradation is caused by the formation of water-soluble low molar mass fragments through chain cleavage[53]. For mass loss to be recorded, these fragments must be released from the materials by counter-diffusion. The time-scale for this to happen can span the course of weeks, resulting in the prolonged induction period seen in the linear, unmodified PLA (Stage 1A in Figure 3.9(a)). During that time-frame, all molar mass averages decreased drastically (Figure 3.5). The rapid loss in mass illustrated by Stage 2A in Figure 3.9(a), signifies that the water soluble, low molar mass reaction products have counter-diffused and have been released from the material. This is consistent with

literature reports for neat PLA, where an initial period of low mass loss rates is observed, followed by higher rates of loss after significant hydrolytic exposure times with a total loss of approximately 40-50%[14,55].

On the other hand, in addition to an initial plateau, the modified PLAs demonstrated a complex profile illustrated by Figure 3.9(b). An induction period is observed (Stage 1B), which is clearly associated with the time needed for the diffusion of water into the polymer bulk, followed by a high rate of loss (Stage 2B), a plateau with minimal mass loss (Stage 3B), and finally a period with a high rate of loss (Stage 4B). The latter has a slope that is similar to the unmodified material and is associated with the counter-diffusion of the reaction products.

The degradation profile is expected to depend on properties such as the crystallinity and the architecture of the polymer chains. The PLA1/TAM samples differ from the unmodified parent material in both their molar mass distributions (Figure 3.5) and in their crystallinity (Table 3.1). We note that the degradation profile of the PLA1/BN samples, which also have higher crystallinity, did not differ compared to the neat PLA1. On the other hand, the branched PLA1/GMA, behaved similar to PLA1/TAM, even though its crystallinity is similar to that of the linear PLA1 (Table 3.1). This suggests that the branched chain architecture is primarily responsible for the changes in the degradation behavior.

As shown in Figure 3.3(b), LCB PLA has a broad MMD, with pronounced tails both in the low and high molar mass region. The first region of mass loss in LCB PLA (Stage 2B in Figure 3.9(b)) appears to be associated with the disappearance of the low molar mass fractions of the polymer chains (as revealed by comparing Figure 3.3(b) to Figure 3.3(a)). The degradation of these segments would result in low molar mass oligomers, which would readily diffuse out of the polymer resulting in the initial phase of rapid degradation. On the other hand, unmodified PLA, which is comprised of linear chains and does not have the same low molar mass fractions imparted from modification as the branched PLA, experiences minimal mass loss in the same time frame.

Furthermore, branched PLA would contain a higher number of chain ends compared to the unmodified linear polymers. It has been found that the carboxyl end group in PLA plays a crucial role in

degradation[56]. An increase in the number of branches (chain ends) in PLA results in enhanced hydrolyzability[59]. The elevated rate of hydrolysis in LCB structures can be attributed to the hydrophilicity of carboxyl groups helping to attract more water molecules, and the higher number of terminal hydroxyl groups around which cleavage of the ester groups occurs[53]. The larger numbers of carboxylic chain ends may also hinder close packing, further facilitating water penetration and counter-diffusion of oligomers[60]. Therefore, it is evident that the branching architecture and the increased number of terminal hydroxyl groups in the modified samples contributed to an enhanced initial hydrolytic degradation rate[53,60].

Once the initial phase of loss of low and high molar mass oligomers is complete in the branched formulations, the rest of the material follows closely the trends of the linear PLAs, consistent with the degradation profile that would be expected for the remaining mostly linear chains. Examining the trends shown in the molar mass distributions of Figure 3.5, we also note that the almost complete loss in the M_z of the branched samples occurs within the first 10 days. Since hydrolysis of ester bonds of PLA occurs randomly, longer chains with high molar mass would be more susceptible to cleavage than shorter chains[61], explaining the susceptibility of the high molar mass fractions to degradation. Furthermore, it is worth noting that in Figure 3.5(c), the TAM-modified PLA experienced a much higher rate of loss in M_z compared to all other formulations, including PLA1/GMA, even though the latter also contains branching. This trend points to an influence of TAM structures on hydrolysis. Owing to the free-radical mechanism, TAM-modified PLA consists of mixtures of linear and highly branched chains. It is also possible that complex LCB TAM structures, interpenetrated with the PLA matrix, exist[35]. The TAM-grafted chains and TAM-structures, which are primarily present in the higher molar mass fractions appear to be more susceptible to degradation than the unmodified, linear chains.

3.4.3 Thermal Properties

This work confirmed previous findings that hydrolytic degradation affects substantially the thermal properties of PLA[13,16,17,44,52,55]. Upon prolonged hydrolysis, the cold crystallization peak disappeared while a strong melting peak remained present in the first heating scan (Figure 3.6). This resulted in a higher

crystallinity of the degraded materials based on Equation 3.2 and was indicative of the transformation of amorphous regions into crystalline phases[17]. Double melting peaks similar to those present in the degraded PLA samples, have been observed in other work, attributed both to lamellar rearrangement and the melting of hydrolytic degradation products of PLA[16,17].

The samples exhibited increases in the degree of crystallinity of over 200% during the first 20 days (Figure 3.7(a)). The increase in crystallinity is generally attributed to the crystallization of the amorphous parts and/or erosion of the amorphous parts and explains the increase in the opacity of the samples shown in Figure 3.2[52]. Hydrolysis of semi-crystalline PLA is expected to initially proceed in the amorphous regions, transforming these domains to crystalline phases[17]. Eventually, the crystallinity may decrease if the degradation process is extended beyond the total hydrolysis of the amorphous regions[17]. An increase in crystallinity can also be attributed to the shortening of polymer chains which results in enhanced mobility, allowing the chains to rearrange into a more crystalline structure.

In this work we show that the strong increase in crystallinity with time from the first heating scan (Figure 3.7(a)), can also be attributed to the conditioning during the hydrolytic degradation experiments. Given that this study was conducted at 60°C, slightly above the T_g of PLA, the conditions were similar to exposing the samples to annealing, which would allow the polymer chains to crystallize as they gain mobility. Enhanced crystallization may also be attributed to the plasticizing effect of water [52]. On the other hand, the second heating scan, which eliminates the previous thermal history, shows an overall decrease in crystallinity for all samples (Figure 3.7(b)), thus proving that the increase in the crystallinity was attributed the hydrolysis conditions only.

We further undertook a separate short-term study to differentiate the effects of plasticizing, due to the presence of water, and annealing, due to the conditioning above T_g, on the crystallinity of the samples. Unmodified PLA1 and modified PLA1/0.1/0.3 were maintained in two environments: water at room temperature and air at 60°C, which were chosen to simulate the effects of plasticizing and annealing, respectively. For a duration of three weeks, the same procedures used for the full-scale degradation experiment were implemented, and DSC was performed on the extracted samples to evaluate any

changes. Table 3.4 shows the changes in thermal properties observed in PLA1/0.1/0.3 after 3 weeks. This data is representative of similar changes seen in PLA1.

In the presence of water at 20°C, the changes in the thermal properties were minimal. Dry conditioning at 60°C resulted in substantial changes, with a crystallinity increase of over 200% compared to the initial material, proving the overwhelming effect of annealing. These changes are even more pronounced when facilitated by the plasticizing effect of water at this temperature, such as the conditions of the 12-week study. These findings prove that the increase in crystallinity as hydrolysis proceeds can be attributed to a combined annealing and plasticizing effect and it is thus dependent on the conditions of the degradation experiments.

Table 3.4: *Thermal properties of PLA1/0.1/0.3 at various conditions*

Sample	First Heating					Cooling	Second Heating			
	T_{cc1} [a]	T_{cc2} [b]	T_m [c]	T_g [d]	χ_c [e]	T_c [f]	T_{cc1}	T_m	T_g	χ_c
Initial Material	98	155	170	62	14	126	-	167	59	47
Water at 20°C	88	152	168	59	17	133	-	168	59	55
Air at 60°C	-	151	169	-	43	133	-	168	59	55
Water at 60°C	-	-	159	-	56	-	86	141	44	25

[a] T_{cc1} – cold crystallization peak temperature measured in heating

[b] T_{cc2} – cold crystallization peak temperature measured in heating just before melting

[c] T_m – melting peak temperature measured in heating

[d] T_g – glass transition temperature

[e] χ_c – percentage crystallinity

[f] T_c – crystallization peak temperature measured in cooling

All temperatures are reported in °C.

3.5 Conclusions

This study investigated the effects of long-chain branching through TAM-modification on the hydrolytic degradation of PLA at 60°C. Within a 12-week time frame, linear and branched samples experienced substantial degradation, with notable losses in mass, molar mass, structural integrity, and changes in thermal properties.

A comparison of mass loss and molar mass loss profiles suggested a bulk mechanism as the predominant erosion phenomenon for all formulations. Additionally, increases in crystallinity were caused by the combined effects of annealing and plasticizing at the given experimental conditions. Hydrolytic degradation caused significant reductions in molar mass (>90%) along with narrowing of the molar mass distributions within the first 20 days of exposure.

The mass loss profiles of the modified formulations differed from those of the neat PLA due to the preferential degradation of low and high molar mass segments from the polymer chains and counter-diffusion of the resulting oligomers. These results demonstrated that reactive modification of PLA to introduce LCB did not hinder the hydrolytic degradation of PLA, thus making this modification approach highly promising for various commodity applications that would benefit from the use of degradable biopolyesters.

3.6 References

(1) Garlotta, D. *J. Polym. Environ.* **2001**, *9* (2), 63.

(2) Dorgan, J. R.; Williams, J. S.; Lewis, D. N. *J. Rheol. (N. Y. N. Y).* **1999**, *43* (5), 1141.

(3) Rasal, R. M.; Janorkar, A. V; Hirt, D. E. *Prog. Polym. Sci.* **2010**, *35* (3), 338.

(4) Dorgan, J. R.; Lehermeier, H.; Mang, M. *J. Polym. Environ.* **2000**, *8* (1), 1.

(5) Dorgan, J. R.; Janzen, J.; Clayton, M. P.; Hait, S. B.; Knauss, D. M. *J. Rheol. (N. Y. N. Y).* **2005**, *49* (3), 607.

(6) Palade, L.-I.; Lehermeier, H. J.; Dorgan, J. R. *Macromolecules* **2001**, *34* (5), 1384.

(7) Lim, L.-T.; Auras, R.; Rubino, M. *Prog. Polym. Sci.* **2008**, *33* (8), 820.

(8) Di, Y.; Iannace, S.; Di Maio, E.; Nicolais, L. *Macromol. Mater. Eng.* **2005**, *290* (11), 1083.

(9) Pilla, S.; Kramschuster, A.; Yang, L.; Lee, J.; Gong, S.; Turng, L.-S. *Mater. Sci. Eng. C* **2009**, *29* (4), 1258.

(10) Corre, Y.-M.; Maazouz, A.; Duchet, J.; Reignier, J. *J. Supercrit. Fluids* **2011**, *58* (1), 177.

(11) Mihai, M.; Huneault, M. A.; Favis, B. D. *Polym. Eng. Sci.* **2010**, *50* (3), 629.

(12) Takamura, M.; Nakamura, T.; Takahashi, T.; Koyama, K. *Polym. Degrad. Stab.* **2008**, *93* (10), 1909.

(13) Iñiguez-Franco, F.; Auras, R.; Ahmed, J.; Selke, S.; Rubino, M.; Dolan, K.; Soto-Valdez, H. *Polym. Test.* **2018**, *67*, 190.

(14) Dong, W.; Zou, B.; Yan, Y.; Ma, P.; Chen, M. *Int. J. Mol. Sci.* **2013**, *14* (10), 20189.

(15) Elsawy, M. A.; Kim, K.-H.; Park, J.-W.; Deep, A. *Renew. Sustain. Energy Rev.* **2017**, *79*, 1346.

(16) Huang, Y.; Zhang, C.; Pan, Y.; Zhou, Y.; Jiang, L.; Dan, Y. *Polym. Degrad. Stab.* **2013**, *98* (5), 943.

(17) Ndazi, B. S.; Karlsson, S. *Express Polym. Lett.* **2011**, *5* (2), 119.

(18) Gogolewski, S.; Jovanovic, M.; Perren, S. M.; Dillon, J. G.; Hughes, M. K. *J. Biomed. Mater. Res.* **1993**, *27* (9), 1135.

(19) Li, S. M.; Garreau, H.; Vert, M. *J. Mater. Sci. Mater. Med.* **1990**, *1* (3), 123.

(20) Li, S. M.; Garreau, H.; Vert, M. *J. Mater. Sci. Mater. Med.* **1990**, *1* (4), 198.

(21) Li, S. M.; Garreau, H.; Vert, M. *J. Mater. Sci. Mater. Med.* **1990**, *1* (3), 131.

(22) Hocking, P. J.; Timmins, M. R.; Scherer, T. M.; Fuller, R. C.; Lenz, R. W.; Marchessault, R. H. *J. Macromol. Sci. Part A* **1995**, *32* (4), 889.

(23) Holland, S. J.; Jolly, A. M.; Yasin, M.; Tighe, B. J. *Biomaterials* **1987**, *8* (4), 289.

(24) Lyu, S.; Schley, J.; Loy, B.; Lind, D.; Hobot, C.; Sparer, R.; Untereker, D. *Biomacromolecules* **2007**, *8* (7), 2301.

(25) Hakkarainen, M. In *Degradable Aliphatic Polyesters*; Springer Berlin Heidelberg: Berlin, Heidelberg, 2002; Vol. 157, pp 113–138.

(26) Tsuji, H.; Ikada, Y. *Polym. Degrad. Stab.* **2000**, *67* (1), 179.

(27) Tsuji, H.; Miyauchi, S. *Polym. Degrad. Stab.* **2001**, *71* (3), 415.

(28) Vert, M.; Schwarch, G.; Coudane, J. *J. Macromol. Sci. Part A* **1995**, *32* (4), 787.

(29) Shih, C. *J. Control. Release* **1995**, *34* (1), 9.

(30) Gilding, D. K.; Reed, A. M. *Polymer (Guildf).* **1979**, *20* (12), 1459.

(31) Agrawal, C.; Huang, D.; Schmitz, J. P.; Athanasiou, K. A. *Tissue Eng.* **1997**, *3* (4), 345.

(32) Aso, Y.; Yoshioka, S.; Li Wan Po, A.; Terao, T. *J. Control. Release* **1994**, *31* (1), 33.

(33) Nerkar, M.; Ramsay, J. A.; Ramsay, B. A.; Kontopoulou, M. *Macromol. Mater. Eng.* **2014**, *299* (12), 1419.

(34) Tiwary, P.; Park, C. B.; Kontopoulou, M. *Eur. Polym. J.* **2017**, *91*, 283.

(35) Tiwary, P.; Kontopoulou, M. *ACS Sustain. Chem. Eng.* **2018**, *6* (2), 2197.

(36) Fischer, E. W.; Sterzel, H. J.; Wegner, G. *Kolloid-Zeitschrift und Zeitschrift für Polym.* **1973**, *251* (11), 980.

(37) Jarerat, A.; Tokiwa, Y. *Macromol. Biosci.* **2001**, *1* (4), 136.

(38) Torres, A.; Li, S. M.; Roussos, S.; Vert, M. *J. Appl. Polym. Sci.* **1996**, *62* (13), 2295.

(39) Fang, H.; Zhang, Y.; Bai, J.; Wang, Z.; Wang, Z. *RSC Adv.* **2013**, *3* (23), 8783.

(40) Wang, Y.; Yang, L.; Niu, Y.; Wang, Z.; Zhang, J.; Yu, F.; Zhang, H. *J. Appl. Polym. Sci.* **2011**, *122* (3), 1857.

(41) You, J.; Lou, L.; Yu, W.; Zhou, C. *J. Appl. Polym. Sci.* **2013**, *129* (4), 1959.

(42) Wu, W.; Parent, J. S.; Sengupta, S. S.; Chaudhary, B. I. *J. Polym. Sci. Part A Polym. Chem.* **2009**, *47* (23), 6561.

(43) El Mabrouk, K.; Parent, J. S.; Chaudhary, B. I.; Cong, R. *Polymer (Guildf).* **2009**, *50* (23), 5390.

(44) Zhang, X.; Espiritu, M.; Bilyk, A.; Kurniawan, L. *Polym. Degrad. Stab.* **2008**, *93* (10), 1964.

(45) Fukushima, K.; Tabuani, D.; Dottori, M.; Armentano, I.; Kenny, J. M.; Camino, G. *Polym. Degrad. Stab.* **2011**, *96* (12), 2120.

(46) Schick, C. *Anal. Bioanal. Chem.* **2009**, *395* (6), 1589.

(47) Siepmann, J.; Gopferich, A. *Adv. Drug Deliv. Rev.* **2001**, *48* (2–3), 229.

(48) Burkersroda, F. von; Schedl, L.; Göpferich, A. *Biomaterials* **2002**, *23* (21), 4221.

(49) Tsuji, H.; Saeki, T.; Tsukegi, T.; Daimon, H.; Fujie, K. *Polym. Degrad. Stab.* **2008**, *93* (10), 1956.

(50) Pitt, C. G.; Zhong-wei, G. *J. Control. Release* **1987**, *4* (4), 283.

(51) Höglund, A.; Odelius, K.; Albertsson, A.-C. *ACS Appl. Mater. Interfaces* **2012**, *4* (5), 2788.

(52) Gorrasi, G.; Pantani, R. *Polym. Degrad. Stab.* **2013**, *98* (5), 1006.

(53) Tsuji, H.; Hayashi, T. *J. Appl. Polym. Sci.* **2015**, *132* (20), 41983.

(54) Saha, S. K.; Tsuji, H. *Polym. Degrad. Stab.* **2006**, *91* (8), 1665.

(55) Mitchell, M. K.; Hirt, D. E. *Polym. Eng. Sci.* **2015**, *55* (7), 1652.

(56) de Jong, S. J.; Arias, E. R.; Rijkers, D. T. S.; van Nostrum, C. F.; Kettenes-van den Bosch, J. J.; Hennink, W. E. *Polymer (Guildf).* **2001**, *42* (7), 2795.

(57) ASTM Standard D5338. *Determining Aerobic Biodegradation of Plastic Materials Under Controlled Composting Conditions, Incorporating Thermophilic Temperatures*; 2015.

(58) ASTM Standard D6400. *Labeling of Plastics Designed to be Aerobically Composted in Municipal or Industrial Facilities*; 2012.

(59) Numata, K.; Srivastava, R. K.; Finne-Wistrand, A.; Albertsson, A.-C.; Doi, Y.; Abe, H. *Biomacromolecules* **2007**, *8* (10), 3115.

(60) Andersson, S. R.; Hakkarainen, M.; Inkinen, S.; Sodergard, A.; Albertsson, A. *Biomacromolecules* **2012**, *13* (4), 1212.

(61) Kale, G.; Auras, R.; Singh, S. P. *J. Polym. Environ.* **2006**, *14* (3), 317.

Chapter 4

Improvements in the crystallinity and mechanical properties of PLA by nucleation and annealing[†]

4.1 Introduction

As a result of significant research and development efforts, PLA is becoming the sustainable material of choice for applications such as packaging, fibers, and other commodity materials which traditionally use petroleum-based polymers[1–3]. However, widespread adoption of PLA in industry is significantly hindered by its inherent slow crystallization kinetics[4,5], low melt strength[4,6–8], poor mechanical properties[1,5], and low heat deflection temperature (HDT)[2,3]. The high cooling rates used in conventional polymer processing techniques are not conducive to the development of significant crystallinity in PLA, thus necessitating extra annealing steps. This contributes to increased cycle times and higher production costs, along with difficulty in the demolding and ejection of parts[9–11], therefore restricting PLA from use in conventional polymer processing applications, such as injection molding, blow molding, and film processing[2,3,12].

Due to a growing demand for sustainable materials, many manufacturers seek to use PLA in more durable and high heat applications. As a result, there is a pressing need to develop strategies to overcome its inherent limitations. Common approaches include block copolymerization, chemical modification, and the use of nucleating agents, plasticizers, blends, and chain extenders[13]. The incorporation of a nucleating agent is one of the most economical and widely used methods for accelerating the crystallization process and increasing the crystallinity content of PLA[9].

Nucleating agents can be categorized into two types: i) those which remain as dispersed solid particulate in the polymer melt, such as organic dicarboxylic acid salts[14,15] and ii) those that dissolve in the polymer

[†] A version of this chapter is under review for publication: **Simmons, H.**; Tiwary, P.; Colwell, J.E.; Kontopoulou, M. Improvements in the crystallinity and mechanical properties of PLA by nucleation and annealing. *Polymer Degradation and Stability.* **2019.**

melt and phase separate during cooling to produce heterogeneous nuclei, such as sorbitol and its derivatives[16]. Upon cooling, these nucleating agents crystallize in the form of nanoscale three-dimensional fibrillar networks, which serve as nucleating sites[17–20]. It is thought that the polymer lamellae subsequently grow epitaxially on the nanofibrillar network[21,22].

Several nucleating agents for PLA such as talc[23], calcium carbonate[24], cellulose[25,26], and LAK 301, an aromatic sulphonate derivative (potassium salt of 5-sulphoisophthalic acid dimethyl ester)[9] have been reported in the literature. LAK is an organic nucleating agent which differs from the more traditional particulate fillers due to its ability to dissolve in the polymer melt, similarly to the sorbitol derivatives described above. It has been found to be highly effective in achieving property and processing improvements when combined with PLA in small amounts[9,27,28].

In addition to the use of nucleating agents, reactive modification approaches have also been employed to produce PLA containing long-chain branching (LCB), which results in improvements in the properties and processability of PLA[29–33]. Recently our group accomplished improvements in the melt strength, crystallization properties, and foaming of PLA, by employing peroxide-initiated grafting of the multi-functional co-agent triallyl trimesate (TAM) in a reactive extrusion process[34–37]. PLA modified with TAM has been shown to contain LCB, and exhibits enhanced crystallization kinetics as a result of the nucleating effect in the presence of branching and of oligomerized coagent[36]. In addition to these benefits, TAM-modification does not compromise the degradability of PLA[38]. Given the positive effects of peroxide and TAM on the properties of PLA, these components were used in a proprietary technology to develop a novel, fully bio-based nucleating agent, biofiller (BF), which consists of cross-linked PLA particles[39]. The compounding of cross-linked polymers into neat linear formulations is known to induce nucleation[39].

The remarkable crystallization properties of TAM-modified PLA[34,36], were previously demonstrated through DSC characterization, which employs controlled cooling conditions. The conditions encountered in industry differ, thus making it imperative to investigate the performance of these materials under a range of molding conditions. In this work, we investigate the thermal and mechanical properties of

compression molded PLA branched by reactive extrusion using TAM coagent, as well as PLA samples containing various amounts of the BF nucleation agent. These are compared to PLA combined with LAK, a highly effective nucleating agent. We implement post-processing annealing, to achieve further property enhancements. The effects of annealing on the hydrolytic degradation of PLA are also investigated.

4.2 Materials and Methods

4.2.1 Materials

PLA 3251D, designated as PLA (MFI 35g·10 min^{-1} at 190°C / 2.16 kg, injection molding grade, weight average molar mass of 84 $kg \cdot mol^{-1}$, dispersity of 1.5) was obtained from Natureworks®. LAK 301 was obtained from Takemoto Oil & Fat Co and used as a nucleating agent. Dicumyl peroxide, DCP (98% purity, Sigma-Aldrich), triallyl trimesate, TAM (98% purity, Monomer-Polymer and Dajac Labs), and tetrahydrofuran (THF, HPLC grade, Sigma-Aldrich) were used as received. The BF additive was prepared according to a proprietary process, by coating powdered PLA with 1 wt% DCP and 1 wt% TAM in an acetone solution and allowing the solvent to evaporate[39]. The mixture was then charged to a batch mixer operating at 185°C and 100 rpm for 10 min, producing a highly cross-linked material.

4.2.2 Reactive Extrusion and Compounding

Reactive modification of PLA with TAM was performed in a twin screw co-rotating extruder (TSE, Coperion ZSK 18 ML) equipped with a strand die, water cooling bath, and pelletizer, as described in previous work[36]. A masterbatch was prepared by solution coating PLA powder with DCP, TAM, and acetone, and allowing the solvent to evaporate. The masterbatch was mixed with dried PLA to yield a 0.1 wt% DCP and 0.3 wt% TAM formulation, designated as PLA/TAM. The extruder operated with a temperature of 190°C throughout, with a temperature of 170°C in the feed zone, feeder speed of 30 min^{-1}, screw speed of 120 min^{-1}, and an average residence time of 2.5 min to allow for a complete reaction (the half-life time of DCP is 0.3-0.8 min at 190°C[40]). The neat PLA samples were processed in the TSE using the same conditions.

LAK was compounded with PLA using a Haake Polylab R600 internal batch mixer equipped with roller rotors and with a chamber volume of 70 cm^3. PLA was coated with an acetone solution containing 1 wt% LAK 301 and the solvent was allowed to evaporate. The resulting mixture was charged to the mixer at 185°C at 120 rpm, using a fill factor of 70%, and mixed for 5 min. The formulation which contains 1 wt% LAK 301 is designated as PLA/LAK. Similarly, the BF was added to PLA using the Haake Polylab R600 batch mixer in ratios of 1-10 wt% BF at 185°C and 120 rpm for 5 min. The sample designation used in this work is PLA/xBF where 'x' denotes the weight percentage of BF.

4.2.3 Sample Preparation and Annealing

Following processing, PLA samples were dried for 24 h under vacuum at 60°C. Samples were prepared for mechanical testing and degradation by melting and shaping PLA through compression molding for 5 minutes using a Carver Hydraulic Press at 180°C. These samples were cooled at room temperature and are designated as compression molded (CM).

Selected samples were subjected to further annealing treatment immediately following the melting step by exposing the mold to temperatures ranging from 80-120°C for an additional 5 minutes. After annealing, the samples were cooled at room temperature and are designated as annealed (CM x°C, where 'x' denotes the annealing temperature). The sample preparation and annealing methodology remained consistent between the various PLA formulations used in this work.

4.2.4 Gel Permeation Chromatography (GPC)

GPC characterization of molded samples was conducted using a Viscotek 270 max separation module equipped with triple detectors: differential refractive index (DRI), viscosity (IV), and light scattering (low angle, LALS; and right angle, RALS). The separation module was maintained at 40°C and contained two porous PolyAnalytik columns in series with an exclusion molar mass limit of $20x10^6$ $g \cdot mol^{-1}$. HPLC grade THF was used as the eluent at a flow rate of 1 $ml \cdot min^{-1}$.

Samples were prepared for GPC analysis by dissolving a film cross-section in THF to achieve a solution of a 2 mg·ml^{-1} concentration. Chromspec 13 mm UV syringe filters with a 0.22 µm pore size were used to filter the samples prior to measurement.

4.2.5 Differential Scanning Calorimetry (DSC)

The non-isothermal crystallization behaviour of neat, branched, and nucleated PLA was studied through differential scanning calorimetry (DSC) using a TA Instruments DSC Q1000. Samples weighing 5-10 mg were sealed in aluminum hermetic pans and heated to 210°C at a rate of 5°C·min^{-1}. Following the first heating scan, the samples were held isothermally for 3 min at 210°C. To determine the crystallization onset and peak, the samples were cooled to -30°C at a rate of 5°C·min^{-1}. The second heating scan was conducted between -30 and 210°C at a rate of 5°C·min^{-1}. The percent crystallinity, χ_c, was determined using Equation 4.1:

$$\chi_c = \frac{\Delta H_m - \Delta H_{cc}}{\Delta H_{100}\left(\frac{\phi_{PLA}}{100}\right)} \times 100 \tag{4.1}$$

where ΔH_m is the enthalpy of melting, ΔH_{cc} is the enthalpy of cold crystallization, ΔH_{100} is the theoretical enthalpy of melting for a 100% crystalline polymer, which is 93 J·g^{-1} for PLA [41], and ϕ_{PLA} is the polymer matrix weight percentage of the samples.

4.2.6 X-ray Diffraction (XRD)

X-ray diffraction (XRD) analysis of compression molded discs (32 mm diameter, 2 mm thickness) was conducted with a Philips X'Pert Pro diffractometer using Co kα radiation (λ = 1.79 Å). Measurements were performed at 40 kV and 45 mA, with data recorded in the range of 2θ = 10-30°.

4.2.7 Mechanical Properties and Heat Deflection Temperature (HDT) Testing

Flexural tests were performed on 127 mm x 13 mm x 3 mm compression molded specimens with an Instron 3369 universal testing machine using a three-point loading system with a cross head speed of 2 mm·min^{-1} according to ISO 178[42]. An impact tester from Satec System Inc. equipped with a 7 lb hammer

was used to perform unnotched Izod impact tests on 63.5 mm x 13 mm x 3 mm compression molded specimens according to ASTM D256[43].

Heat deflection temperature (HDT) measurements were performed on 127 mm x 13 mm x 3 mm compression molded specimens. Samples were lowered in a silicon oil bath and the temperature was increased from 23°C at a heating rate of 120°C·h^{-1} until 0.25 mm deflection occurred under a load of 1.82 MPa, consistent with ASTM D648[44]. All mechanical tests were performed 48 h after molding.

4.2.8 Hydrolytic Degradation

Thin films with a thickness of 200 µm were prepared for hydrolytic degradation tests by compression molding and annealing at 100°C. Long-term hydrolytic degradation tests were conducted at 60°C in a Thermo Scientific Forma 3911 environmental chamber using methods described in previous work[38]. Individual films having dimensions of 1x3 cm^2 were placed in scintillation vials containing 20 ml of phosphate buffer solution (PBS). The total duration of the experiment was 12 weeks (84 days), with sampling intervals of 1 week. Films were weighed after 24 h drying in a vacuum oven at 60°C to obtain the mass loss measurements. The degradation medium was replaced upon each extraction.

Due to their lower molar mass compared to the original material, GPC characterization of the degraded samples was performed using a Waters 2960 separation module connected to a Waters 410 differential refractometer (DRI), which allowed for better detection of low molar masses. Four Styragel columns were maintained at 35°C with HPLC grade THF as the eluent at a flow rate of 0.3 ml·min^{-1}. The DRI detector was calibrated by polystyrene standards with narrow dispersities over the range of 300-850,000 g·mol^{-1}. GPC analysis was performed on samples dissolved in THF at a concentration of 2 mg·ml^{-1} and filtered using Chromspec 13 mm UV syringe filters with a 0.22 µm pore size.

4.3 Results and Discussion

4.3.1 Thermal Properties and Crystallinity

Thermograms of selected compression molded samples, obtained by DSC, are shown in Figure 4.1(a). The detailed thermal properties, including cold crystallization temperature (T_{cc}), melting temperature (T_m), and glass transition temperature (T_g) of all compositions are summarized in Table A.1.

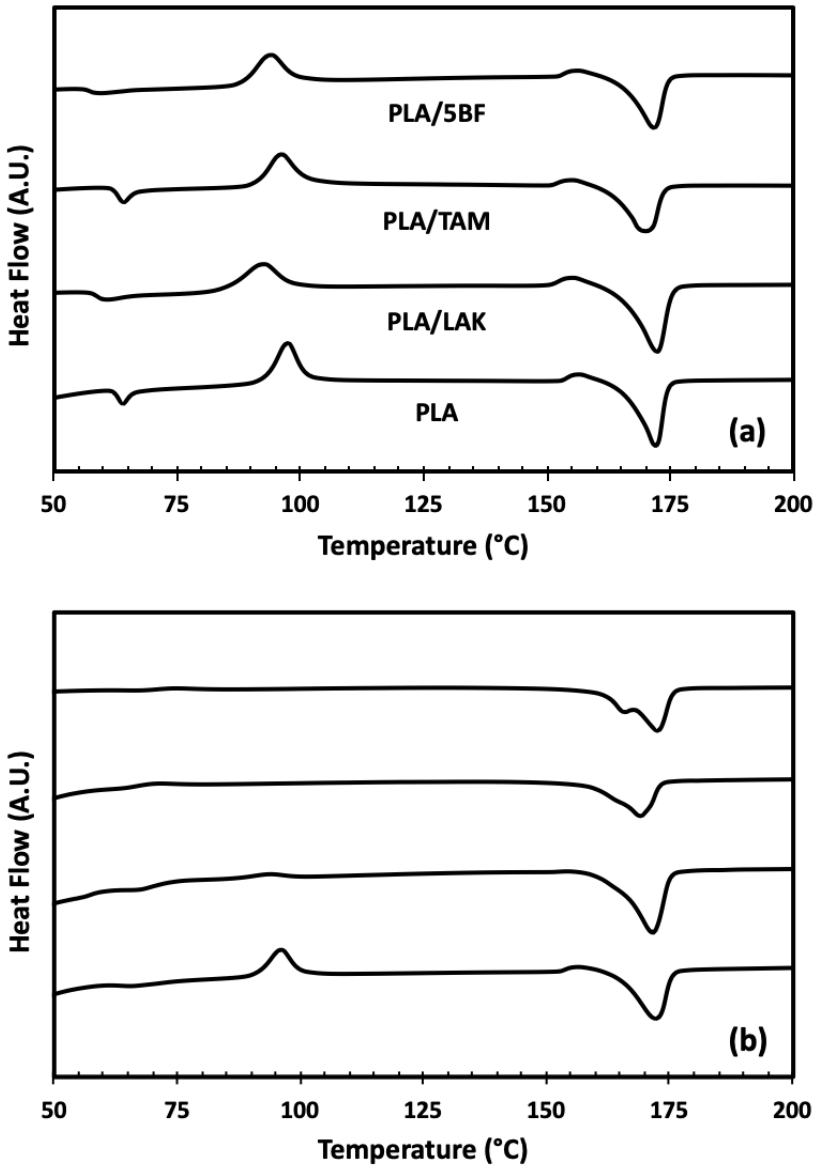

Figure 4.1: *First heating DSC curves for PLA samples compression molded (a) and annealed at 100°C (b). Curves are shifted vertically by an arbitrary factor and exothermic peaks are up.*

As seen in Figure 4.2, the compression molded PLA/LAK had slightly improved crystallinity compared to the neat PLA. The branched PLA/TAM exhibited a crystallinity of 13%, whereas the PLA/BF formulations containing 5 wt% BF and above showed an impressive improvement in crystallinity, higher than 20%. These results suggest that the PLA-based BF acts as a very effective nucleating agent, owing to its good compatibility with the matrix material.

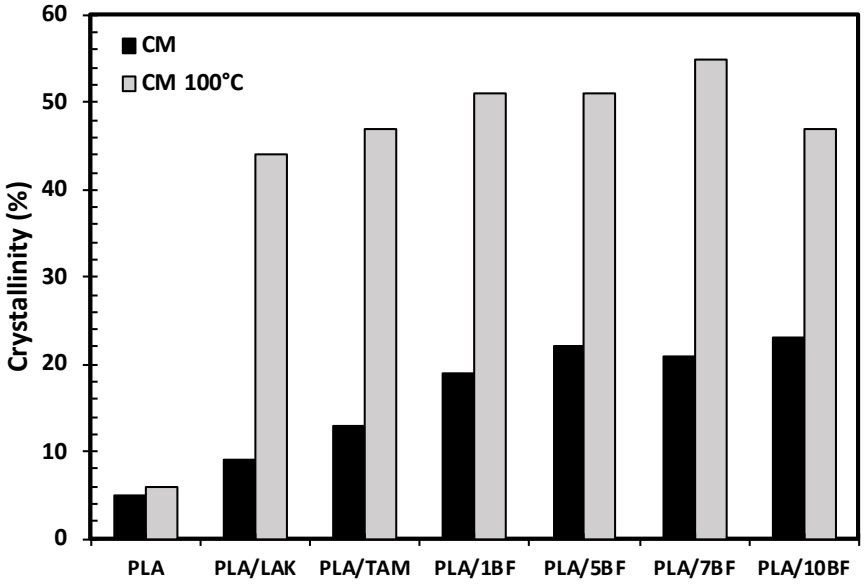

Figure 4.2: *Crystallinity of all formulations compression molded and annealed at 100°C*

Nucleating agents enhance crystallinity by introducing sites for nucleation and increasing the crystallization rates. However, achieving high crystallinity in nucleated PLA after molding operations remains difficult. To achieve a high degree of crystallinity, the cooling rate must be reduced (leading to a long cycle time), or alternatively, annealing of the parts offline may be implemented[45,46]. Annealing involves submitting samples to a controlled temperature for a limited time[47]. This manifests in changes in the sample crystallinity, since PLA can crystallize between its glass transition and melting temperature[48,49]. Annealing treatment can impart significant improvements in the thermal and mechanical properties of PLA[45,50–54]. In this work annealing was performed by conditioning the compression molded samples at different temperatures.

The effect of annealing at 100°C on the thermal properties is illustrated in Figure 4.1(b) and summarized in Table A.1. The annealed non-nucleated neat PLA sample did not exhibit remarkable changes in its

thermal properties, and only a slight increase in crystallinity was achieved (Figure 4.2). However, remarkable enhancements in the crystallinity up to 45% for PLA/TAM and PLA/LAK and up to 50% for the formulations containing the BF nucleating agent were achieved.

The disappearance of the cold crystallization peak (Figure 4.1(b)) in the branched (PLA/TAM) and nucleated samples (PLA/LAK, PLA/5BF) confirms that the crystallization process was promoted at the slower cooling rates provided by annealing conditions[55]. This is a phenomenon which has been previously observed when nucleating agents are added to PLA, and demonstrates the efficiency of a nucleating agent in enhancing the crystallization process[56,57]. Our results show that the nucleated formulations of PLA are more responsive to annealing treatment, and there is a combined effect of nucleation and thermal treatment in improving the crystallinity of a sample.

Figure 4.3 shows the effect of annealing temperature on crystallinity. The most dramatic effects were obtained when the annealing temperature was increased from 80°C to 100°C, whereas the improvements were marginal above this temperature. Therefore 100°C is deemed as an appropriate temperature for annealing of these samples, while avoiding possible degradation concerns at higher temperatures.

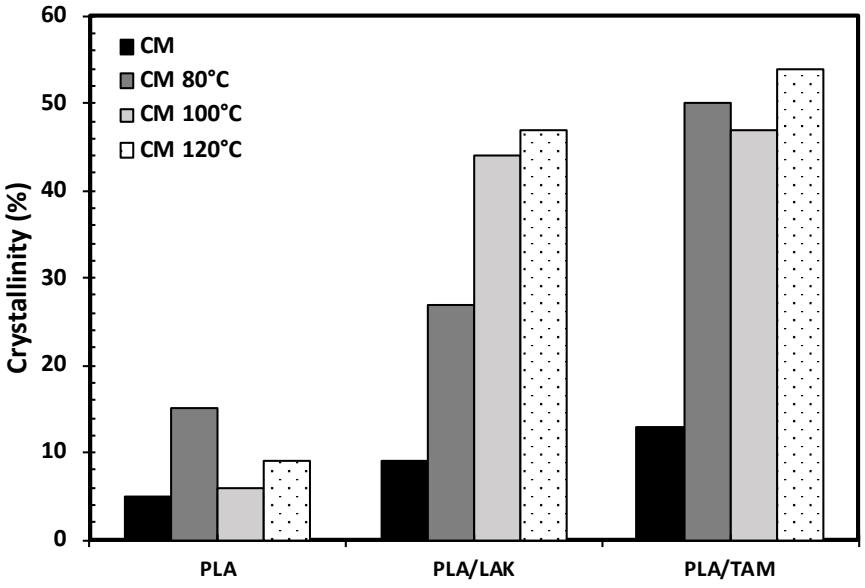

Figure 4.3: *Effect of annealing temperature on sample crystallinity*

X-ray diffraction (XRD) was used to identify the type of crystals formed within the various PLA compositions (Figure 4.4). PLA is known to crystallize in three different crystal forms: α, β, and γ[58,59].

The most common crystal structure is α, with two distinct phases, α (stable) and α′ (disordered)[58–62]. Differences between the crystalline structures are associated with chain conformation and packing between the disordered and ordered forms. Compression molded PLA/5BF and PLA/TAM, exhibit only two low intensity diffraction peaks at 16.5° and 18.9°, corresponding to the (110)/(200) and (203) reflection of the disordered α′ crystals, respectively[61,62]. The presence of these peaks, along with their low intensity indicates the development of some crystallinity in these samples compared to the compression molded neat PLA, consistent with the results shown in Figure 4.2.

Notable differences in the XRD patterns were observed between the compression molded and annealed samples. Upon annealing, the (110)/(200) reflection increased in intensity, providing evidence of higher crystallinity. Several diffraction peaks of lower intensity were also present in the annealed samples at 14.8°, 18.9°, and 22.2°, corresponding to the (010), (203), and (015) reflections respectively[61–63]. The occurrence of the lower intensity reflections supports the development of α-crystals upon annealing at 100°C. It should be noted that in addition to the (010), (110)/(200), and (203) reflections detected in this work, for the presence of α-crystal, literature reports peaks at 12.5°, 20.8°, 23.0°, 24.1°, and 25.1° corresponding to the (004)/(103), (204), (115), (016), and (206) planes respectively[61]. Evidently, at an annealing temperature of 100°C, neither the α or α′ crystal form was developed exclusively and instead a combination of the two crystal forms is present. The α′ and α crystal forms are known to exclusively develop at 85°C and 145°C, respectively[58,60–62]. Therefore the annealing temperature of 100°C falls directly in a transition region between the α and α′ crystal forms[58,64,65].

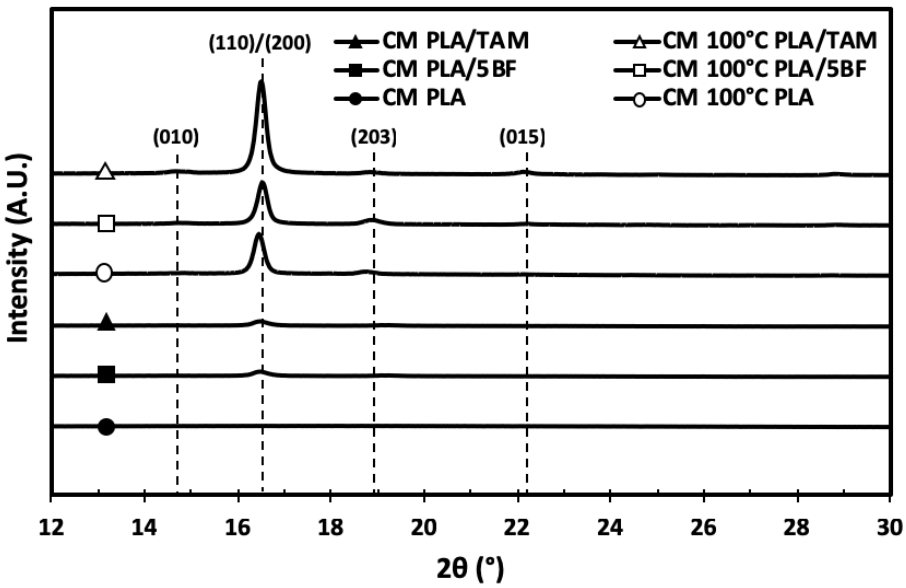

Figure 4.4: *XRD patterns for PLA, PLA/5BF, and PLA/TAM compression molded and annealed at 100°C. Curves are shifted vertically by an arbitrary factor.*

The glass transition temperature, T_g, was sensitive to the various modification strategies and to annealing. In the compression molded samples, the modified PLA have lower and less well-defined T_g compared to the linear neat PLA (Figure 4.5). However, upon annealing, increases of over 10°C in the T_g of PLA/TAM and the PLA/BF samples were observed. These results suggest that post-molding treatment is an effective method to increase T_g, with a positive influence on important properties, such as the HDT, as described in the next section.

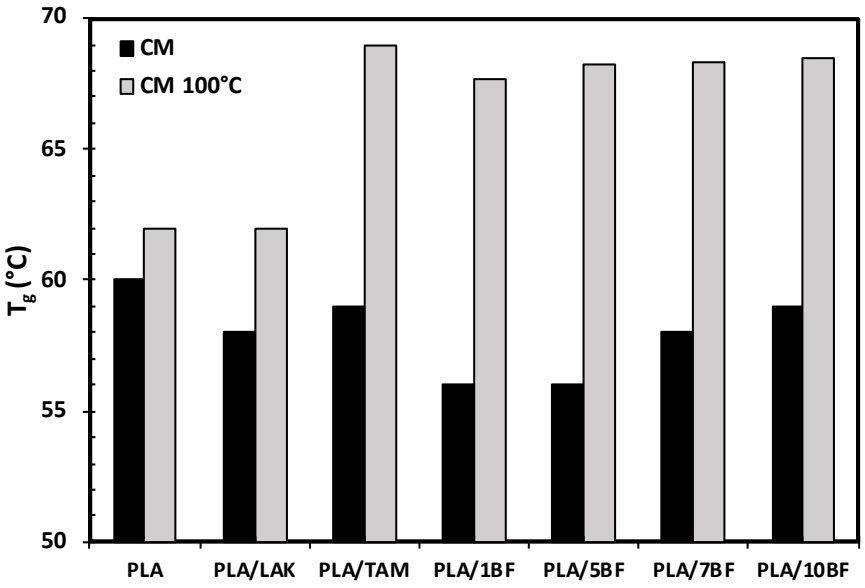

Figure 4.5: *T_g of all formulations compression molded and annealed at 100°C*

Figure 4.6 shows the effect of annealing temperature on T_g. For both LAK and TAM-modified PLA, similar improvements in T_g were obtained across all annealing temperatures, while the T_g of neat PLA remained relatively unchanged upon annealing, with only a moderate improvement when annealed at 100°C.

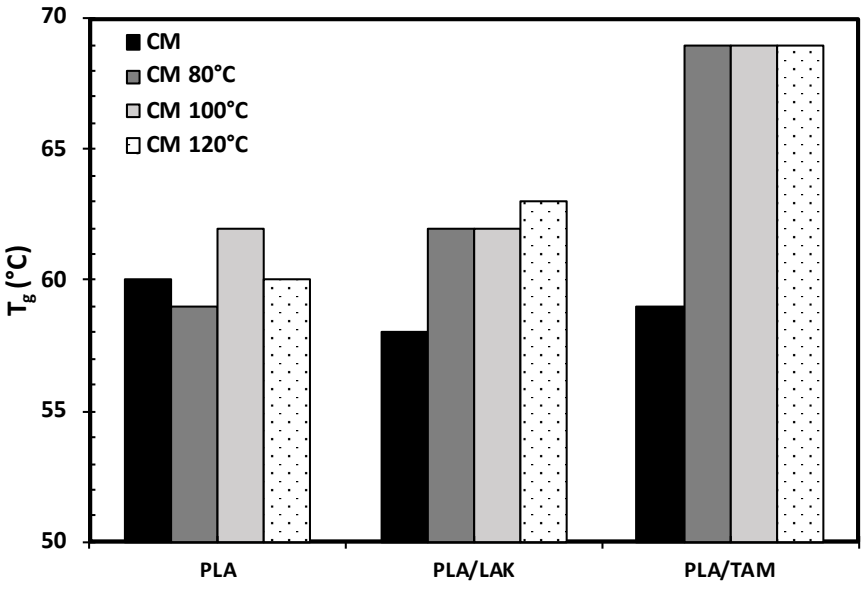

Figure 4.6: *Effect of annealing temperature on T_g*

4.3.2 Mechanical Properties and Heat Deflection Temperature (HDT)

It is well known that the properties of molded polymeric parts such as the crystalline morphology, spherulite size, and crystallinity are largely governed by the processing conditions[45,66,67]. The mechanical properties such as flexural modulus, impact strength, and HDT depend on crystalline structure, molecular weight, and chain architecture[59], and are important factors in determining the end-use applications of PLA. In this section, we establish structure-property relations between the thermal and mechanical properties of the PLA formulations under investigation.

Prior to annealing, all of the formulations exhibited similar flexural moduli, with only modest improvements seen in the branched and nucleated samples compared to neat PLA (Figure 4.7). However, improvements were observed post-annealing, with PLA/TAM and PLA containing above 7 wt% BF, experiencing over 40% increases in flexural moduli compared with the neat material, while also matching within statistical error the performance of PLA/LAK, which was the benchmark material.

The presence of stable nucleation sites and an increase in chain mobility at higher molding temperatures facilitate crystallization[35,36,68,69], as shown in Section 4.3.1 above. The combined effect of these two phenomena is evident in the flexural moduli of annealed PLA formulations. A comparison of the crystallinity (Figure 4.2, Table A.1) and the flexural moduli (Figure 4.7, Table A.2), reveals a direct correlation. The neat PLA does not develop significant crystallinity even upon annealing, and consequently its flexural modulus showed only modest improvement. In contrast, the nucleated formulations experienced substantial increases in crystallinity, followed by large increases in the flexural moduli as a result of annealing.

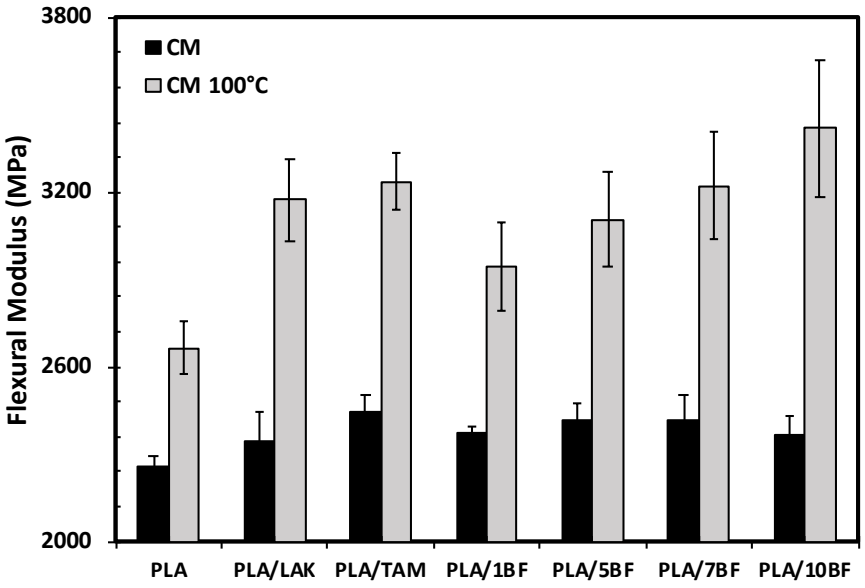

Figure 4.7: *Flexural modulus of all formulations compression molded and annealed at 100°C*

The effects of annealing temperature on the flexural moduli are shown in Figure 4.8 for three selected materials. Evidently, the flexural modulus of PLA/TAM is most strongly influenced by annealing treatment, showing improvement across all temperatures, while PLA/LAK only exhibits substantial improvements when annealed at 100°C and 120°C.

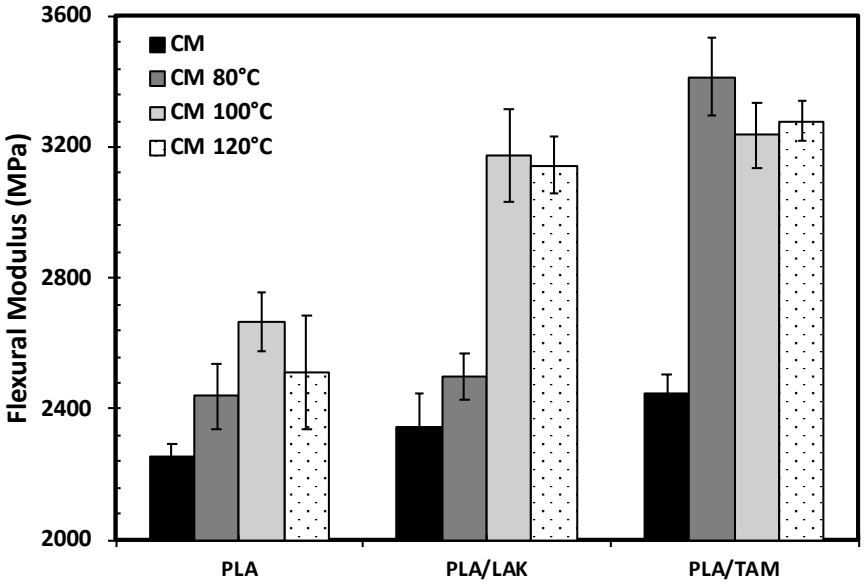

Figure 4.8: *Effect of annealing temperature on flexural modulus*

The unnotched Izod impact strength of the non-annealed and annealed samples are presented in Figure 4.9. There were no significant differences in the impact strength of the compression molded samples, except for the PLA/5BF composition. PLA/LAK and PLA/TAM exhibited improvements in their impact strength upon annealing treatment that were comparable within statistical error.

The impact strength of the BF-based PLAs decreased upon annealing. This may be attributed to the higher crystallinity of these materials, which would typically affect impact strength negatively. Accordingly, PLA/LAK and PLA/TAM, which had lower crystallinity (Figure 4.2) had better impact properties. This suggests that there is a balance between the increase in the crystallinity and the impact properties. Differences in the crystalline structure may also be responsible for these observations. Nevertheless, in all cases, nucleation and branching of PLA did not compromise the properties of the initial PLA material, except for the composition containing 10 wt% BF.

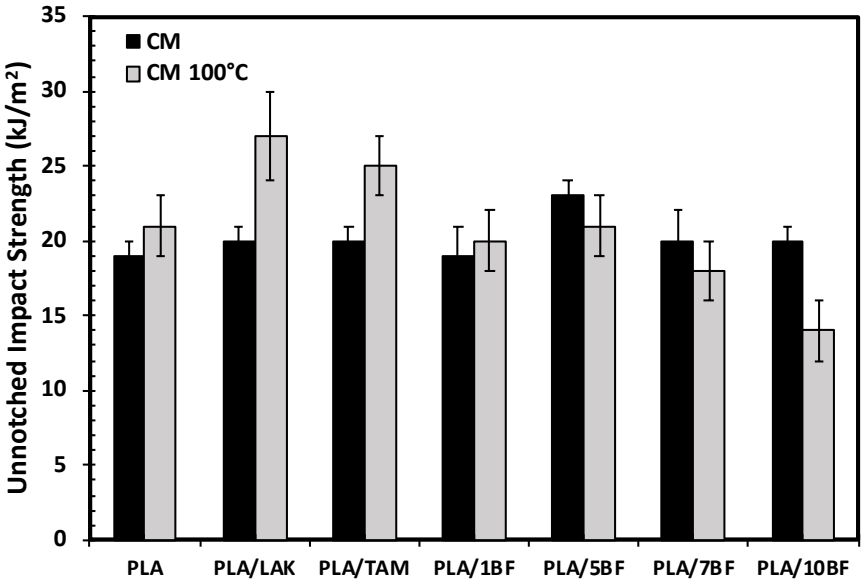

Figure 4.9: *Impact strength of all formulations molded and annealed at 100°C*

The effect of annealing temperature on the impact strength is summarized in Figure 4.10. While modest improvements are observed at annealing temperatures of 80°C and 100°C, the impact strength of the nucleated samples is compromised at a temperature of 120°C, decreasing nearly to the values of the initial compression molded material.

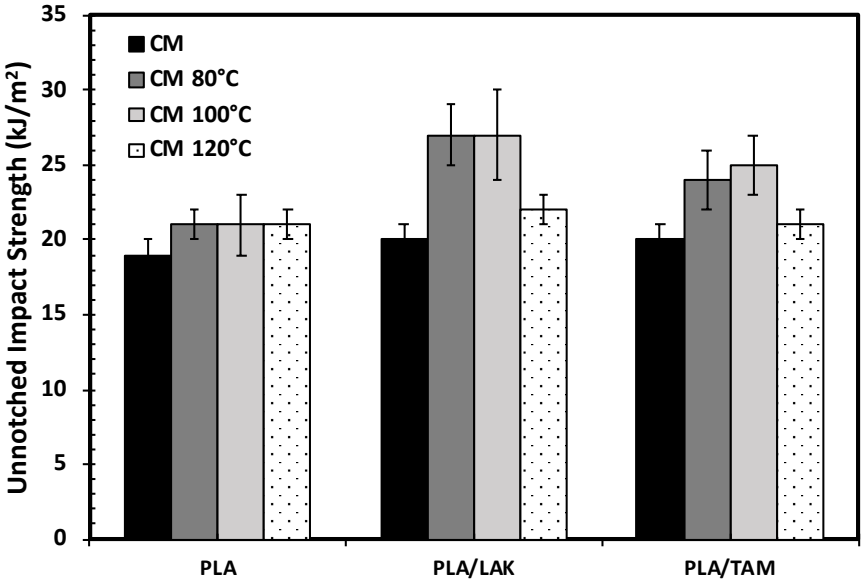

Figure 4.10: *Effect of annealing temperature on impact strength*

It is well known that PLA can degrade upon thermal processing, due to reactions which occur such as hydrolysis, inter-chain transesterification, and depolymerization by back-biting (intramolecular transesterification)[12,70–72]. As a result of such reactions, the molecular weight, and hence the mechanical properties decrease[29,73]. The tendency of PLA to undergo thermal degradation is related to both the processing temperature and the residence time.

The results suggest that thermal degradation took place when samples were annealed at 120°C and support the use of lower annealing temperatures (≤100°C) to maximize mechanical properties and crystallinity, while avoiding degradation.

The HDT, which is the temperature at which a material loses its load bearing capacity, can be improved by adding nucleating agents and by exposing the sample to annealing conditions. Figure 4.11 illustrates the changes in HDT of the PLA samples annealed at 100°C relative to a baseline HDT of 55°C for the

non-annealed samples. The annealed PLA/TAM exhibited the largest increase in HDT, by 7°C, followed closely by PLA/5BF. This enhancement can be correlated to the increase in T_g also observed for these materials (Figure 4.5).

Taking into consideration differences in composition and experimental methodology, the annealed HDT values are comparable with literature. Nagarajan et al. conducted studies with PLA and LAK, finding that a 1 wt% loading of LAK and exposure to a heated injection mold at 90°C for 60 s resulted in an HDT of 65°C[74]. More substantial changes in HDT (>85°C) have been recorded for higher mold temperatures exceeding 110°C[74]; however, such mold conditions can compromise the mechanical properties of the material, as was observed for the annealing temperature of 120°C in this work (Figure 4.8, Figure 4.10).

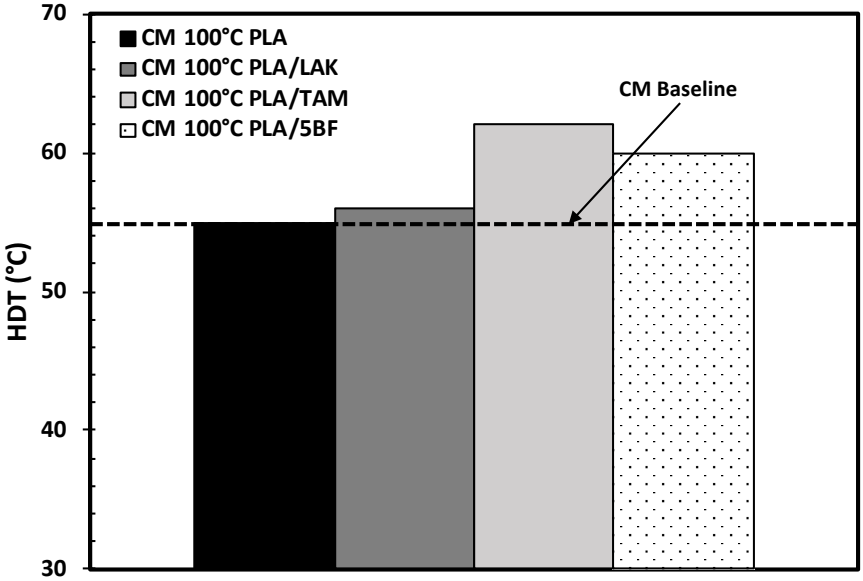

Figure 4.11: *HDT of PLA samples annealed at 100°C*

4.3.3 Hydrolytic Degradation

In addition to being derived from bio-based, renewable materials, PLA is also considered to be biodegradable, under certain conditions. The hydrolytic degradation behaviour of PLA is strongly dependent on parameters such as molecular weight, crystallinity, geometry, and surrounding environment (temperature, moisture, pH, presence of micro-organisms, etc)[75]. Given the influence of crystallinity on degradation behaviour (Figure 4.2), it is of interest to investigate the effects of higher crystallinity on the

degradation of PLA. In this section we investigate the effect of annealing at 100°C on the long-term hydrolytic degradation profile of neat and modified PLA.

Figure 4.12 shows the mass loss of the PLA samples as a function of degradation time. All samples show the same principal erosion behaviour; the matrices start to lose mass after an induction period of minimal mass loss. However, the time point at which mass loss begins is quite different between the compression molded and annealed samples. The original PLA sample showed an initial period of minimal mass loss of about 70 days, followed by rapid mass loss toward the end of the degradation period. The delay in the onset of mass loss coupled with immediate and rapid loss in molecular weight was attributed to a bulk erosion mechanism that is prevalent in these samples[38].

On the contrary, all annealed formulations, which had higher crystallinity, experienced substantial mass loss and followed similar profiles, with an induction period of only 14 days, followed by constant and linear loss. Given the immediate onset of molar mass loss in the annealed samples (Figure 4.13), it is evident that these samples also follow a bulk erosion mechanism.

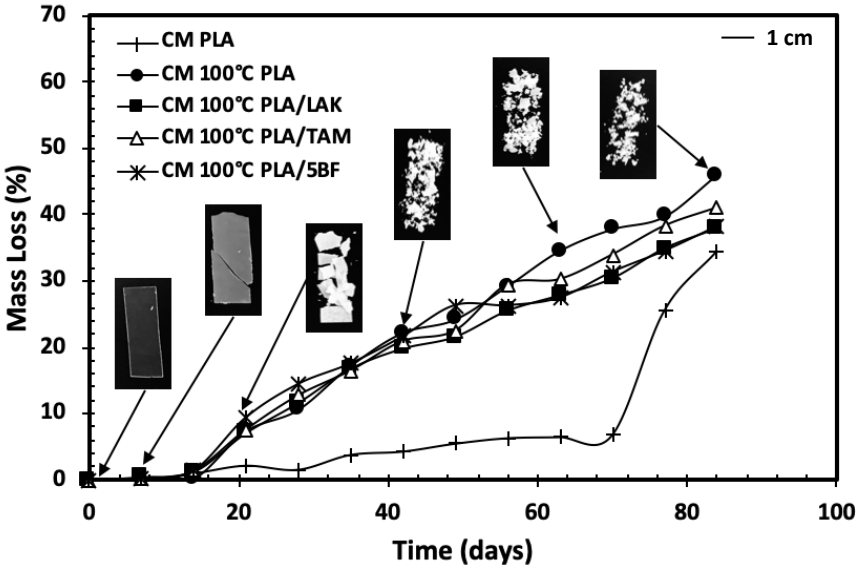

Figure 4.12: *Mass loss and representative visual changes as a function of hydrolysis time for PLA samples compression molded and annealed at 100°C. Lines are drawn to guide the eye.*

Several researchers have reported accelerated degradation rates with increasing polymer crystallinity[76,77]. Tsuji and Ikada propose that higher crystallinities introduce more defects into the amorphous region,

which allows for easier diffusion of water into such regions[76]. Accelerated hydrolysis of PLA with high crystallinity may also be ascribed to an enhanced catalytic effect caused by the exclusion of the terminal group from the crystalline region during crystallization. This results in an increased density of hydrophilic and catalytic carboxyl terminal groups in the amorphous region[76].

Despite the differences in the induction period of mass loss, all samples followed a bulk erosion mechanism and achieved over 30% mass loss at the end of the study irrespective of their prior thermal treatment. The annealed samples experienced higher rates of mass loss and surpassed the overall mass loss over the course of the study compared to the non-conditioned PLA.

As degradation proceeded, significant physical changes were also observed in the samples (Figure 4.12), including increased brittleness and fragmentation, along with a notable increase in sample opacity as degradation proceeded. This is a well-known consequence of degradation, attributed to increased crystallinity in the polymer matrix as a result of the preferential degradation of amorphous regions[38,78,79]. No significant visual differences between the non-annealed and annealed samples were observed upon hydrolytic degradation in this work.

Molar mass loss occurs upon hydrolytic degradation, with its rate dictated by the type of erosion mechanism present. Across all formulations, significant decreases in the molar mass averages were observed (Figure 4.13), attributed to the hydrolytic degradation process and the loss of low and high molar mass fragments. In all molar mass averages, the rate of loss was highest in the first three weeks of the study, reaching over 70% loss. Beyond the sixth week of the study, the molar mass loss plateaued amongst all molar mass averages and across all PLA formulations. These trends are consistent with those seen previously for non-annealed samples[38].

Comparison of the M_z averages (Figure 4.13(c)), reveals that PLA/TAM exhibited the highest rates of loss in the first two weeks, while the neat, LAK, and BF-modified PLA formulations did not experience such rates of loss in M_z in the same timeframe. PLA/TAM contains a higher number of chain ends compared to unmodified PLA, owed to the presence of LCB and complex TAM structures interpenetrated with the PLA matrix[36,38]. The carboxyl end group has been found to play a crucial role in degradation,

hindering close packing and providing enhanced hydrolyzability[80–82]. Branching architecture, particularly that provided by TAM, has also been found previously to be responsible for changes in degradation behaviour, and a more accelerated rate of molar mass loss[38,80,83].

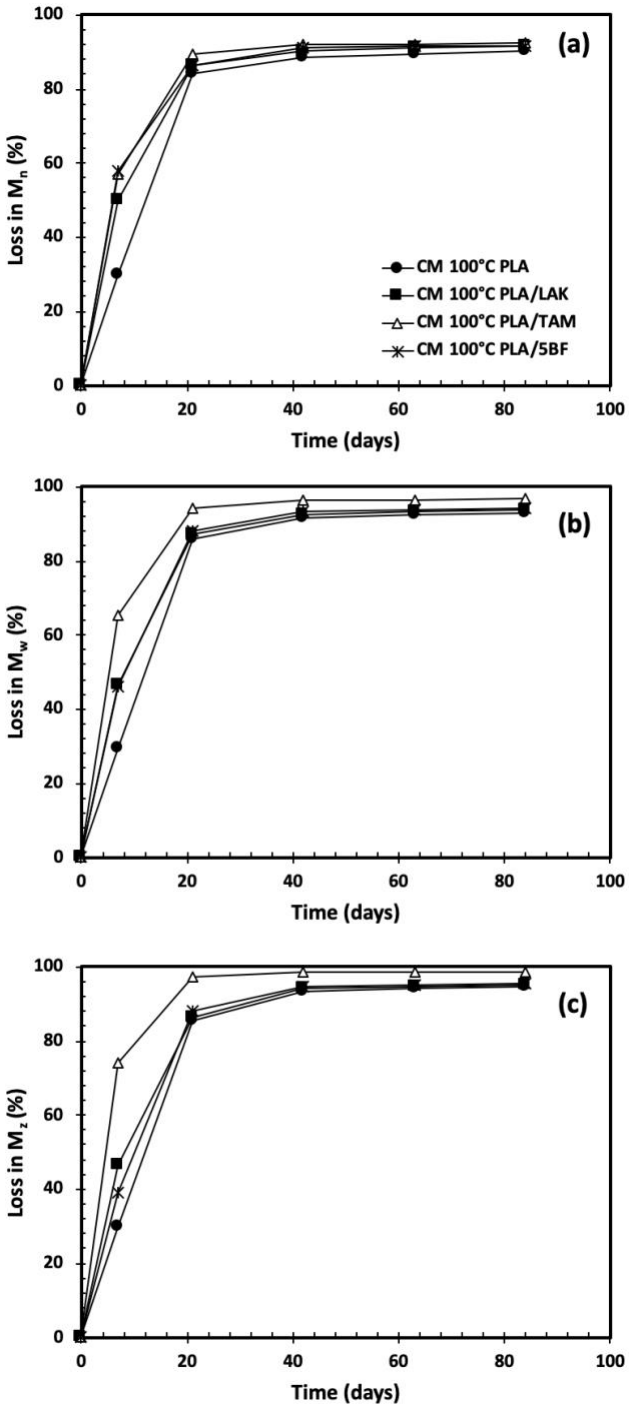

Figure 4.13: *Molar mass averages for PLA samples as a function of time (a) M_n; (b) M_w; and (c) M_z for PLA annealed at 100°C*

Irrespective of the formulation, comparable rates of specimen mass loss and molar mass loss were achieved to our previous work, which focused on the degradation of non-annealed neat and TAM-modified PLA under the same environmental conditions[38]. These results demonstrate that the use of annealing to introduce crystallinity in neat, branched, and nucleated PLA did not hinder the hydrolytic degradation of PLA on a 12-week time scale.

4.4 Conclusions

We have demonstrated strategies to obtain PLA with high crystallinity and enhanced mechanical properties, as well as HDT. The two proposed methods include the introduction of long-chain branching by reactive extrusion, and the addition of a PLA-based, cross-linked nucleating agent. In the former case, the improvements in crystallization behaviour are attributed to the nucleating effect of the long-chain branched structures. In the latter approach, the improvements were attributed to the exceptional nucleating capacity of the BF nucleating agent, which owing to its PLA-based nature had good compatibility with the matrix material.

Further improvements to the crystallinity were achieved through annealing at temperatures in the range of 80-120°C, demonstrating the combined effects of controlled cooling and nucleating agents in promoting crystallization. The improvements in crystallinity achieved by annealing translated to significant improvements in the flexural modulus, with all modified formulations experiencing over 30% increases relative to non-annealed neat PLA. Additionally, the impact strength of the original materials was maintained upon annealing. An annealing temperature of 100°C was selected as optimum, due to maximum property improvements achieved at this temperature and thermal degradation occurring above 100°C. Improvements in the glass transition temperatures of over 10°C were also achieved upon annealing, resulting in a 7°C increase in HDT.

Given the known influence of crystallinity on degradation, the effects of nucleation and annealing on the hydrolysis of PLA were studied. Within a 12-week timeframe, annealed PLA samples experienced substantial loss in sample mass, molar mass, and structural integrity, comparable to those previously

recorded for the degradation of non-annealed PLA. The results of this work demonstrated that annealing is an effective method to provide the required crystallinity for PLA while maintaining its degradability. This extends the range of use of PLA in commodity applications that require biodegradable polymers with high heat resistance and durability.

4.5 References

(1) Auras, R.; Tak, L. T.; Selke, S. E. M.; Tsuji, H. *Poly(Lactic Acid): Synthesis, Structures, Properties, Processing, and Application.*; John Wiley & Sons, Inc.: Hoboken, NJ, USA, 2010.

(2) Drumright, R. E.; Gruber, P. R.; Henton, D. E. *Adv. Mater.* **2000**, *12* (23), 1841.

(3) Auras, R.; Harte, B.; Selke, S. *Macromol. Biosci.* **2004**, *4* (9), 835.

(4) Dorgan, J. R.; Williams, J. S.; Lewis, D. N. *J. Rheol. (N. Y. N. Y).* **1999**, *43* (5), 1141.

(5) Rasal, R. M.; Janorkar, A. V; Hirt, D. E. *Prog. Polym. Sci.* **2010**, *35* (3), 338.

(6) Dorgan, J. R.; Lehermeier, H.; Mang, M. *J. Polym. Environ.* **2000**, *8* (1), 1.

(7) Dorgan, J. R.; Janzen, J.; Clayton, M. P.; Hait, S. B.; Knauss, D. M. *J. Rheol. (N. Y. N. Y).* **2005**, *49* (3), 607.

(8) Palade, L.-I.; Lehermeier, H. J.; Dorgan, J. R. *Macromolecules* **2001**, *34* (5), 1384.

(9) Nagarajan, V.; Mohanty, A. K.; Misra, M. *J. Appl. Polym. Sci.* **2016**, *133* (28), 1.

(10) El-Hadi, A.; Schnabel, R.; Straube, E.; Müller, G.; Henning, S. *Polym. Test.* **2002**, *21* (6), 665.

(11) Huang, T.; Yamaguchi, M. *J. Appl. Polym. Sci.* **2017**, *134* (24), 44960.

(12) Lim, L.-T.; Auras, R.; Rubino, M. *Prog. Polym. Sci.* **2008**, *33* (8), 820.

(13) Mekonnen, T.; Mussone, P.; Khalil, H.; Bressler, D. *J. Mater. Chem. A* **2013**, *1* (43), 13379.

(14) Beck, H. N. *J. Appl. Polym. Sci.* **1967**, *11* (5), 673.

(15) Binsbergen, F. L. *Polymer (Guildf).* **1970**, *11* (5), 253.

(16) Thierry, A.; Straupe, C.; Lotz, B.; Wittmann, J. C. *Polym. Commun.* **1990**, *31*, 299.

(17) Yamasaki, S.; Ohashi, Y.; Tsutsumi, H.; Tsujii, K. *Bull. Chem. Soc. Jpn.* **1995**, *68* (1), 146.

(18) Shepard, T. A.; Delsorbo, C. R.; Louth, R. M.; Walborn, J. L.; Norman, D. A.; Harvey, N. G.; Spontak, R. J. *J. Polym. Sci. Part B Polym. Phys.* **1997**, *35* (16), 2617.

(19) Wilder, E. A.; Spontak, R. J.; Hall, C. K. *Mol. Phys.* **2003**, *101* (19), 3017.

(20) Libster, D.; Aserin, A.; Garti, N. *Polym. Adv. Technol.* **2007**, *18* (9), 685.

(21) Thierry, A.; Fillon, B.; Straupé, C.; Lotz, B.; Wittmann, J. C. *Prog. Colloid Polym. Sci.* **1992**, *87*, 28.

(22) Mathieu, C.; Thierry, A.; Wittmann, J. C.; Lotz, B. *J. Polym. Sci. Part B Polym. Phys.* **2002**, *40* (22), 2504.

(23) Battegazzore, D.; Bocchini, S.; Frache, A. *Express Polym. Lett.* **2011**, *5* (10), 849.

(24) Liang, J.-Z.; Zhou, L.; Tang, C.-Y.; Tsui, C.-P. *Compos. Part B Eng.* **2013**, *45* (1), 1646.

(25) Frone, A. N.; Berlioz, S.; Chailan, J.-F.; Panaitescu, D. M. *Carbohydr. Polym.* **2013**, *91* (1), 377.

(26) Kowalczyk, M.; Piorkowska, E.; Kulpinski, P.; Pracella, M. *Compos. Part A Appl. Sci. Manuf.* **2011**, *42* (10), 1509.

(27) Dan Sawyer. In *Midwest Biopolymers & Biocomposites Workshop*; Natureworks LLC: Ames, Iowa, 2010.

(28) Anderson, K. A.; Randall, J. R.; Kolstad, J. J. Polylactide molding compositions and molding

process. WO2011085058A1, 2011.

(29) Di, Y.; Iannace, S.; Di Maio, E.; Nicolais, L. *Macromol. Mater. Eng.* **2005**, *290* (11), 1083.

(30) Pilla, S.; Kramschuster, A.; Yang, L.; Lee, J.; Gong, S.; Turng, L.-S. *Mater. Sci. Eng. C* **2009**, *29* (4), 1258.

(31) Corre, Y.-M.; Maazouz, A.; Duchet, J.; Reignier, J. *J. Supercrit. Fluids* **2011**, *58* (1), 177.

(32) Mihai, M.; Huneault, M. A.; Favis, B. D. *Polym. Eng. Sci.* **2010**, *50* (3), 629.

(33) Takamura, M.; Nakamura, T.; Takahashi, T.; Koyama, K. *Polym. Degrad. Stab.* **2008**, *93* (10), 1909.

(34) Nerkar, M.; Ramsay, J. A.; Ramsay, B. A.; Kontopoulou, M. *Macromol. Mater. Eng.* **2014**, *299* (12), 1419.

(35) Tiwary, P.; Park, C. B.; Kontopoulou, M. *Eur. Polym. J.* **2017**, *91*, 283.

(36) Tiwary, P.; Kontopoulou, M. *ACS Sustain. Chem. Eng.* **2018**, *6* (2), 2197.

(37) Tiwary, P.; Kontopoulou, M. *J. Rheol. (N. Y. N. Y).* **2018**, *62* (5), 1071.

(38) Simmons, H.; Kontopoulou, M. *Polym. Degrad. Stab.* **2018**, *158*, 228.

(39) Chaloupli, N. N.; Kontopoulou, M.; Simmons, H.; Tiwary, P. Biobased Additive for Thermoplastic Polyesters. Publication No. WO/2019/010574., 2019.

(40) Arkema Inc. *DI-CUP® Dicumyl Peroxide Technical Information*; Philadelphia, 2009.

(41) Fischer, E. W.; Sterzel, H. J.; Wegner, G. *Kolloid-Zeitschrift und Zeitschrift für Polym.* **1973**, *251* (11), 980.

(42) ISO 178. *Plastics - Determination of flexural properties*; 2019.

(43) ASTM Standard D256. *Determining the Izod Pendulum Impact Resistance of Plastics*; 2010.

(44) ASTM Standard D648. *Standard Test Method for Deflection Temperature of Plastics Under Flexural Load in the Edgewise Position*; 2018.

(45) Harris, A. M.; Lee, E. C. *J. Appl. Polym. Sci.* **2008**, *107* (4), 2246.

(46) Goto, K.; Nakano, S.; Kuriyama, T. *Strength, Fract. Complex.* **2006**, *4* (3), 185.

(47) Pérez-Fonseca, A. A.; Robledo-Ortíz, J. R.; González-Núñez, R.; Rodrigue, D. *J. Appl. Polym. Sci.* **2016**, *133* (31), 43750.

(48) Andjelić, S.; Scogna, R. C. *J. Appl. Polym. Sci.* **2015**, *132* (38), 42066.

(49) Ivey, M.; Melenka, G. W.; Carey, J. P.; Ayranci, C. *Adv. Manuf. Polym. Compos. Sci.* **2017**, *3* (3), 81.

(50) Tabi, T.; Sajo, I. E.; Szabo, F.; Luyt, A. S.; Kovacs, J. G. *Express Polym. Lett.* **2010**, *4* (10), 659.

(51) Dong, T.; Yu, Z.; Wu, J.; Zhao, Z.; Yun, X.; Wang, Y.; Jin, Y.; Yang, J. *Polym. Sci. Ser. A* **2015**, *57* (6), 738.

(52) Srithep, Y.; Nealey, P.; Turng, L.-S. *Polym. Eng. Sci.* **2013**, *53* (3), 580.

(53) Wach, R. A.; Wolszczak, P.; Adamus-Wlodarczyk, A. *Macromol. Mater. Eng.* **2018**, *303* (9), 1800169.

(54) Takayama, T.; Todo, M.; Tsuji, H. *J. Mech. Behav. Biomed. Mater.* **2011**, *4* (3), 255.

(55) Debeli, D. K.; Tebyetekerwa, M.; Hao, J.; Jiao, F.; Guo, J. *Polym. Compos.* **2018**, *39* (S3), E1867.

(56) Song, P.; Wei, Z.; Liang, J.; Chen, G.; Zhang, W. *Polym. Eng. Sci.* **2012**, *52* (5), 1058.

(57) Xu, T.; Zhang, A.; Zhao, Y.; Han, Z.; Xue, L. *Polym. Test.* **2015**, *45*, 101.

(58) Zhang, J.; Duan, Y.; Sato, H.; Tsuji, H.; Noda, I.; Yan, S.; Ozaki, Y. *Macromolecules* **2005**, *38* (19), 8012.

(59) Pan, P.; Inoue, Y. *Prog. Polym. Sci.* **2009**, *34* (7), 605.

(60) Zhang, J.; Tashiro, K.; Tsuji, H.; Domb, A. J. *Macromolecules* **2008**, *41* (4), 1352.

(61) Pan, P.; Kai, W.; Zhu, B.; Dong, T.; Inoue, Y. *Macromolecules* **2007**, *40* (19), 6898.

(62) Pan, P.; Zhu, B.; Kai, W.; Dong, T.; Inoue, Y. *J. Appl. Polym. Sci.* **2008**, *107* (1), 54.

(63) Righetti, M. C.; Gazzano, M.; Di Lorenzo, M. L.; Androsch, R. *Eur. Polym. J.* **2015**, *70*, 215.

(64) Shen, L.-Q.; Xu, Z.-K.; Xu, Y.-Y. *J. Appl. Polym. Sci.* **2002**, *84* (1), 203.

(65) Miyata, T.; Masuko, T. *Polymer (Guildf).* **1997**, *38* (16), 4003.

(66) Tsuji, H.; Ikada, Y. *Polymer (Guildf).* **1995**, *36* (14), 2709.

(67) Park, S.-D.; Todo, M.; Arakawa, K. *J. Mater. Sci.* **2005**, *40* (4), 1055.

(68) Najafi, N.; Heuzey, M.-C.; Carreau, P. J.; Therriault, D.; Park, C. B. *Rheol. Acta* **2014**, *53* (10–11), 779.

(69) Zhang, Y.; Tiwary, P.; Parent, J. S.; Kontopoulou, M.; Park, C. B. *Polymer (Guildf).* **2013**, *54*, 4814.

(70) Kopinke, F. D.; Mackenzie, K. *J. Anal. Appl. Pyrolysis* **1997**, *40–41*, 43.

(71) Yang, S.-L.; Wu, Z.-H.; Meng, B.; Yang, W. *J. Polym. Sci. Part B Polym. Phys.* **2009**, *47* (12), 1136.

(72) Kim, I.; Jeong, Y. G. *J. Polym. Sci. Part B Polym. Phys.* **2010**, *48* (8), 850.

(73) Garlotta, D. *J. Polym. Environ.* **2001**, *9* (2), 63.

(74) Nagarajan, V.; Zhang, K.; Misra, M.; Mohanty, A. K. *ACS Appl. Mater. Interfaces* **2015**, *7* (21), 11203.

(75) Höglund, A.; Odelius, K.; Albertsson, A.-C. *ACS Appl. Mater. Interfaces* **2012**, *4* (5), 2788.

(76) Tsuji, H.; Ikada, Y. *Polym. Degrad. Stab.* **2000**, *67* (1), 179.

(77) Chye Joachim Loo, S.; Ooi, C. P.; Hong Elyna Wee, S.; Chiang Freddy Boey, Y.; Loo, S. C. J.; Ooi, C. P.; Wee, S. H. E.; Boey, Y. C. F.; Chye Joachim Loo, S.; Ooi, C. P.; Hong Elyna Wee, S.; Chiang Freddy Boey, Y. *Biomaterials* **2005**, *26* (16), 2827.

(78) Jarerat, A.; Tokiwa, Y. *Macromol. Biosci.* **2001**, *1* (4), 136.

(79) Torres, A.; Li, S. M.; Roussos, S.; Vert, M. *J. Appl. Polym. Sci.* **1996**, *62* (13), 2295.

(80) Tsuji, H.; Hayashi, T. *J. Appl. Polym. Sci.* **2015**, *132* (20), 41983.

(81) de Jong, S. J.; Arias, E. R.; Rijkers, D. T. S.; van Nostrum, C. F.; Kettenes-van den Bosch, J. J.; Hennink, W. E. *Polymer (Guildf).* **2001**, *42* (7), 2795.

(82) Numata, K.; Srivastava, R. K.; Finne-Wistrand, A.; Albertsson, A.-C.; Doi, Y.; Abe, H. *Biomacromolecules* **2007**, *8* (10), 3115.

(83) Andersson, S. R.; Hakkarainen, M.; Inkinen, S.; Sodergard, A.; Albertsson, A. *Biomacromolecules* **2012**, *13* (4), 1212.

Chapter 5

Conclusions and Future Recommendations

5.1 Thesis Conclusions

Reactive extrusion in the presence of peroxide and TAM provides an effective and industrially relevant means to introduce branching in PLA, yielding improvements in processing characteristics and properties. This work addressed two major gaps in the research on coagent-modified PLA: the effect of LCB on degradation, and the optimization of thermal and mechanical properties through controlled process conditions.

TAM-modified PLA experienced substantial degradation within a 12-week time frame, with losses in mass (>30%), molar mass (>90%), structural integrity, and changes in thermal properties. Due to the immediate decrease in molar mass over the first three-weeks of the study and the initial lag period for mass loss in the same timeframe, a bulk mechanism was proposed as the predominant erosion phenomenon. The significant increase in crystallinity of the degraded samples beyond 50% was attributed to the combined effects of annealing and plasticizing under the experimental conditions. Differences in the degradation profiles of the neat and modified PLA were observed due to the preferential degradation of low and high molar mass segments from the polymer chains and counter-diffusion of the resulting oligomers. It is noteworthy that the LCB introduced by reactive extrusion did not affect the capacity of the modified PLA to degrade.

Improvements to the crystallinity of PLA from 5% to nearly 20% were achieved both through the introduction of LCB by reactive extrusion, and the addition of BF, a novel PLA-based, cross-linked nucleating agent. Such improvements were attributed to the nucleating effects of LCB structures in the former approach, and the exceptional nucleating ability of the BF, due to its good compatibility with the matrix material, in the latter approach.

Further improvements in crystallinity (>50%) were achieved by annealing at 80-120°C, illustrating the combined effects of controlled cooling and nucleating agents in promoting crystallization. These improvements translated to over 30% increases in the flexural moduli, while the impact strength of the original materials was maintained. Improvements in the glass transition temperatures by as much as 12°C were also achieved upon annealing, resulting in a 7°C increase in HDT. In addition, the hydrolytic degradation was found to be unhindered by the increased crystallinity in the annealed samples.

The results of this work demonstrate that the use of reactive modification to introduce LCB in PLA, the addition of the BF, and the controlled cooling achieved by annealing conditions all serve as effective methods to improve the properties and crystallinity of PLA, without sacrificing degradability. These improvements will extend the range of use of PLA in various commodity applications that require degradable polymers.

5.2 Future Work

There are many opportunities for future work in this field, several of which are described below.

I. Given the promising results obtained from a 12-week hydrolytic degradation study, a long-term degradation study under composting conditions would present a lot of opportunities for further understanding the degradation mechanisms of coagent-modified PLA. The composting study should be investigated according to ASTM and ISO standards and would determine the true sustainability of the coagent-modified PLA and its potential to replace PBPs in applications requiring degradable polymers.

II. Further study into the kinetics of degradation and the diffusivity of various PLA formulations would prove useful in understanding the mechanisms and phases of degradation.

III. It would be interesting to examine the degradation extracts in detail, particularly soil extracts in the case of a composting study, to determine the products of degradation at various stages. This would prove critical for the market acceptance of coagent-modified PLA as a

biodegradable and compostable material, ensuring no toxic or harmful compounds are produced during degradation, and that the end products abide by composting standards.

IV. Scale-up of the processing of the BF-modified PLA to a twin-screw extruder and injection molding set-up would better simulate industrial processing conditions and yield better sample quality compared to compression molding. The use of injection molding also opens up significant opportunities to further investigate the effects of cooling rates on the crystallization through the use of heated molds and controlled cooling.

V. Further optimization of annealing conditions could be completed. Investigating the effects of annealing time and temperature using statistical methods such as design of experiments (DOE) would highlight optimal conditions for the post-processing treatment of coagent-modified PLA, which could be proposed to industry for implementation when using such materials.

Appendix A

Thermal and mechanical properties of annealed PLA

Table A.1: *Thermal properties of PLA samples at various annealing temperatures*

Sample	Annealing Temperature	T_{cc1} [a]	T_{cc2} [b]	T_m [c]	T_g [d]	χ_c [e]
PLA	CM	98	157	172	60	5
	CM 80°C	95	157	173	59	15
	CM 100°C	96	157	173	62	6
	CM 120°C	97	157	173	60	9
PLA/LAK	CM	93	155	172	58	9
	CM 80°C	95	156	173	62	27
	CM 100°C	94	n/a	172	62	44
	CM 120°C	n/a	n/a	172	63	47
PLA/TAM	CM	98	155	170	59	13
	CM 80°C	n/a	n/a	170	69	50
	CM 100°C	n/a	n/a	169	69	47
	CM 120°C	n/a	n/a	168	69	54
PLA/1BF	CM	92	152	172	56	19
	CM 100°C	n/a	n/a	172	68	51
PLA/5BF	CM	94	156	172	56	22
	CM 100°C	n/a	n/a	166, 173	68	51
PLA/7BF	CM	93	156	173	58	21
	CM 100°C	n/a	n/a	167, 172	68	55
PLA/10BF	CM	95	156	172	59	23
	CM 100°C	n/a	n/a	173	68	47

[a] T_{cc1} – cold crystallization peak temperature

[b] T_{cc2} – cold crystallization peak temperature measured just before melting

[c] T_m – melting peak temperature

[d] T_g – glass transition temperature

[e] χ_c – percentage crystallinity

n/a – Temperature was not detected

All temperatures are reported in °C and measured during the first heating scan.

Table A.2: *Mechanical properties of PLA samples at various annealing temperatures*

Sample	Annealing Temperature	Flexural Modulus (MPa)	Unnotched Izod Impact Strength[a] ($kJ \cdot m^{-2}$)
PLA	CM	2256 ± 38	19 ± 0.9
	CM 80°C	2440 ± 99	21 ± 1
	CM 100°C	2665 ± 89	21 ± 2
	CM 120°C	2513 ± 173	21 ± 1
PLA/LAK	CM	2343 ± 102	20 ± 1
	CM 80°C	2499 ± 71	27 ± 2
	CM 100°C	3174 ± 142	27 ± 3
	CM 120°C	3145 ± 88	22 ± 1
PLA/TAM	CM	2446 ± 57	20 ± 1
	CM 80°C	3145 ± 118	24 ± 2
	CM 100°C	3236 ± 98	25 ± 2
	CM 120°C	3280 ± 60	21 ± 1
PLA/1BF	CM	2371 ± 22	19 ± 2
	CM 100°C	2948 ± 152	20 ± 2
PLA/5BF	CM	2419 ± 57	23 ± 1
	CM 100°C	3106 ± 161	21 ± 2
PLA/7BF	CM	2416 ± 89	20 ± 2
	CM 100°C	3223 ± 182	18 ± 2
PLA/10BF	CM	2364 ± 67	20 ± 1
	CM 100°C	3421 ± 234	14 ± 2

[a] All Izod impact specimens exhibited complete break.